Comprehensive characterization of the complex *lola* locus in *Drosophila melanogaster* reveals novel roles *in vivo*

Dissertation

zur Erlangung des Grades

Doktor der Naturwissenschaften

Am Fachbereich Biologie

der Johannes Gutenberg-Universität Mainz

vorgelegt von

Nadja Dinges

geboren am 01.07.1988

in Nürnberg

Tag der mündliche Prüfung: 22. März 2018

Table of Contents

1. Introduction 10
1.1 Alternative splicing enhances proteome diversity 10
1.2 Alternative *trans*-splicing occurs in different species 11
1.3 *Trans*-splicing in *Drosophila* relies on the RNA sequences TSA and TSB 12
1.4 The complex *lola* locus encodes for distinct BTB-ZF protein isoforms 14
1.5 Lola functions as a transcription factor during *Drosophila* development 18
1.6 The transcription factor Lola regulates nervous-system development 19
1.7 Lola acts beyond the nervous system 24
1.8 Octopamine regulates various processes in *Drosophila* 26
2. Aim of this study 31
3. Materials & Methods 33
3.1 Buffer compositions 33
3.2 Fly work 35
3.2.1 Fly stocks 35
3.2.2 Genomic DNA Extraction 36
3.2.3 Gateway cloning 36
3.2.4 p-element mediated germline transformation 36
3.2.5 Generation of CRISPR/Cas9 mutant flies 37
3.2.6 Lifespan assay 37
3.2.7 Drug feeding assay 38
3.2.8 Locomotion assay 38
3.2.9 Fertility assay 38
3.2.10 Generation of MARCM clones 38
3.3 Molecular methods 39
3.3.1 Transcriptome analysis 39
3.3.1.1 Collection of *lola-F* mutant embryos 39
3.3.1.2 Collection *of lola-O* mutant embryos 39
3.3.1.3 RNA isolation 39
3.3.1.4 DNase I treatment on isolated RNA 40
3.3.1.5 cDNA library preparation 40
3.3.1.6 Computational analysis 41
3.3.1.7 GO Term method and plot outline 41

3.3.2 Transcriptome analysis of FACS-sorted cells 41
3.3.3 cDNA synthesis and qRT-PCR 42
3.3.4 Targeted DamID 42
3.3.4.1 Sample preparation 42
3.3.4.2 Computational analysis 43
3.4 Immunohistochemistry 43
3.4.1 *In-situ* hybridization 43
3.4.1.1 Preparation of digoxigenin-labeled RNA probes 43
3.4.1.2 *In-situ* hybridization on embryos 44
3.4.1.3 Fluorescent *in-situ* hybridization on third instar larval brains 44
3.4.2 Immunostaining 45
3.4.2.1 Whole mount embryo immunostaining 45
3.4.2.2 Third instar larval brain immunostaining 45
3.4.3 Western blotting 46
3.5. Quantification and statistical analysis 46
3.6 List of antibodies used in this study 47
3.7 List of oligonucleotides used in this study 48
4. Results 53
4.1 CRISPR/Cas9-induced *lola* isoform-specific knock-out 53
4.2 *lola* mutants display diverse phenotypes 57
4.2.1 Proof of principle experiments validate previously identified isoform-specific functions 58
4.3 Lola-A and Lola-H regulate locomotion in opposite directions 62
4.4 Lola-F regulates axon guidance processes at the embryonic ventral midline by activating numerous axon guidance genes 64
4.4.1 Lola-F is required during embryonic development 64
4.4.2 *lola-F* is expressed in neurons and neural stem cells of the developing nervous system 66
4.4.3 Depletion of Lola-F affects axon guidance along the embryonic ventral midline 67
4.4.4 Establishment of neural identity is unaffected in the absence of Lola-F 69
4.4.5 Lola-F is required in neurons to regulate axonal pathfinding along the embryonic ventral midline 71
4.4.6 Majority of Lola isoforms is expressed in neurons during embryonic development 73

4.4.7 None of the remaining neuronal Lola isoforms is essential for axonal guidance in the VNC 75
4.4.8 Lola-F positively regulates several axon guidance genes 77
4.4.9 Futsch is a key target in Lola-F-mediated axonal guidance 79
4.4.10 Ectopic neuronal Lola-F expression has no effect on Futsch levels 82
4.4.11 The loss of Lola-F has no effect on larval brain development 84
4.4.12 Conclusion: Lola-F is the main isoform involved in axonal guidance along the embryonic VNC 86
4.5 The splice variant Lola-O regulates neurotransmitter biogenesis in *Drosophila* 87
4.5.1 CRISPR/Cas9 induced mutations targeting Lola-O 87
4.5.2 *lola-O* mutant flies display a strong degeneration phenotype 89
4.5.3 Lola-O mediates its activity through a neuronal function 91
4.5.4 Lola-O is expressed in a subset of neuronal cells 93
4.5.5 Octopamine is involved in various physiological functions 95
4.5.6 *lola-O* is specifically expressed in octopaminergic neurons in the larval brain 96
4.5.7 Depletion of Lola-O is partially rescued by ectopic octopamine 98
4.5.8 Expressing *lola-O* cDNA in octopaminergic neurons rescues most of *lola-O* mutant defects 100
4.5.9 Depletion of Lola-O affects expression of genes involved in neurogenesis and metabolism 102
4.5.10 *Tbh* levels are reduced in the absence of Lola-O activity 104
4.5.11 Lola-O regulates the octopamine pathway via regulation of *Tbh* 106
4.5.12 Lola-O regulates *Tbh* levels indirectly 107
4.5.13 Conclusion: Lola-O regulates octopamine synthesis via indirect regulation of the enzyme TBH 109
5. Discussion 111
5.1 CRISPR/Cas9 mediated KO to analyse physiological functions *in vivo* 111
5.2 Lola-F regulates axonal pathfinding along the embryonic ventral midline 112
5.3 Lola might acquire novel functions by forming homo- and hetero-dimers 114
5.4 Functional redundancy between Lola isoforms 114
5.5 Cell-type specificity of different Lola isoforms 117
5.6 *lola trans*-splicing is isoform specific 117
5.6 Novel connection between Lola and octopamine synthesis 118

6. Graphical abstract 120
7. Summary / Zusammenfassung 122
7.1 Summary 122
7.2 Zusammenfassung 123
8. Article 124
9. Literature 139
Annex 148
List of reagents used in this study 148
List of enzymes used in this study 149
List of commercially available kits used in this study 150
Abbreviation list 151
Curriculum Vitae 156
Acknowledgement 154

Table of Figures

Figure 1: Proposed model of the *trans*-splicing mechanism on the example of *lola*.....14
Figure 2: Structure of the *lola* locus.....16
Figure 3: Lola regulates embryonic axon guidance along the ventral midline.....21
Figure 4: Scheme of the octopaminergic pathway. 27
Figure 5: CRISPR/Cas9 approach to systematically mutate each Lola isoform. 54
Figure 6: Chromatograms of heterozygous *lola* mutations inducing a frameshift. 56
Figure 7: *lola-B* deficient 3rd instar larval brains appear wildtypic.....58
Figure 8: Scheme of the CRISPR/Cas9 induced mutation targeting *lola-J*. 60
Figure 9: *lola-N* mutant MARCM clones in the *Drosophila* adult brain. 61
Figure 10: Proof of principle experiments to validate the CRISPR/Cas9-mediated *lola* KO screen. 62
Figure 11: *lola-A* and *lola-H* mutant flies reveal locomotion abnormalities in opposing directions. 63
Figure 12: Validation of the *lola-F* specific alleles. 65
Figure 13: *lola-F* mRNA is enriched in the embryonic and larval CNS. 66
Figure 14: Lola-F regulates axon guidance during embryonic development. 68
Figure 15: Proper neural identities are established in *lola-F* mutant embryos. 70
Figure 16: Lola-F regulates embryonic axonal guidance in an isoform-specific manner. 72
Figure 17: *lola* isoform expression in FACS-sorted neurons. 74
Figure 18: The remaining lethal *lola* alleles display a wildtypic VNC. 76
Figure 19: Lola-F positively regulates axon guidance genes. 78
Figure 20: *futsch* levels are reduced in the absence of Lola-F activity. 79
Figure 21: Ectopic Futsch levels partially rescue axonal midline crossing of *lola-F* mutant embryos. 81
Figure 22: Ectopic neuronal Lola-F cDNA expression has no effect on Futsch levels. 83
Figure 23: *lola-F* mutant MARCM clones in third instar larval brains show wildtypic characteristics. 85
Figure 24: The *lola-O* specific mutation depletes the entire ZF domain. 88
Figure 25: Depletion of Lola-O accelerates degeneration of adult flies. 90
Figure 26: Lola-O is required in neurons to regulate various physiological processes. 92

Figure 27: Lola-O is expressed in a specific subset of cells in the third instar larval brain.....94

Figure 28: *Tbh* deficient flies display a phenotype reminiscent to *lola-O* mutants. 95

Figure 29: Lola-O localizes to TBH-positive octopaminergic cells. 97

Figure 30: Ectopic octopamine partially rescues the phenotype associated with the loss of Lola-O.....99

Figure 31: Lola-O activity is required in octopaminergic cells.....101

Figure 32: GO-term analysis for differentially regulates genes in *lola-O* mutant embryos.....103

Figure 33: *lola-O* mutants reveal reduced TBH levels. 105

Figure 34: Ectopic neuronal *Tbh* expression is sufficient to partially rescue the phenotype. 106

Figure 35: Lola-O directly binds and positively regulates *Bacchus*. 108

INTRODUCTION

1. Introduction

While the exact number of human genes is yet to be determined, the current estimation from the Human Genome Project completed in 2003 annotated 22,300 genes (Pertea and Salzberg, 2010). In contrast, the genome of *Drosophila melanogaster* is believed to contain 19,800 genes, while the grape *Vitis vinifera* harbours more than 26,000 genes (Adams, 2000; Vitulo et al., 2014). Thus, comparing the genome sizes between these organisms clearly illustrates that the number of genes alone is not sufficient to explain the complexity of higher organisms. Instead, additional regulatory layers are required to control gene expression (Lander *et al.*, 2001). Among them are mechanisms such as RNA editing, RNA modifications, usage of multiple transcription start and termination sites and alternative pre-mRNA splicing (AS) (Timothy W Nilsen and Graveley, 2010). AS is a process by which exons are alternatively included or excluded from the mature mRNA, leading to the expression of different mRNA variants, which potentially encode for distinct protein isoforms. Hence, AS constitutes an essential mechanism to expand proteome diversity by increasing the number of proteins generated from a single gene (Johnson, 2003; Timothy W. Nilsen and Graveley, 2010).

1.1 Alternative splicing enhances proteome diversity

As every splicing reaction, AS relies on core splicing signals comprising the 5' splice site (SS), the 3' SS and the branch point sequence (BPS) (Robberson, Cote and Berget, 1990; Berget, 1995). These *cis*-acting sequences are present in every intron and are recognized during spliceosome assembly in the splicing reaction. The spliceosome is a large ribonucleoprotein complex that catalyses the splicing reaction. It contains more than 100 proteins and five small nuclear RNAs (snRNA U1-U6) (Nilsen, 2003; Zhou et al., 2002). During pre-mRNA splicing, both 5' and 3' SSs and the BPS associate with snRNAs in a tightly regulated step-wise manner, leading to the release of a lariat-intron and the ligation of both exons (Will and Lührmann, 2011).

AS requires additional regulatory layers to control the inclusion or exclusion of alternatively spliced exons. Factors that coordinate AS include *cis*-acting regulatory sequences and *trans*-acting regulators (Wang and Burge, 2008). A splicing factor may

serve as a positive regulator when bound to a *cis*-regulatory enhancer element, but can also carry a repressive function when bound to a *cis*-acting silencer sequence (Schaal and Maniatis, 1999; Pozzoli and Sironi, 2005; Lim *et al.*, 2011). Intronic and exonic splicing enhancers are typically bound by positive *trans*-acting elements, the serine/arginine-rich (SR) proteins, whereas splicing silencers generally associate with negative regulating factors, such as the heterogenous nuclear ribonucleoproteins (hnRNPs) (Pozzoli and Sironi, 2005). Overall, the interaction between these elements determines the initiation or inhibition of spliceosome assembly on splice sites (Wang and Burge, 2008). Furthermore, secondary pre-mRNA structure can influence these interactions by bringing together splicing elements or by masking *cis*-acting sequences that would otherwise serve as binding elements for a splicing factor (Reid *et al.*, 2009; Warf and Berglund, 2010).

In most organisms, AS happens predominantly as *cis*-splicing, the most commonly used and well-described mechanism (Konarska *et al.*, 1985). Here, exons of one single pre-mRNA molecule are ligated to form the mature mRNA. With recent advances in next generation sequencing, however, it became apparent that its counterpart, the *trans*-splicing process, is used much more frequently than previously assumed (Cáceres and Kornblihtt, 2002; Horiuchi and Aigaki, 2006). In *trans*-splicing, exonic sequences from two different pre-mRNA transcripts are fused to form the mature mRNA, with exons deriving either from the same (intragenic *trans*-splicing) or two otherwise unrelated genes (intergenic *trans*-splicing).

1.2 Alternative *trans*-splicing occurs in different species

Trans-splicing has very long been considered to be specific of lower eukaryotes, such as nematodes and trypanosomes (Sutton and Boothroyd, 1986; Krause and Hirsh, 1987). Recent innovations in transcriptome sequencing, however, also enabled the identification of *trans*-spliced RNA in higher organisms. Intriguingly, *trans*-splicing has been shown to give rise to oncogenic fusion transcripts in human, suggesting that *trans*-spliced RNA may precede chromosomal rearrangement observed in human tumours (Kowarz *et al.*, 2011). More recently, Wu et al. identified a *trans*-spliced non-coding RNA that is required to maintain pluripotency in human embryonic stem cells

(Wu *et al.*, 2014). This non-coding RNA is highly abundant in pluripotent cells in comparison to differentiated cells. Its *cis*-spliced counterpart is equally expressed in both cell types, suggesting that an active mechanism controls *trans*-splicing during cell differentiation. Taken together, these findings suggest that the mechanism of *trans*-splicing is more abundant than previously considered and may even carry essential physiological functions in higher organisms.

While methods to identify *trans*-spliced RNA have improved over the years, the underlying mechanism and its regulating factors in higher organisms remain to be determined. In contrast, *trans*-splicing has been well characterized in trypanosomes, in which all pre-mRNAs are spliced in *trans*. In this case, the splicing reaction involves a 39-nucleotide spliced leader (SL) sequence that is *trans*-spliced 5' to each mRNA precursor (Boothroyd and Cross, 1982). In addition, *trans*-splicing is also used extensively in the nematode *C. elegans*, where 62 % of transcripts are processed by *trans*-splicing of a 22-nucleotide SL exon to the 5'-end of the pre-mRNA (Blumenthal, 2012). More precisely, the SL partially replaces the native 5' untranslated region (UTR), a process that was recently shown to positively influence translational efficiency (Yang *et al.*, 2017).

1.3 *Trans*-splicing in *Drosophila* relies on the RNA sequences TSA and TSB

In *Drosophila*, about 20-37% of multi-exon genes are alternatively spliced (Gibilisco *et al.*, 2016). While males generally express more number of genes, AS is more abundant in female flies. The vast majority of alternatively spliced genes are processed via *cis*-splicing. The knowledge about the existence of *trans*-splicing in *Drosophila* was limited until recently to only two loci, *longitudinals lacking* (*lola*) and *modifier of mdg4* (*mod(mdg4)*). Both genes are among the most complex ones found in this model organism and share common features with respect to their gene architecture. They span over large regions on the genome and contain a constitutive N-terminal region combined with alternatively spliced C-terminal exons. More

recently, mRNA-sequencing of *Drosophila* hybrids identified about 80 additional potentially *trans*-spliced RNA (McManus *et al.*, 2010). The genome of *Drosophila* harbours species-specific single nucleotide polymorphisms (SNPs), which facilitates the tracking of *trans*-splicing in *Drosophila* hybrids by identifying the chromosomal origin of individual exons. All validated *trans*-spliced RNA harbour complex gene architectures, suggesting that *trans*-splicing may facilitate the expression of genes whose structure would otherwise create challenges to the transcription and *cis*-splicing machineries.

While *trans*-splicing was considered for a long time an experimental artefact arising from strand-switching of polymerases during cDNA synthesis, interallelic complementation assays, however, were able to experimentally validate *lola trans*-splicing *in vivo* for different isoforms (Horiuchi, Giniger and Aigaki, 2003). The same study demonstrated that chromosomal pairing is crucial for *lola trans*-splicing, implying an important role of chromatin structure in this process.

Only two years ago, Gao and colleagues made important discoveries helping to understand the *trans*-splicing process by identifying two intronic RNA sequences, named TSA and TSB, which promote *trans*-splicing in *Drosophila* (Figure 1; Gao et al., 2015). The 13-nucleotide motif TSA is located in the intron downstream of the last *lola* constitutive exon. It recruits and base-pairs with the 5'-end of the U1 snRNA and thus initiates the binding of U1 small nuclear RNP (snRNP). This established RNA-protein interaction is sufficient to initiate the *trans*-splicing process. In contrast, TSB increases efficiency of the splicing reaction by forming a conserved secondary structure, which acts as a *trans*-splicing enhancer. The subsequent recruitment of spliceosomal factors is predicted to initiate a bridging interaction between the 3'-transcript and the TSA/TSB-containing intron, leading to the formation of a Y-shaped intermediate. The exact molecular mechanism underlying this reaction is however unclear. In particular it remains to be characterized how the 3'-transcript is spliced prior its ligation with the constitutive region.

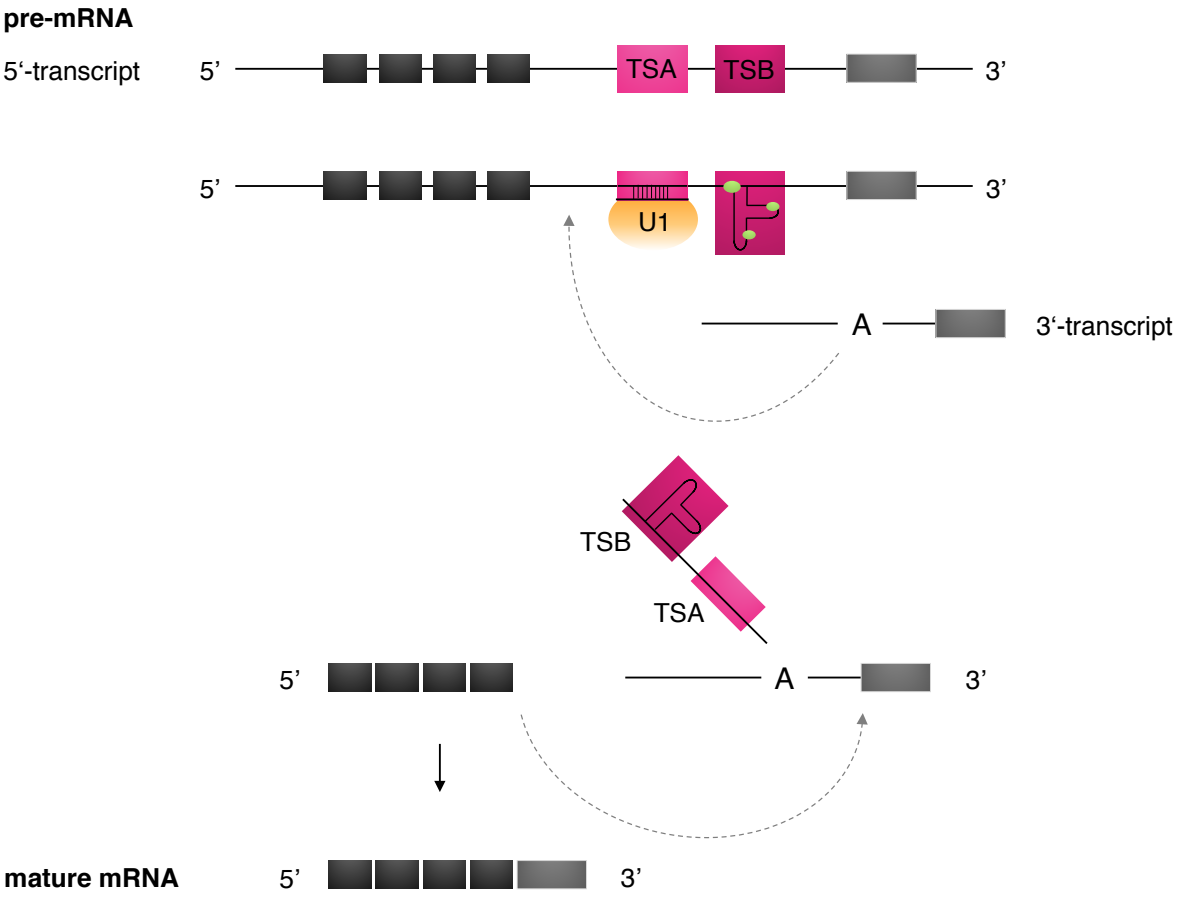

Figure 1: Proposed model of the *trans*-splicing mechanism for *lola pre*-mRNA.

The *trans*-splicing RNA motifs TSA and TSB are located in the last constitutive 5’ intron. TSA is sufficient to promote *trans*-splicing in *Drosophila* by recruiting and binding the U1 snRNP. TSB forms a conserved secondary structure that enhances the *trans*-splicing reaction, resulting in the formation of a Y-structured intermediate. Black boxes indicate constitutive exons, grey boxes depict isoform-specific C-terminal exons. Green circles indicate spliceosomal factors. “A” highlights the BPS. Model adapted from Gao et al., 2015.

1.4 The complex *lola* locus encodes for distinct BTB-ZF protein isoforms

First identified in 1994 by Giniger and colleagues, *lola* stood up by its unusually complex architecture for *Drosophila.* The *lola* locus spans over 61 kb on the genome and comprises 32 exons, classified into four 5’-UTR exons, five N-terminal constitutive exons and 23 C-terminal isoform specific exons (Figure 2; Crowner et al., 2002; Giniger et al., 1994; Goeke et al., 2003; Madden et al., 1999). By a combination

of alternative *cis*- and *trans*-splicing, about 80 different mRNA isoforms are expressed, which encode for 20 known protein isoforms that are named Lola-A to Lola-T. Each *lola* mRNA isoform comprises one 5'-UTR exon, all four constitutive exons and one or two C-terminal isoform specific exons.

The N-terminal constitutive region encodes for a Broad-Complex, Tramtrack and Bric a brac (BTB) domain, which has functionally been shown to initiate protein homo-, hetero- and multi-dimerization (Bardwell and Treisman, 1994; Bonchuk *et al.*, 2011). Previous evidences suggest that Lola isoforms might interact with each other via this BTB domain. Yeast two hybrid assays confirmed homo-dimerization for the Lola N-terminus (Giot *et al.*, 2003). Additionally, the splice variant Lola-F was shown to interact with at least two other Lola isoforms during embryonic development (Zhang *et al.*, 2003).

In *Drosophila* as well as in human, approximately 25 % of BTB proteins harbour an additional zinc finger (ZF) domain (Cavarec, Jensen, Casella, S. a Cristescu, *et al.*, 1997; Stogios *et al.*, 2005; Erin L. Davies *et al.*, 2013). Interestingly, the majority of Lola isoforms belongs to this subgroup of BTB-ZF proteins. More precisely, 17 isoforms contain putative ZF motifs encoded by their isoform specific C-terminal exon, while three isoforms (Lola-A,-G,-M) lack any recognizable C-terminal motif.

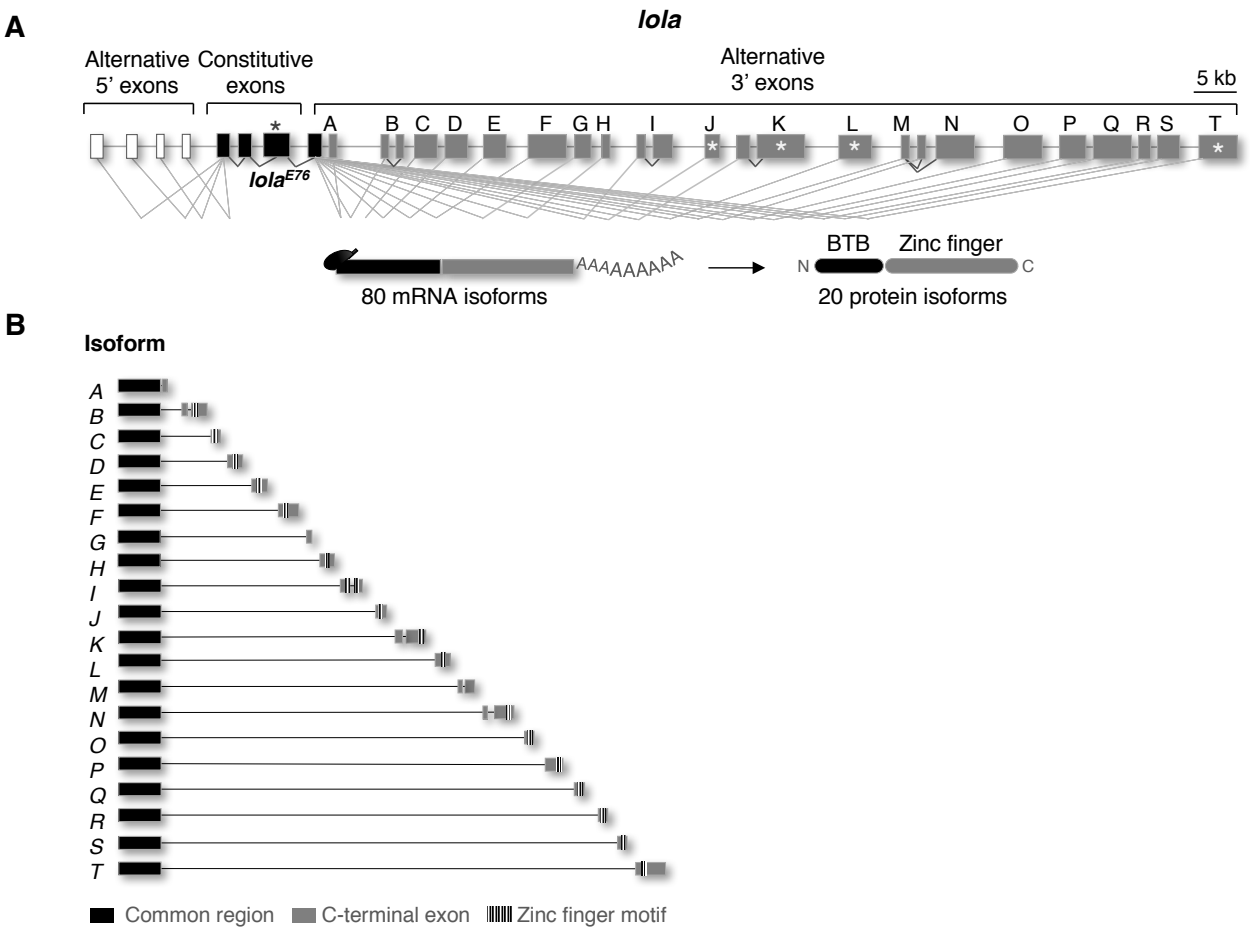

Figure 2: Structure of the *lola* locus.

(**A**) *lola* comprises 32 exons including 5' UTR exons (white box), constitutive exons (black) and 3'-alternative exons (grey). 80 mRNA isoforms encode for 20 protein isoforms, each sharing an N-terminal BTB domain (black) but hold isoform-specific exons encoding for a C-terminal zinc-finger domain in 17 isoforms. Previously characterized mutations are marked by an asterisk. (**B**) Scheme of the 20 *lola* isoforms (Lola-A-Lola-T). C-terminal exons are sequentially located on the genome. ZF motifs are depicted in stripes.

ZF motifs are well known for their regulatory role in transcription, which is acquired by direct binding to nucleotides (Elrod-Erickson *et al.*, 1996). Typically, ZFs are characterized by one or two Cysteines (Cys) found in close proximity of two Histidines (His), which fold into the characteristic α-helix that is packed against two antiparallel ß-strands (Lee *et al.*, 1989). Crucial for the stability of a ZF protein is an integrated zinc ion that coordinates the formation of the typical ZF-tertiary structure. ZF variability is obtained by positional combinations of Cys and His residues, resulting in different kinds of ZF motifs, such as the classical types Cys_2His_2 (C_2H_2), $Cys_2HisCys$ (C_2HC), or Cys_2His (C_2H) (Krishna, Majumdar and Grishin, 2003). In addition, binding specificity is expanded by the pair-wise presence of distinct ZFs,

leading to numerous possible ZF combinations. Overall, ZF domains exhibit less sequence conservation compared to other structural motifs, suggesting that BTB-ZF proteins represent transcriptional regulators with the ability to bind unique consensus sequences (Bardwell and Treisman, 1994; Bonchuk *et al.*, 2011).

The majority of Lola isoforms harbour tandem ZFs of the DNA-binding types C_2HC-C_2H_2 (Lola-B-D,-F,-H,-J-L,-O-R and -T) and C_2HC-C_2HC (Lola-I and Lola-N). Single-ZF proteins are found in isoforms Lola-E and -S, both harbouring a C_2H_2-ZF type (Ohsako *et al.*, 2003). Further specificity of Lola ZFs is obtained by variations in isoform-specific linker sequences. Slight variations in linker sequences were shown to alter the binding specificity of ZF motifs, suggesting that individual Lola isoforms are capable of binding unique DNA-consensus sequences (Fukushima, Yoshida and Takatsuji, 2012). Previously performed bacteria one-hybrid assays support this hypothesis and identified unique putative consensus sequences for distinct Lola isoforms (Enuameh *et al.*, 2013). Moreover, sequence comparisons of Lola ZFs between *Drosophila melanogaster* and *Anopheles gambiae* reveal a high level of conservation for some isoforms, suggesting that individual Lola functions might be evolutionary conserved among insects (see Table 1).

Isoform	ZF type	ZF identity between *D. melanogaster* & *A. gambiae*
Lola-F	C_2HC-C_2H_2	81%
Lola-I	C_2HC-C_2HC	87%
Lola-K	C_2HC-C_2H_2	90%
Lola-L	C_2HC-C_2H_2	94%
Lola-N	C_2HC-C_2HC	74%
Lola-O	C_2HC-C_2H_2	88%
Lola-T	C_2HC-C_2H_2	90%

Table 1: ZF-sequence identity of the most conserved Lola isoforms between *Drosophila melanogaster* and *Anopheles Gambiae*. Data was obtained from Goeke et al., 2003

1.5 Lola functions as a transcription factor during *Drosophila* development

The hypothesis that Lola directly binds DNA and thereby regulates gene expression was first evidenced by the discovery that Lola transcriptionally represses the *copia* retrotransposon in the CNS during embryonic development (Cavarec, Jensen, Casella, S. A. Cristescu, *et al.*, 1997). In contrast, *lola* appears to have an opposite function in the gonads since *lola* mutants have decreased *copia* transcript levels in this tissue. These results suggest that Lola is also able to act as a positive transcriptional regulator in some tissues, even though an indirect effect cannot be ruled out.

Given the structural variability of Lola isoforms, specificity might partially be obtained by distinct tissue- and cell-type specific expressions (see Table 2). While few isoforms are expressed ubiquitously during embryonic development, *in-situ* hybridizations revealed specific tissue-specific expression for the majority of isoforms, suggesting that individual Lola isoforms might function in a cell-type specific manner during embryonic development (Goeke *et al.*, 2003).

Isoform	Tissue-specific expression	Cell-type specific expression
Lola-A	Not described	
Lola-B	CNS	Tracheal pits
Lola-C	Ectoderm	Cells in ventral neurogenic region; tracheal pits
Lola-D	CNS	Cells in ventral neurogenic region
Lola-E	CNS, Ectoderm, Muscle	Ventral furrow; dorsal layer in CNS
Lola-F	CNS, Ectoderm	
Lola-G	Not described	
Lola-H	Mesoderm	Cells in ventral neurogenic region; ventral furrow
Lola-I	CNS, Gut, Epithelium	Dorsal layer in CNS
Lola-J	Ectoderm	Tracheal pits
Lola-K	CNS, Epithelium	
Lola-L	CNS, Muscle	
Lola-M	Not described	

Lola-N	Ubiquitous; CNS (Southall et al., 2014)	Neurons (Southall *et al.*, 2014)
Lola-O	Not described	
Lola-P	Ubiquitous	Cells in dorsal epidermis; ventral furrow
Lola-Q	CNS, Muscle, Gut	
Lola-R	CNS, Muscle, Gut	Gonads
Lola-S	CNS, Muscle	
Lola-T	CNS, Mesoderm	Cluster of brain cells; abdominal histoblasts; imaginal discs; somatic gonadal precursors (Tripathy *et al.*, 2014)

Table 2: Tissue- and cell-type-specific expression of Lola isoforms. If not stated otherwise, data was obtained by *in-situ* hybridization from Goeke et al., 2003.

1.6 The transcription factor Lola regulates nervous-system development

Although Lola isoforms harbour unique ZF domains with distinct binding motifs (Enuameh *et al.*, 2013), Lola ZFs reveal a high homology among their linker sequences, raising the question about potential functional redundancies between isoforms (Ohsako *et al.*, 2003). Accordingly, Wissel et al. (2016) recently found that two Lola isoforms act redundantly during larval neuroblast (Nb) development (Wissel *et al.*, 2016). RNAi mediated double knock-down (KD) of Lola-F and Lola-L lead to an over-proliferation of Nbs, while single KD of either of these isoforms had no effect. While the underlying molecular mechanism in the regulation of Nb proliferation has not been analysed further, these findings demonstrate for the first time that Lola splice variants can carry physiological roles in a redundant manner.

Lola controls axonal guidance along the embryonic ventral midline

Lola was first named after its regulatory role in axon growth and guidance during embryonic development (Figure 3; Crowner et al., 2002; Goeke et al., 2003; Horiuchi et al., 2003; Ohsako et al., 2003). While numerous studies have characterized genes associated with axon growth and guidance, the molecular mechanism underlying this complex process in *Drosophila* is still not fully understood. The *Drosophila* embryonic ventral nerve cord (VNC) consists of segmentally repeated arrangements of axonal projections that, similar to vertebrates, organize into ipsilateral and contralateral projections. One well-characterized axon-guidance gene is *frazzled* (*fra*), which encodes for a receptor present on the surface of axons in the CNS. Midline-glia-secreted Netrins (NetrinA and NetrinB), attract axons by activating the Frazzled receptor, thereby steering axonal projections along the embryonic midline (Harris, Sabatelli and Seeger, 1996; Kolodziej *et al.*, 1996). Furthermore, *Drosophila* motoraxons harbour three Robo receptors that bind midline secreted Slit, leading to repulsion of these axons from the ventral midline (Kidd *et al.*, 1998; Brose *et al.*, 1999). Previous studies showed that Lola positively regulates expression levels of both genes, *robo* and *Slit* (Crowner et al., 2002). In the absence of Lola, *Slit* expression in midline glia was reduced by about 50 %, while ectopic Lola expression in the ventral midline was sufficient to elevate Slit levels. Furthermore, Robo levels were reduced in the absence of all Lola isoforms and the receptor re-localized to commissural axon tracts from which it is generally excluded. The reduced *Slit/robo* levels in *lola* null mutant embryos subsequently perturbs axon guidance cues along the ventral midline and leads to multiple aberrant axonal midline crossings (**Figure 3**). Another key Lola target is the actin-nucleation factor Spire, which is essential to control axonal growth (Gates, Kannan and Giniger, 2011). Microarray assays using *lola* null mutant embryonic RNA revealed increased *spire* transcript levels, suggesting that Lola negatively regulates *spire* expression to ensure proper axon extensions.

In conclusion, the combinatorial effect of Lola on Slit, Robo and Spire levels is believed to account for the severe axonal guidance defects observed under the loss of all Lola isoforms. However, due to the complexity of the *lola* locus, it has not been possible to assign this regulatory role to one individual Lola isoform, raising the question

whether a single or a combination of Lola isoforms account for the axon guidance function during *Drosophila* embryogenesis.

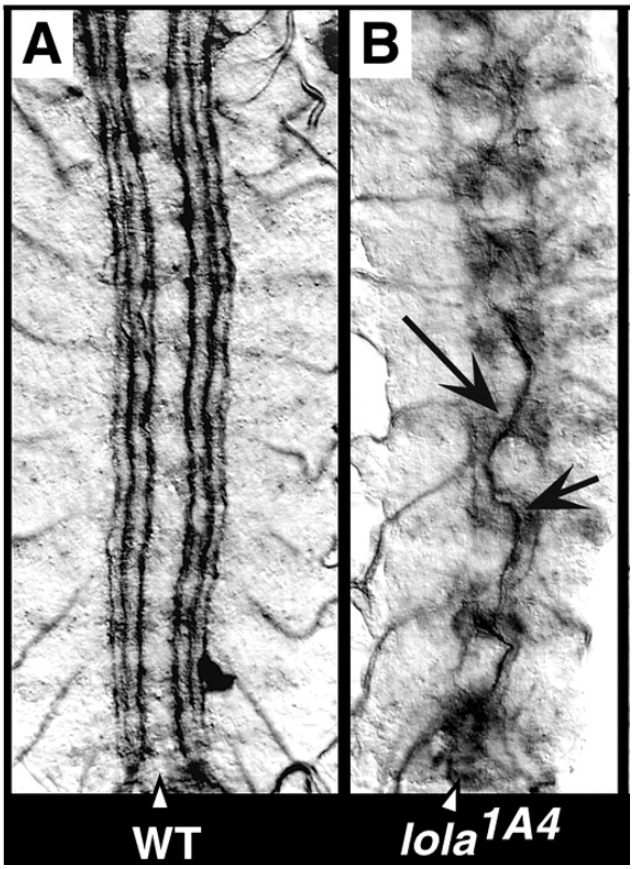

Figure 3: Lola regulates embryonic axon guidance along the ventral midline.

(A) Anti-Fasciclin2 immunostaining shows wildtype axonal tracts running along the ventral midline in three parallel bundles. Axons do not cross the ventral midline. (B) *lola*^{1A4} null mutant embryos display axonal midline crossings and stalled axon extension, leading to a disrupted VNC. Ventral view on stage 15 embryos, anterior is top. Arrowheads depict embryonic ventral midline. Obtained and modified from Goeke et al., 2003.

Distinct Lola splice variants regulate peripheral ISNb growth and guidance

While majority of Lola studies have been performed using *lola* null mutant alleles that carry a mutation in the BTB-encoding constitutive region, advances in genome engineering and random mutagenesis allowed functional characterization of few distinct isoforms.

Until recently, four Lola isoforms (Lola-J, K, -L, and -T) were shown to carry essential roles in development of the nervous system. In *Drosophila*, 36 motoneurons in each hemisegment come together to form six major nerves that target and innervate different muscle regions. Among them is the well-characterized intersegmental nerve b (ISNb), which is formed by four motoneurons and innervates the ventral muscles of the body wall by four neuromuscular junctions (NMJs) (Landgraf and Thor, 2006). Intriguingly, three of the characterized Lola isoforms regulate the development and guidance of the ISNb. Mutations targeting exons Lola-K and -L, respectively, lead to stalled ISNb growth accompanied by perturbed formation of NMJs indicating that these isoforms regulate similar processes in a non-redundant manner (Goeke *et al.*, 2003). The absence of these isoforms is homozygous lethal by the end of embryogenesis, which possibly arises from impaired peripheral ISNb muscle innervations and subsequent perturbed locomotion. Last year, Peng et al. (2016) described a role for another Lola isoform, Lola-J, in ISNb guidance via negative regulation of the cGMP-dependent protein kinase (PKG) (Peng *et al.*, 2016). The second messenger PKG was previously reported to function in axonal pathfinding by establishing guidance cues for axon growth through different intracellular signalling pathways (Renger *et al.*, 1999). Co-immunoprecipitation (Co-IP) experiments revealed an interaction between PKG and Lola-J via its C-terminal ZF domain, suggesting that Lola-J directly binds and represses PKG to ensure ISNb axonal guidance during embryonic development.

Additional roles of Lola in the nervous system

The predominant role of Lola in axonal pathfinding is further emphasized by its function in olfactory projection neuron identity and targeting specificity (Spletter *et al.*, 2007). In adult flies, the olfactory system comprises projection neurons (PNs), which send their dendrites to single glomeruli in the antenna lobe (AL). For further processing of olfactory information, axons are recruited from the AL to higher olfactory centres, a process that is likely specified by the expression of PN cell-surface molecules that determine wiring specificity (Jefferis *et al.*, 2005). Investigations on $lola^{E76}$ null mutant clones identified Lola as an essential regulator of wiring specificity

of axons and dendrites of PNs during pupal development (Spletter *et al.*, 2007). In the absence of Lola, PNs have dendritic and axonal targeting defects and subsequently fail to innervate their corresponding glomeruli in the AL. Although further studies are needed to fully understand how Lola regulates axon guidance of PNs, it is assumed that Lola transcriptionally represses multiple genes controlling PN identity and wiring specificity. *In-situ* hybridizations revealed moderate expression of most *lola* isoforms in the adult AL, thus making it difficult to assign this function to one specific Lola isoform.

In 2014, Southall and colleagues generated $lola^{E76}$ null mutant MARCM clones and discovered subsequent tumour formations in the larval brain (Southall *et al.*, 2014). In the absence of all Lola isoforms, Nb genes were up-regulated in postmitotic neurons, leading to the de-differentiation of those neurons and a subsequent reversion into Nbs. Ectopic neuronal Lola-N expression was sufficient to prevent tumour growth in $lola^{E76}$ null mutant clones, suggesting a potential role for this isoform in maintaining neuronal identity. In order to identify direct target genes of Lola-N, a specific approach called DNA adenine methyltransferase identification (DamID) was performed. DamID was originally developed to identify protein-DNA binding *in vivo* by the group of van Steensel and Henikoff (van Steensel and Henikoff, 2000; Marshall *et al.*, 2016). In brief, a protein of interest is fused to an *E. coli* DNA adenine methyltransferase (Dam), which methylates adenine in the *GATC* sequence context. The binding specificity is provided by the protein of interest. While this technique is useful to identify target genes it suffers from low sequence resolution. Nevertheless, by performing the DamID for Lola-N, Southall and colleagues found predominant binding to Nb genes and cell-cycle genes and suggested that Lola-N directly binds and represses Nb genes in neurons. Furthermore, they determined a Lola-N specific consensus sequence as *CGATCG*. Of note, this sequence is highly similar to the consensus sequence of the Dam, raising the possibility of a potential technical bias. Together, this work demonstrates a crucial function for Lola in neurogenesis. Perhaps more importantly, this study was the first to demonstrate that Lola acts as a transcription factor that regulates gene expression by direct binding to DNA.

1.7 Lola acts beyond the nervous system

Lola isoforms were shown to control multiple aspects of gonad formation and maintenance. Gonads comprise two cell types, the germ cells and somatic cells, termed SGPs, which create a niche to provide survival signals to the germ cells (Boyle and DiNardo, 1995; Richardson and Lehmann, 2010). Following specification, SGP clusters encounter migrating germ cells and both cell types remain loosely associated until SGPs fuse and surround individual germ cells in a process named 'ensheathment' to form an elongated gonad. Subsequently, gonads round up in a so-called 'compaction' step, leaving the embryonic gonad with an appearance of a tight ball-like structure. During this step-wise mechanism, Lola-T is expressed in SPGs and regulates SGP cluster formation, the germ cell ensheathment and the final gonad compaction (Tripathy *et al.*, 2014). In *lola-T* mutant embryos, the mechanism of gonad formation is perturbed on both the compaction and ensheathment level, suggesting a crucial but yet not fully understood role for Lola-T in gonadal development.

After gonad formation, isoforms Lola-K and Lola-L were both reported to be required cell autonomously for germline stem cell (GLC) identity in the *Drosophila* testis. GLCs were rapidly lost in profit of differentiation in the absence of either Lola-K or Lola-L activity, confirming a similar but non-redundant function for both isoforms in maintaining stem-cell identity in the *Drosophila* germline.

In addition to this described male-specific function of Lola-K and Lola-L, Lola plays essential roles in female ovarian maturation processes. During oogenesis, nurse cells undergo regression after dumping their cytoplasmic contents into the oocyte (Cavaliere, Taddei and Gargiulo, 1998; NEZIS *et al.*, 2000). Apoptosis of nurse cells is developmentally regulated and is accompanied by highly condensed chromatin (NEZIS *et al.*, 2000). In $lola^{E76}$ null mutant germline clones, nurse cells exhibit abnormal nuclear organization with diffused chromatin that is unable to condense (Paige Bass, Cullen and McCall, 2007). As a consequence, nurse cell apoptosis is blocked in the absence of Lola, suggesting that Lola functions in completing chromatin condensation in nurse cells, a crucial process during programmed cell death in the

ovary. The identification of Lola isoform(s) required in this process remains to be determined.

Moreover, Lola is involved in the *Drosophila* eye development, where it regulates two binary cell-fate decisions guided by Notch inductive signalling (Zheng and Carthew, 2008). The *Drosophila* compound eye comprises 800 light-sensing cell-clusters, so-called ommatidia, which itself contain eight photoreceptors (R1-R8) (Silver and Rebay, 2005). Zheng and Carthew showed that Lola is expressed in all photoreceptor cells but is required cell-autonomously in R3 for its specification. Likewise, Lola promotes R7 fate by antagonizing Notch-depended gene expression. In the absence of Lola, ommatidia display a reversed polarity with photoreceptors of abnormal shapes and sizes, while most ommatidia miss both photoreceptor types R3 and R7.

Lola further controls the expression of Glutamate receptor (GluR) and p-21 activated kinase (PAK) at the NMJ (Fukui et al., 2012). Upon Lola KD, postsynaptic quantal size and *GluR* abundance is decreased. Interestingly, synaptic-response tests showed that increased neuronal activity leads to a reduction in *lola* mRNA levels. Based on these results, Fukui and colleagues proposed that Lola coordinates expression of multiple postsynaptic components at the NMJ in a dynamic manner to ensure proper signal transmission upon stimulation.

During early development, the highly conserved isoform Lola-F was shown to interact with the histone H3S10 kinase JIl-1 (Zhang *et al.*, 2003). Lola-F localizes to the nucleus where its activity is developmentally regulated and restricted to early embryogenesis. Co-immunoprecipitation (Co-IP) assays identified a direct interaction between Lola-F and JIL-1. The molecular function of JIL-1 was determined to the maintenance of euchromatic chromosomal regions by antagonizing Su(var)3-9-mediated heterochomatinization (Boeke *et al.*, 2010), suggesting that Lola-F might coordinate the establishment of an epigenetic state compatible with gene expression via interaction with JIL-1.

Altogether, previous work demonstrated the involvement of Lola in multiple developmental processes. Currently, specific functions have been assigned for six

isoforms (Lola-F, -J, -K, -L, -N and -T), raising the question about the physiological function of the remaining 14 Lola isoforms. Previous findings demonstrated distinct tissue-specific roles for at least two isoforms, indicating that some Lola isoforms have pleiotropic functions. In conclusion, Lola is amongst the most complex loci in *Drosophila* and we are only starting to unveil its extent of complexity by deciphering isoform-specific functions *in vivo*.

1.8 Octopamine regulates various processes in *Drosophila*

The proper regulation of nervous-system dependent processes is essential for living organisms in order to maintain homeostasis of distinct cellular processes, including hormone production and control of motor functions, involving muscle contraction, vision, and memory. Precise regulations of motor functions requires a fine-tuned control of neurotransmitter secretion, a process that when impaired has been linked to severe human diseases, such as neurodegeneration, autism and seizure disorders (Francis PT, 2005; Werner and Coveñas, 2011; Robertson, Ratai and Kanwisher, 2016).

The *Drosophila* monoamine octopamine is the homologue of the human noradrenaline and norepinephrine. It can act as a neurotransmitter, neurohormone and neuromodulator to regulate various physiological functions (Wierenga and Hollingworth, 1990; Roeder, 1999; Selcho *et al.*, 2012; Zhou *et al.*, 2012; Yang *et al.*, 2015b; Kurz *et al.*, 2017). The synthesis of octopamine begins with the modification of tyrosine into tyramine, a reaction that is catalysed by the enzyme Tyrosine-decarboxylase 2 (Tdc2; **Figure 4**). While tyramine can act on its own as a neurotransmitter in locomotion control (Pflüger and Duch, 2011, Ryglewski, 2017), majority of this molecule is hydrolysed into octopamine via activity of the Tyramine-ß-hydroxylase (TBH) (Monastirioti, Linn and White, 1996).

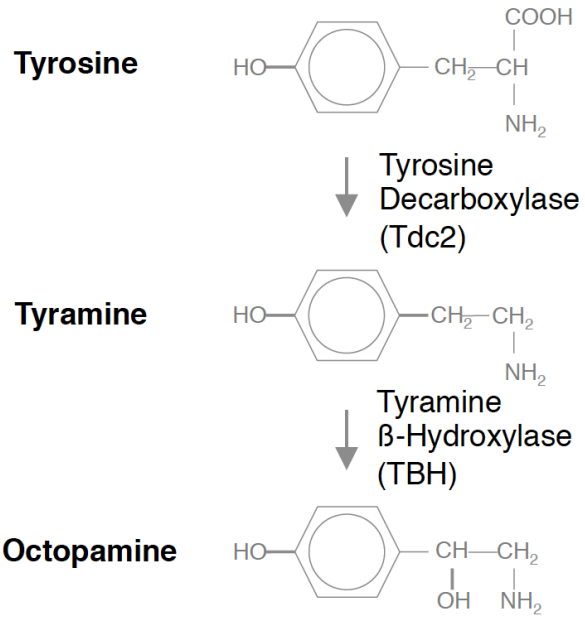

Figure 4: Scheme of the octopaminergic pathway.

Synthesis of octopamine starts with tyrosine, which is decarboxylated into tyramine by the Tyrosine Decarboxylase 2 (Tdc2). Tyramine is hydrolysed into octopamine by the Tyramine-ß-Hydroxylase (TBH).

In *Drosophila,* octopamine regulates a vast variety of behaviours and physiological responses. Octopamine was shown to desensitize sensory inputs, to regulate arousal, initiation and maintenance of rhythmic behaviours, to mediate learning, to control oviposition and to influence longevity (Hammer and Menzel, no date; Menzel *et al.*, 1996, 1999; Schwaerzel *et al.*, 2003; Li *et al.*, 2016). The synthesis of octopamine begins during late embryonic development (stage 14), in a total number of 27 ventral unpaired median (iVUM) neurons along the embryonic midline (Wheeler et al., 2008). Later in development, approximately 42 octopaminergic neurons regulate octopamine synthesis in the larval brain (Selcho *et al.*, 2012). Larval octopaminergic neurons are categorized into type II motorneurons, which extend their axons to form synaptic connections with muscles via type II boutons (Koon and Budnik, 2012). While type I boutons are typically larger in size and use glutamine as their neurotransmitter, type II synapses have smaller boutons containing a variety of neurotransmitters (Atwood, Govind and Wu, 1993). Upon loss of TBH, the number of type II boutons and the synaptic strength of octopaminergic neurons are drastically reduced, which results in larval locomotion defects (Koon *et al.*, 2010). The regulatory

role of octopamine goes beyond larval stages by coordinating oviposition in female adult flies (Monastirioti, Linn and White, 1996; Kurz *et al.*, 2017). Perturbation of octopamine levels results in female sterility due to egg retention in the oviduct, a phenotype that was recently described to be mediated by misexpression of peptidoglycan in octopaminergic neurons (Monastirioti, Linn and White, 1996; Kurz *et al.*, 2017). Peptidoglycan, a polymer that forms the cell wall of most bacteria, initiates an immune response upon bacterial infection and thus introduces behavioural changes including egg retention (Bosco-Drayon *et al.*, 2012). Kurz and colleagues suggest a model in which bacterial infections lead to reduced octopamine levels, which in turn induces egg-retention (Kurz *et al.*, 2017). While the precise underlying effect of peptidoglycan expression on octopamine signalling is not entirely understood, this study takes a step forward in deciphering the diverse physiological effects of octopamine on *Drosophila* behaviour.

As a homologue to the human norepinephrine, which is also known to be the "fight-or-flight-hormone", octopamine synthesis drastically increases in *Drosophila* upon starvation-caused stress induction (Yang *et al.*, 2015a). Irrespective of this, only little is known about the dynamics underlying octopamine synthesis in insects. Studies on honeybees have shown that octopamine synthesis increases with age, which might also be the case for *Drosophila* and other invertebrates (Harris and Woodring, 1992). While approaches have been made in characterizing downstream processes of octopamine-related functions, little is known about how octopamine synthesis is regulated on the transcriptional level. Nonetheless, the yet poorly characterized nuclear protein Bacchus (Bacc) was shown to negatively regulate *Tbh* expression (Chen *et al.*, 2013). Studies on *Bacc* mutants revealed that the heterozygous loss of *Bacc* elevates *Tbh* expression by 1.5-fold, while *Tdc2* levels remain unaffected. Homozygous mutant flies displayed an even more drastic increase in *Tbh* levels by 3-fold, which is accompanied by a rise in octopamine levels of almost 2-fold. These findings demonstrate that Bacc expression requires a fine-tuned regulation to guarantee accurate synthesis octopamine.

Octopamine transmits its action through four different G-protein coupled receptors, the Octopamine receptor in mushroom bodies (Oamb), Octopamine ß1 receptor

(Octß1R), Octopamine ß2 receptor (Octß2R) and Octopamine ß3 receptor (Octß3R) (Evans and Robb, 1993; Elphick and Egertova, 2001; Maqueira, Chatwin and Evans, 2005; El-Kholy *et al.*, 2015; Yang *et al.*, 2015b). The function of Octß1R receptors is mediated via an increase in intracellular calcium and has been shown to coordinate rhythmic behaviours (Elphick and Egertova, 2001; Balfanz *et al.*, 2005; Maqueira, Chatwin and Evans, 2005). Oct2ßR, in turn, regulates neuromuscular functions and ovulation by increasing cyclic adenosine monophosphate (cAMP) levels (Evans and Robb, 1993; Li *et al.*, 2015). The most abundant and best-studied receptor is Oamb, whose role has been described in several octopamine-regulated functions such as learning, ovulation, the starvation-induced stress response and male courtship behaviour (Lee, Rohila and Han, 2009; Zhou *et al.*, 2012; Luo *et al.*, 2014).

Taken together, octopamine is involved in a large array of behaviours and can superficially be considered equivalent to norepinephrine in vertebrates, to which it shares functional but also structural similarities. Both molecules are involved in fight-or-flight-responses, motivational behaviours and aggression. However, it is not yet entirely clear how expression of the two key enzymes, TBH and Tdc2, is regulated and which factors control octopamine synthesis in a spatio-temporal manner.

AIM OF THIS STUDY

2. Aim of this study

lola is amongst the most complex genes found in *Drosophila melanogaster*, encoding 20 known protein isoforms that have essential roles in embryonic nervous system development. First identified in 1994, Lola has been shown to fulfil a crucial regulatory role in axonal pathfinding in the *Drosophila* embryo. The complexity of this BTB-ZF transcription factor was further emphasized by recent findings revealing various nervous-system dependent and independent functions in a tissue- and cell-type specific manner. At the beginning of my PhD, only two Lola isoforms were characterized in overtaking distinct physiological functions during embryonic development. Most studies were performed using *lola* null mutant alleles, making it difficult to decipher isoform-specific Lola functions in the absence of distinct mutant alleles.

With the CRISPR/Cas9 system, a novel tool has been established to sequence-specifically alter the genome, which subsequently allows to generate mutations for distinct protein isoforms. Taking advantage of this novel powerful tool, my study aimed to generate loss-of-function mutations for each Lola isoform in order to physiologically and molecularly characterize Lola isoform-specific functions *in vivo*.

MATERIALS

&

METHODS

3. Materials & Methods

3.1 Buffer compositions

PBS (10x)	NaCl 1.37 M; KCl 27 mM; KH_2PO_4 11.5 mM; Na_2HPO_4 63 mM
DNA lysis buffer (1x)	100 mM Tris-Hcl pH7.5; 100 mM EDTA; 100 mM Nacl; 0.5% SDS
Larval CNS fixation buffer (1x)	8 g PFA; 5 µl NaOH 10 M; 100 ml sodium phosphate buffer (0.2M, pH 7.4); adjust to 200 ml with H_2O; heat to 60°C, filter and store at -20°C
Sodium phosphate buffer (0.2 M, pH 7.4)	27.55 g Na_2HPO_4; 6.24 g NaH_2PO_4; adjust to 1 l with H_2O; adjust pH 7.4
Embryo fixation solution (1x)	400 µl 1xPBS; 500 µl n-heptane; 100 µl 37% formaldehyde
HB4-hybridization buffer (1x)	50 ml formamide; 25 ml 20xSSC; 200 µl Heparin (50 mg/ml); 100 µl Tween20; 500 mg Torula Yeast RNA extract; adjust to 1 l with H_2O
SSC buffer (20x)	175.3 g NaCl (3 M) 88.2 g Sodium citrate (0.3 M) adjust to 1 l with H_2O adjust pH 7.2

AP-buffer (1x)	100 mM NaCl; 50 mM MgCl2; 100 mM Tris pH 9.5; 0.1 % Tween20
TNT-buffer (1x)	100 mM Tris pH 7.5; 150 mM NaCl; 0.1 % Tween20
Protein lysis buffer (1x)	140 mM NaCl; 10 mM Tris-HCl pH 8; 1 mM EDTA pH 8; 0.5 % Triton X-100
WB running buffer (10x)	30 g Tris; 144 g Glycine; 50 ml 20% SDS; adjust to 1 l with H_2O
WB transfer buffer (10x)	22.5 g Tris; 103.3 g Glycine; 200 ml MeOH; adjust to 1 l with H_2O
Protein loading buffer (6x)	360 mM Tris-Cl pH 6.8; 12 % SDS; 60 % glycerol; 30 % ß-mercaptoethanol; 0.06 % bromophenol blue
TBS (10x)	30.2 g Tris; 73 g NaCl; 14 ml HCl; adjust to 1 l with H_2O
Hemolymph-like (HL) Buffer	25 mM KCl 4.8 mM $NaHCO_3$ 90 mM NaCl 80 mM D-Glucose 5 mM Trehalose 5 mM Glutamin 10 mM HEPES 0.25 % Trypsin-EDTA

3.2 Fly work

3.2.1 Fly stocks

If not otherwise stated, fly experiments were performed on standard fly medium at 25°C.

Fly strains used for CRISPR/Cas9-induced *lola* mutations

Name	Genotype	Source
TBX-0002	*y1 v1 P{nos-phiC31\int.NLS}X; attP40*	National Insitute of Genetics (NIG)
TBX-0008	*y2 cho2 v1/Yhs-hid; Sp/CyO*	National Insitute of Genetics (NIG)
Cas-0001	*y2 cho2 v1; attP40{nos-Cas9}/CyO*	National Insitute of Genetics (NIG)

Additional fly strains used during this study

Name	Genotype (chromosome)	Source
Wild type	w^{1118}	Bloomington *Drosophila* Stock Center
Balancer	Ap^{xa}, *Cyo / Tm6c*	Bloomington *Drosophila* Stock Center
Balancer	*Sco/CyO-GFP*	Bloomington *Drosophila* Stock Center
Balancer	*w*; P{sqh-mCherry.M}*	Bloomington *Drosophila* Stock Center
lola deficiency	*Df(2R)ED2076*	Bloomington *Drosophila* Stock Center
Octopamine driver line	*Tdc2*-GAL4 (II)	Bloomington *Drosophila* Stock Center
Ubiquitous driver line	*Tubulin*-GAL4 (II)	Bloomington *Drosophila* Stock Center
Neuronal driver line	$elav^{C155}$-GAL4 (X)	Bloomington *Drosophila* Stock Center
lola BAC (Lola-O-GFP)	*PBac(lola.J-GFP.FLAG)* (III)	Bloomington *Drosophila* Stock Center
lola BAC (Lola-T-GFP)	*PBac(lola.GR-GFP.FLAG)* (III)	Bloomington *Drosophila* Stock Center
EP UAS-Futsch	*P{w[futsch[EP1419]* (X)	Bloomington *Drosophila* Stock Center
TBH mutants	Tbh^{nm18}	M. Monastirioti
MARCM ready	*hs-FLP,UAS-mCD8::GFP; act-GAL4;FRT82B,tubP-Gal80*	C. Berger
UAS –Dam control	*UAS-LT3-Dam* (III)	A. Brand
UAS- Dam-RNA Pol II	*UAS-LT3-Dam-Pol II* (III)	A. Brand
UAS –Dam-Lola-O	*UAS-LT3-Dam-Lola-O* (II)	This study
UAS-Lola-F	*UAS-Flag/HA-Lola-F* (III)	This study
UAS-Lola-H	*UAS-Flag/Myc-Lola-H* (III)	This study
UAS-Lola-O	*UAS-Flag/Myc-Lola-O* (III)	This study
UAS-TBH	*UAS-Flag/HA-TBH* (III)	This study

3.2.2 Genomic DNA Extraction

Flies of the respective genotype were collected in 100 µl DNA lysis buffer (see 3.1), homogenized using a sterile pestle and incubated at 65°C for 60 minutes. 400 µl of KAc (5M) were added and proteins were precipitated on ice for 10 minutes. The sample was centrifuged for 15 minutes at full speed (RT), the supernatant was transferred into a new tube and the DNA was precipitated by adding 500 µl isopropanol. The DNA was pelleted at full speed for 30 minutes (RT), the pellet was washed with 75% EtOH and air-dried before the DNA was re-suspended in water.

3.2.3 Gateway cloning

The coding sequence (CDS) of *lola-H, lola-O, lola-F* and *Tbh* was amplified from cDNA using Phusion High Fidelity Polymerase and inserted into Gateway plasmids with N-terminal Flag-Myc(4x) or Flag-HA(4x) tag (pPFMW or pPFHW, respectively; obtained from *Drosophila* Genomics Resource Centre at Indiana University). The cloning strategy included two steps. First, the CDS was cloned into the entry vector pENTR TOPO by a topoisomerase-catalysed reaction using the pENTR/D-TOPO Cloning Kit, followed by a recombination with the final Gateway plasmid using the Gateway® LR recombination reaction. Both reactions were performed according to the kit protocol with the exception that half-reactions were used. Lola-H and Lola-O were Flag-Myc tagged and Lola-F and TBH were Flag-HA-tagged. All constructs were sequenced at *GATC Biotech* prior to microinjection.

3.2.4 p-element mediated germline transformation

For p-element insertion, DNA plasmids were microinjected (800 ng/µl) in-house together with a Δ2-3 helper plasmid (100 ng/µl) into w^{1118} blastoderm embryos (Rubin and Spradling, 1982; Laski, Rio and Rubin, 1986). Microinjected flies were subsequently crossed to flies of the Ap^{xa}, *Cyo;Tm6c* balancer and F1 flies were screened for yellow eyes. The constructs for *lola-O* and *lola-H* were injected at *BestGeneInc*.

3.2.5 Generation of CRISPR/Cas9 mutant flies

To induce deletion mutations in specific *lola* exons, a pair of two gRNAs in the C-terminal exon was designed (https://shigen.nig.ac.jp/fly/nigfly) and cloned into pBFv-U6.2B as previously described (Kondo and Ueda, 2013). Briefly, 5 µg vector (pBFv-U6.2 and pBFv-U6.2B) was BbsI-digested and gel-purified. The gRNAs were annealed in a 100 µl volume (20 µl Phusion® High Fidelity Buffer, 40 µl forward primer, 40 µl reverse primer) by heating at 95°C for 5 minutes and a gradual cooling to RT. Each gRNA was alternatingly cloned into either pBFv-U6.2 or pBFv-U6.2B, respectively and each plasmid containing one gRNA was EcoRI/NotI digested and gel-purified. The gRNA pair was cloned into the final vector pBFv-U6.2B, sequenced and injected (250 ng/µl) in-house into blastoderm *y*^{1} *v*^{1} *P(nos-phiC31\int.NLS)X; attP40* embryos. Microinjected flies were crossed with *y*^{2} *cho*^{2} *v*^{1}*/Y*$^{hs\text{-}hid}$*; Sp/CyO* and F1 flies were screened for brown-coloured *cho*^{2} eyes. Transgenic flies were further crossed with *y*^{2} *cho*^{2} *v*^{1}*; attP40(nos-Cas9)/CyO* and offspring from the F1 generation were PCR screened for the expected deletion mutation using primer sequences flanking the gRNA sequences (see 3.6.). PCR amplicons of the expected size were sequenced at *GATC Biotech* and obtained *lola* alleles were maintained over the balancer chromosome *CyO-GFP* to allow an immediate identification of mutant flies based on the absence of *CyO* and GFP expression.

3.2.6 Lifespan assay

20 control or experimental flies were collected within 10 hours of eclosion, gender separated and maintained on standard medium at 25°C. Survival was analysed every two days and flies were transferred to new vials twice a week. In order to prevent premature death and accompanying falsification of results due to moist food conditions, vials were consistently covered with Formula 4-24® Instant *Drosophila* Medium (Carolina Biological Supply Company). Experiments were performed in three biological replicates for males and females, respectively. Data in this study represents lifespan curves obtained for male flies.

3.2.7 Drug feeding assay

20 *lola-O* mutant flies were collected within 10 hours of eclosion, sex separated and placed on medium containing 5 mg/ml (males) or 7.5 mg/ml octopamine (females). For this purpose, standard medium was covered with 2 ml of solution containing octopamine of the respective concentration and tubes were allowed to dry over-night. Flies were examined daily for survival and phenotypic penetrance and were transferred to new tubes containing fresh octopamine twice a week. 20 flies were used for each condition in three individual biological replicates. For control purposes, octopamine was additionally fed to w^{1118} flies.

3.2.8 Locomotion assay

20 freshly hatched male and female flies of the respective genotype were separated and directly placed into measuring cylinders. The locomotion was assessed using the climbing assay described previously (Bahadorani and Hilliker, 2008). Briefly, flies were tapped to the bottom and the number of flies passing 8 cm in a given 10-seconds time window was counted. To analyse hyperactivity of *lola-A* deficient flies the time interval was shortened to 5 seconds. Measurements were repeated five times for three independent biological replicates. Data in this study represents locomotion assays obtained for male flies.

3.2.9 Fertility assay

10 virgin females were collected and mated with four males for three to four days. Mated females were subsequently shifted to conical flasks covered with apple agar plates containing fresh yeast paste. Apple agar plates were changed every 24 hours and the number of laid eggs was counted. Experiments were conducted in three biological replicates.

3.2.10 Generation of MARCM clones

Flies of the respective genotype were recombined with *FRT42D* sites and mated for three days with MARCM-ready flies at 25°C. Eggs were collected for four hours and developed further for 24 hours. The freshly hatched first-instar larvae (L1 stage)

were transferred to a water bath for a one-hour heatshock at 37°C. Vials were transferred back to 25°C and larvae were aged until third instar larval or adult stage, when the brain was dissected and subjected to immunostaining (see 3.4.2.2). The heatshock of freshly hatched first-instar larvae allows to precisely target and induce recombination in the senescent Nb, which will become mitotically active again in late L1 phase to give rise to a GFP-labelled Nb lineage.

3.3 Molecular methods

3.3.1 Transcriptome analysis

3.3.1.1 Collection of *lola-F* mutant embryos

lola-F^{Stop} flies were recombined with *w*; P{sqh-mCherry.M}* to allow a precise identification of homozygous mutant flies. Embryos were collected at 25°C for two hours and subsequently developed for 13 hours. Using a fluorescent microscope, 100 *lola-F* KO embryos were hand-sorted and collected based on the absence of mCherry expression, while control embryos were collected in parallel. Both mutant and control embryos were transferred into TRIzol reagent and RNA was isolated as described in 3.3.1.3.

3.3.1.2 Collection *of lola-O* mutant embryos

Homozygous *lola-O* mutant embryos were collected at 25°C for two hours and developed for 20 hours, transferred into TRIzol reagent and subjected to RNA isolation (see 3.3.1.3)

3.3.1.3 RNA isolation

Samples were collected in 400 µl TRIzol reagent and homogenized using a sterile pestle. At this stage, samples were either flash frozen in liquid nitrogen and stored in -80°C, or immediately processed further by adding 100 µl chloroform. The emerging two phases were vortexed and incubated for 10 minutes (RT). The samples were centrifuged at 12000 rpm (4°C), the aqueous phase was transferred into a new tube and the RNA was precipitated by adding 267 µl isopropanol. If low RNA

concentrations were expected, precipitation was performed using 1 µl Ambion GlycoBlue™, 1/10 volume NaAc (3 M) and 2.5 volumes 100 % EtOH. Upon incubation at -80° C for one hour, RNA was pelleted by centrifugation at 14800 rpm (4°C) for 30 minutes, washed with 80 % EtOH and eluted in sterile water. If required, RNA quality was assessed on an Agilent 2100 Bioanalyzer using the Agilent RNA 6000 Pico Kit.

3.3.1.4 DNase I treatment on isolated RNA

To eliminate remaining DNA, DNase I (1U/50 µl) was added accordingly to the RNA sample and incubated for 30 minutes at 37°C. To purify the RNA, a phenol-chloroform extraction was performed. For this, the sample volume was adjusted to 200 µl and supplied with 300 µl phenol:chloroform (pH 4.5). The sample was vortexed and centrifuged at 14800 rpm for 5 minutes (RT), before the aqueous phase was transferred into a new tube and supplied with 300 µl chloroform. Upon vortexing and centrifugation at 14800 rpm (5 minutes, RT), the aqueous phase containing the RNA was transferred into a new tube followed by a standard precipitation step (see 3.3.1.3).

3.3.1.5 cDNA library preparation

The purified and DNAse I-treated RNA was analysed on a Nanodrop 2000 (Thermo Fisher Scientific) and concentration was adjusted to 1 µg in 50 µl sterile water. Library preparation was done using the NEBNext® Ultra™ Directional RNA Library Prep Kit for Illumina®. Typically, half-reactions were used, mRNA fragmentation was performed on-beads for 15 minutes at 94°C and library enrichment was done in 11 cycles. Finished libraries were purified twice using Ampure XP Beads (Beckman Coulter) to eliminate oligo-dimers and library concentrations were measured using the Qubit™ dsDNA HS Sensitivity Assay. The library profiles were analysed on an Agilent 2100 Bioanalyzer using the Agilent High Sensitivity DNA Kit. Finally, concentrations were adjusted to 10 nM, cDNA libraries were pooled and submitted for high throughput sequencing on a HiSeq2500 for Lola-F and Next-Seq500 for Lola-O, respectively.

3.3.1.6 Computational analysis

Computational analysis was performed by Nastasja Kreim (IMB Core Facilities, Genomics). *Lola-F*^{Stop}, *lola-O* and corresponding control samples were sequenced paired end. *lola*^{E76} and control were sequenced single read. Demultiplexing and fastq conversion was done with bcl2fastq (v. 1.8.4). Reads were mapped using STAR (v. 2.5.0c) against ensembl release 79 (BDGP6). For *lola-F*^{Stop} and the corresponding control the first read was used for mapping to ensure comparability with *lola* null and corresponding control samples. Mapped reads were filtered for rRNA and mitochondrial RNA reads before further processing. Counts per gene were calculated using htseq-count (v. 0.6.1p1) with ensembl release 79 as a reference. Differentially expression analysis was done using DESeq2 (v. 1.10.0) with an FDR filter of 1%.

3.3.1.7 GO Term method and plot outline

GO term analysis for *lola-F* mutants was performed by Nastasja Kreim (IMB Core Facilities, Genomics). GO Terms overrepresentation was calculated using GOStats (v. 2.38.1) requiring a minimal amount of 5 genes per GO Term and adjusted *p*-value smaller than 1%. Afterwards, terms were summarised using semantic similarity (GOSemSim 1.30.3). Only GO Terms with a OddsRatio larger then 5 are displayed.

3.3.2 Transcriptome analysis of FACS-sorted cells

To induce a neuronal specific mCherry expression, *elav*^{C155}-GAL4 flies were recombined with UAS-*mCherry* flies. Eggs were collected for three hours, followed by 13 hours of aging. Embryos were subsequently bleach-treated for 2 minutes and collected in Schneider's Medium. Cell isolation was performed as previously described (Salmand & Perrin, 2011) with the exception that all solutions were supplied with 0.1 % pluronic acid to avoid clumping of cells. Briefly, embryos were homogenized in 1 ml Schneider's Medium in 10 strokes using a tight dounce homogenizer. The lysate was filtered through a 100 µm mesh and cells were pelleted for 1 minute at 1000 rpm. Cells were resolved in 500 µl HL buffer (see 3.1) supplied with 1 U DNase I and incubated at 37°C for 10 minutes. The reaction was stopped by adding 500 µl Donkey Serum and cells were pelleted for 1 minute at 1000 rpm.

Finally, cells were dissolved in 500 µl Schneider's Medium, filtered through a 30 µm mesh and sorted by fluorescent activated cell sorting (FACS) using the Becton Dickinson Aria III SORP flow cytometer. For RNA preparation, 10 sorted cells per replicate were collected in lysis buffer and subjected to library preparation using the Smart-Seq2 Kit from Illumina®. cDNA libraries were submitted for high throughput sequencing on a NextSeq500.

3.3.3 cDNA synthesis and qRT-PCR

Total RNA was prepared (see 3.3.1.3 and 3.3.1.4) and transcribed into cDNA using M-MLV reverse transcriptase. Typically, 2 µg of DNase treated and purified RNA was used as a starting material for reverse transcription. cDNA synthesis was performed in a 20 µl volume containing 0.7 mM random oligos, 10 mM dNTPs, 1x M-MLV-Buffer, 25 U Murine RNase inhibitor and 200 U M-MLV RT enzyme. The reaction was incubated at 42°C for one hour followed by a 5-minutes enzyme-inactivation step at 85°C.

For the measurement of RNA levels, qRT-PCR analysis was performed using a ViiA7 real-time PCR system (Applied Biosystems). Per 10 µl reaction, 0.5 µl cDNA was mixed with SYBR green PCR master mix and primers of interest. Measurements were done in triplicates. Relative RNA levels were normalized to *Rpl15* levels. Primer sequences are listed in 3.7.

3.3.4 Targeted DamID

3.3.4.1 Sample preparation

UAS-LT3-Dam-Lola-O flies were generated by amplifying the CDS and cloning into pUASTattB-LT3-NDam (kind gift from A. Brand). Upon microinjection and generation of transgenic flies, *UAS-LT3-Dam-Lola-O* and *UAS-LT3-Dam-Pol II* (kind gift from A. Brand) flies were crossed with *Tdc2*-GAL4 to induce octopaminergic expression. Analysis of binding sites was performed on stage 17 embryos (20-22 hours AEL) for *UAS-LT3-Dam*, *UAS-Dam-LT3-Lola-O* and *UAS-LT3-Dam-Pol II* flies. Genomic DNA isolation and subsequent treatments were exactly performed as described (Marshall et al., 2016). Purified methylated DNA was amplified with MyTaq™ HS DNA

Polymerase, sonicated in 5 cycles on a Bioruptor® Pico (Diagenode), PCR-purified using Ampure XP beads (Beckman Coulter) and subjected to library preparation using the NebNext DNA Ultra II library kit. Typically, 500 ng of DNA was used as a starting material and library enrichment was done in 7 cycles. Library concentration was adjusted to 10 nM and pooled libraries were subsequently sequenced on a NextSeq500.

3.3.4.2 Computational analysis

Computational analysis was carried out by Tony Southall (Imperial College, London). The first read was mapped to *Drosophila melanogaster* genome (BDGP6) using bowtie (v. 2.2.9), binned to GATC fragments and normalized against the Dam-only control (Marshall and Brand, 2016). Peaks were called and mapped to genes using a custom Perl program (available on request). In brief, a false discovery rate (FDR) was calculated for peaks (formed of two or more consecutive GATC fragments) for the individual replicates. Then each potential peak in the data was assigned a FDR. Any peaks with less than a 1% FDR were classified as significant. Significant peaks present in both replicates were used to form a final peak file. Any gene within 5 kb of a peak (with no other genes in between) was identified as a potential target gene.

3.4 Immunohistochemistry

3.4.1 *In-situ* hybridization

3.4.1.1 Preparation of digoxigenin-labeled RNA probes

Primers were designed to amplify a unique region within *lola* exons with the reverse primer containing the SP6 sequence (see 3.7). The PCR was performed on embryonic cDNA using Phusion®-DNA polymerase. 250 ng of template PCR product was used to perform an *in-vitro* transcription with the DIG RNA labelling kit. The reaction was incubated over-night at 37°C and probes were carbonated to approximately 300 bp by incubation with carbonate buffer at 65°C for 20 minutes (Cox et al., 1984). The probes were then EtOH precipitated (see 3.3.1.3) and re-suspended in sterile water to obtain a concentration of 100 ng/µl. For *in-situ* hybridizations, the probes were diluted 1:50 in HB4 hybridization buffer (see 3.4.1.2).

3.4.1.2 *In-situ* hybridization on embryos

Embryos were dechorionated in 50 % bleach for 2 minutes and fixed for 23 minutes in fixation solution (see 3.1) while shaking at RT. The lower phase was removed and 1 ml MeOH was added, followed by a one-minute vortexing step to destroy the vitelline membrane. After washing in MeOH several times, embryos were gradually transferred into PBTween (1x PBS; 0.1% Tween20), followed by three washes for 15 minutes and a gradual transfer into HB4 hybridization buffer (see 3.1). After equilibration at RT, embryos were pre-hybridized in HB4 at 56°C for several hours. The diluted RNA probe was denatured at 80°C for 10 minutes, cooled down on ice and embryos were hybridized over-night at 65°C. After hybridization, the probes were stored at -20°C to be re-used for subsequent experiments. Embryos were subsequently incubated in wash buffer (formamide, 2x SSC, 1:1; 0.1% Tween20) for 30 minutes at 65°C, gradually transferred into PBTween at RT and incubated with anti-DIG-AP antibody (1:1000 in PBTween) for two hours (RT). Upon several washes in PBTween and one rinse with AP buffer (see 3.1), probes were visualized using a 1:100 dilution of NBT/BCIP solution in AP buffer. Once the desired signal intensity was reached, the reaction was stopped by washing several times with 1xPBS and samples were mounted in glycerol (80% glycerol in 1x PBS).

For fluorescent *in-situ* hybridizations, fixed embryos were subsequently peroxidase treated for 20 minutes at RT (MeOH, H_2O_2; 9:1) and gradually transferred into PBTween. After the hybridization process described above, samples were incubated with anti-DIG-POD-fab-fragments for two hours at RT (1:500 in PBTween), washed with PBTween several times and blocked by washing for 15 minutes with TNT-buffer (see 3.1). Finally, probes were visualized using the Tyramide Signal Amplification (1:50 dilution in amplification diluent) with an incubation time of 15 minutes (RT). The reaction was stopped by several washes in PBTween and samples were mounted in Vectashield. Analysis was done on a Leica SP5 microscope.

3.4.1.3 Fluorescent *in-situ* hybridization on third instar larval brains

Larval CNS was dissected in cold 1x PBS, fixed for 25 minutes in fixation solution (RT; see 3.1) and peroxidase treated (MeOH:H_2O_2; 9:1) for 20 minutes at RT. After a

gradual transfer into PBTween (1x PBS; 0.1% Tween-20), samples were washed several times and post-fixed for 20 minutes in 1 ml PBTween and 140 µl formaldehyde. The brains were washed again in PBTween, gradually transferred into HB4 buffer and blocked for at least four hours at 65 °C. All subsequent steps were performed without shaking to prevent damaging of the tissue. Upon blocking and dilution of the denatured probe (see 3.4.1.1), hybridization was performed over-night at 65°C. Post-hybridization washes were done at 65°C and comprised a gradual transfer from HB4 to 2x SSC and subsequently to 0.2x SSC. Samples were further processed at RT on a nutator for a gradual transfer into PBTween. Anti-DIG-POD fab-fragments antibody was incubated over-night at 4°C (1:500 in PBTween) and samples were thereafter treated as embryonic samples (see. 3.4.1.2).

3.4.2 Immunostaining

3.4.2.1 Whole mount embryo immunostaining

Embryos were dechorionated and fixed as described in 3.4.1.2. and gradually transferred into PBT (1x PBS; 0.3% Triton X-100). After three 15-minutes washes in PBT, samples were blocked for one hour at RT (PBT; 5 % donkey serum), and subsequently incubated with the primary antibody over-night at 4°C. Embryos were washed again several times in PBT, incubated with the secondary antibody for two hours at RT and washed with PBT to remove excess antibody. Samples were mounted in Vectashield and analysed using a Leica SP5 confocal microscope.

3.4.2.2 Third instar larval brain immunostaining

Larval brains were fixed as explained before (see 3.4.1.3) and thereafter treated as embryonic samples (see 3.4.2.1). In cases where an immunostaining required improvements with regard to immunofluorescence intensity, the incubation time with primary antibodies was extended to a maximum of five days. Likewise, incubations with secondary antibodies were prolonged to over-night at 4°C to enhance penetration efficiency.

For Lola-O-GFP, which is expressed at low levels in the CNS, an antigen-retrieval step was carried out before the actual immunostaining process in order to uncover hidden

antigenic sides. For this purpose, larval CNS first underwent the *in-situ* hybridization procedure (see 3.4.1.3) before the actual immunostaining protocol was applied, starting with an over-night incubation in primary antibody. The mounting of larval CNS was done in Vectashield and a confocal stack through the entire larval brain was recorded using a Leica SP5 confocal microscope.

3.4.3 Western blotting

For western blot analysis, staged embryos of the corresponding genotype were collected, homogenized in 50 µl lysis buffer (see 3.1) and incubated at 4°C for 30 minutes. The lysate was cleared by repeating centrifugations at 4°C. The embryonic protein extract was supplied with protein-loading dye, denatured for 10 minutes at 80°C and loaded on an 8% SDS-PAGE polyacrylamide gel. Proteins were separated for approximately three hours at 90 V in WB-running buffer and subsequently transferred on a PVDF membrane in WB-transfer buffer for 1 hour at 105V. The membrane was blocked for one hour in TBST (1x TBS; 0.1% Tween-20) containing 5% dry milk and probed with primary antibody over-night at 4°C, followed by several washes with TBST and an incubation with secondary antibody for one hour at RT. For visualization, ultra-sensitive enhanced chemiluminescent reagent was used in a 1:1 dilution with water and the signal was detected on a Gel Doc™ XRS+ Gel documentation system (BioRad).

3.5. Quantification and statistical analysis

Statistical parameters and significance are reported in the figures and the figure legends. For comparisons of the means of two groups, one-way ANOVA and t-test were used. Comparisons of multiple groups were conducted using multiple t-tests including Bonferroni normalization of p-values.

3.6 List of antibodies used in this study

Primary antibodies

Name	Dilution (Immunofluorescence IF / Western blotting WB)	Source
Guinea Pig anti-Deadpan	1:50 IF	C. Berger
Rat anti-Elav 7E8A10	1:100 IF	DSHB
Mouse anti-FasII 1D4	1:100 IF	DSHB
Mouse anti-Repo 8D12	1:75 IF	DSHB
Mouse anti-Lola Zf5 7F1-1D5	1:10 IF / 1:100 WB	DSHB
Rabbit anti-GFP	1:500 IF	Lorrey Pines
Rabbit anti-Lola	1:250 WB	E. Giniger
Rat anti-TBH	1:70 IF / 1:100 WB	M. Monastirioti
Mouse anti-22C10	1:10 IF	DSHB
Sheep anti-DIG-POD fab-fragments	1:500 IF	Roche
Sheep anti-DIG-AP	1:1000 IF	Roche
Rabbit anti-GFP	1:500 IF	Torrey Pines
Mouse anti-Tubulin	1:2O00 WB	Biolegend

Secondary antibodies

Name	Dilution	Source
Goat anti-mouse Alexa Fluor 488	1:500	Jackson Immunoresearch
Goat anti-Guinea Pig Alexa Fluor 555	1:250	Jackson Immunoresearch
Goat anti-rat Alexa Fluor 648	1:500	Jackson Immunoresearch
Donkey anti-rabbit HRP	1:1000	Jackson Immunoresearch
Donkey anti-mouse HRP	1:1000	Jackson Immunoresearch

3.7 List of oligonucleotides used in this study

Oligonucleotides used in this study are listed in the following. The abbreviations "F/R" were used to refer to forward and reverse primers, respectively.

gRNA cloning oligos

Name	Sequence (5'-3')	Name	Sequence
gRNA I Lola-A F	CTTC GCTCATATTATCGATTTCAG	gRNA I Lola-J F	CTTC GTGTAGGCCTTCTCGCAGCG
gRNA I Lola-A R	AAAC CTGAAATCGATAATATGAGC	gRNA I Lola-J R	AAAC CGCTGCGAGAAGGCCTACAC
gRNA II Lola-A F	CTTC GTTGTAGTGTACATTAAAAT	gRNA II Lola-J F	CTTC GTCTCTTCGATTCGGCTAAG
gRNA II Lola-A R	AAAC ATTTTAATGTACACTACAAC	gRNA II Lola-J R	AAAC CTTAGCCGAATCGAAGAGA
gRNA I Lola-B F	CTTC GGGAGCATTTCCACCGCTGC	gRNA I Lola-K F	CTTC GTTATATTTTATTTTTTCTG
gRNA I Lola-B R	AAAC GCAGCGGTGGAAATGCTCCC	gRNA I Lola-K R	AAAC CAGAAAAAATAAAATATAAC
gRNA II Lola-B F	CTTC GCACAAGGGCGTCCAAAAGA	gRNA II Lola-K F	CTTC GTGTTGCACGTAAAGAAGCT
gRNA II Lola-B R	AAAC TCTTTTGGACGCCCTTGTGC	gRNA II Lola-K R	AAAC AGCTTCTTTACGTGCAACAC
gRNA I Lola-C F	CTTC GCCACCGATACCGCCACCCG	gRNA I Lola-L F	CTTC GCGGGCATTCCATTCGTTCC
gRNA I Lola-C R	AAAC CGGGTGGCGGTATCGGTGGC	gRNA I Lola-L R	AAAC GGAACGAATGGAATGCCCGC
gRNA II Lola-C F	CTTC GGCGCAAGACGTTGAAAGGT	gRNA II Lola-L F	CTTC GCTGTCGCCATCTAAGCCGC
gRNA II Lola-C R	AAAC ACCTTTCAACGTCTTGCGCC	gRNA II Lola-L R	AAAC GCGGCTTAGATGGCGACAGC
gRNA I Lola-D F	CTTC GATGACTATCACCAGGGATC	gRNA I Lola-M F	CTTC ATCATTTATTGACAAGATTT
gRNA I Lola-D R	AAAC GATCCCTGGTGATAGTCATC	gRNA I Lola-M R	AAAC AAATCTTGTCAATAAATGAT
gRNA II Lola-D F	CTTC GAGATTTTCATTGGACAGGA	gRNA II Lola-M F	CTTC TTTCTATTTCATGACTAAC
gRNA II Lola-D R	AAAC TCCTGTCCAATGAAAATCTC	gRNA II Lola-M R	AAAC GTTAGTCATGAAATAGAAA
gRNA I Lola-E F	CTTC GGCCGCTGCTATAACTGCCG	gRNA I Lola-N F	CTTC GACGACCACATCCACGTCCA
gRNA I Lola-E R	AAAC CGGCAGTTATAGCAGCGGCC	gRNA I Lola-N R	AAAC TGGACGTGGATGTGGTCGTC
gRNA II Lola-E F	CTTC GCCAGAATTACCATAACGTT	gRNA II Lola-N F	CTTC GAAGGGTCCACAGTTCCGAA
gRNA II Lola-E R	AAAC AACGTTATGGTAATTCTGGC	gRNA II Lola-N R	AAAC TTCGGAACTGTGGACCCTTC

gRNA I Lola-F^{Stop} F	CTTC GTCTAGCGAGCCGCTGATAG	gRNA I Lola-O F	CTTC GTTCCAATGGGACTGTTGTA
gRNA I Lola-F^{Stop} R	AAAC CTATCAGCGGCTCGCTAGAC	gRNA I Lola-O R	AAAC TACAACAGTCCCATTGGAAC
gRNA II Lola-F^{Stop} F	CTTC GCTTTCAGCATGACAGGGAT	gRNA II Lola-O F	CTTC GAAGCAGGCGATGTATTTCG
gRNA II Lola-F^{Stop} R	AAAC ATCCCTGTCATGCTGAAAGC	gRNA II Lola-O R	AAAC CGAAATACATCGCCTGCTTC
gRNA I Lola-F^{ZNF} F	CTTC GACTACAAGCACAGCATTTT	gRNA I Lola-P F	CTTC GGTGCGTTTTCTAGTGGCGG
gRNA I Lola-F^{ZNF} R	AAAC AAAATGCTGTGCTTGTAGTC	gRNA I Lola-P R	AAAC CCGCCACTAGAAAACGCACC
gRNA II Lola-F^{ZNF} F	CTTC GCACAGATGACAACGGGCAG	gRNA II Lola-P F	CTTC GGATGGAGATCCCGGCGGCA
gRNA II Lola-F^{ZNF} R	AAAC CTGCCCGTTGTCATCTGTGC	gRNA II Lola-P R	AAAC TGCCGCCGGGATCTCCATCC
gRNA I Lola-G F	CTTC GAGTTTTCCAGGACAAGATA	gRNA I Lola-Q F	CTTC GTGTACTGTATATTGCCCAC
gRNA I Lola-G R	AAAC TATCTTGTCCTGGAAAACTC	gRNA I Lola-Q R	AAAC GTGGGCAATATACAGTACAC
gRNA II Lola-G F	CTTC GAAAGATTAAGACTAGGAAT	gRNA II Lola-Q F	CTTC GGTTGCAAGTATTGCCTCCC
gRNA II Lola-G R	AAAC ATTCCTAGTCTTAATCTTTC	gRNA II Lola-Q R	AAAC GGGAGGCAATACTTGCAACC
gRNA I Lola-H F	CTTC GCACTGGAAGATGGGTCTTT	gRNA I Lola-R F	CTTC GAAGAACCAGCTCCTGTGCC
gRNA I Lola-H R	AAAC AAAGACCCATCTTCCAGTGC	gRNA I Lola-R R	AAAC GGCACAGGAGCTGGTTCTTC
gRNA II Lola-H F	CTTC GAGGCCACCGCATAGGGAGG	gRNA II Lola-R F	CTTC GCGGCCACCGAAGATGAATC
gRNA II Lola-H R	AAAC CCTCCCTATGCGGTGGCCTC	gRNA II Lola-R R	AAAC GATTCATCTTCGGTGGCCGC
gRNA I Lola-I F	CTTC GGGCACTGGTAACGTCCATC	gRNA I Lola-S F	CTTC AGCAGAAAGTAGCTGCAGTC
gRNA I Lola-I R	AAAC GATGGACGTTACCAGTGCCC	gRNA I Lola-S R	AAAC GACTGCAGCTACTTTCTGCT
gRNA II Lola-I F	CTTC GGATGCCACATCATTTATAA	gRNA II Lola-S F	CTTC TTCTTAACGAACATATGCGC
gRNA II Lola-I R	AAAC TTATAAATGATGTGGCATCC	gRNA II Lola-S R	AAAC GCGCATATGTTCGTTAAGAA
gRNA I Lola-J F	CTTC GTGTAGGCCTTCTCGCAGCG	gRNA I Lola-T F	CTTC GTTTTTTGAGGCCGTCTCGG
gRNA I Lola-J R	AAAC CGCTGCGAGAAGGCCTACAC	gRNA I Lola-T R	AAAC CCGAGACGGCCTCAAAAAAC
gRNA II Lola-J F	CTTC GTCTCTTCGATTCGGCTAAG	gRNA II Lola-T F	CTTC GTGACGGCACACAAGCTTAA
gRNA II Lola-J R	AAAC CTTAGCCGAATCGAAGAGA	gRNA II Lola-T R	AAAC TTAAGCTTGTGTGCCGTCAC

Lola CRISPR/Cas9 screening oligos

Name	Sequence (5'-3')	Name	Sequence (5'-3')
lola-A F	CATGGCAGCACGACAGATCTC	*lola-K* F	CCTCTTACTAACCACTATTCGTTC
lola-A R	CTCTGCGCCAAACTCTCGCT	*lola-K* R	GACCTTTTGTTTTTACAACTAGTTTTC
lola-B F	ACTCAATGGTTGTGCCCAAAATC	*lola-L* F	CAAACTCCACAAATACAACACAAATC
lola-B R	CTCAGATCGTGGCTAAGTGCAAG	*lola-L* R	CGGAATCAGTGTGCCAAATTAAGC
lola-C F	CTCGCTTTTTCCATTCTGTTC	*lola-M* F	GCCCTCAGGTATTTTACACAACTAC
lola-C R	GAAGTATTGAACGCATGATTTACC	*lola-M* R	GTGGTTTTAGCATCGCTTATGAGTG
lola-D F	TGCAGCTGATAGACGACTCATC	*lola-N* F	CAACTAACCTTCAGACAAACTAACTC
lola-D R	GTTGTGCGACAGCCAAATAAATG	*lola-N* R	GTGGAGGGGCATTTGCTTTATCTC
lola-E F	GAGGACACAACACGAACATATC	*lola-O* F	TCCAGTTCACTCCACTCCAT
lola-E R	CTACTGAAGAGGCTACGCTAAAC	*lola-O* R	GTTGCCCTTGTTGCTGCTAC
lola-F F	CATTTTCATTTCATACAACCCCCAC	*lola-P* F	CAGCGATGAGTTCTACGGCTATC
lola-F R	CATATCATTTGGAATAAGTGCGTTAC	*lola-P* R	GGTCCACATTCCTGCACAAATTAC
lola-G F	ATCCCGCCCTCGTTCAGTGTTG	*lola-Q* F	GCAAGCAATTAAGAATAAAGCATAC
lola-G R	CCGCCTTAGATACTAGAAAAAAGTC	*lola-Q* R	GAGCTGATGCGAAATTTGATTCTAC
lola-H F	CTCACTTACCCATCCGTCTTC	*lola-R* F	CTCGTATAGCATTAAGTAGTCCAATC
lola-H R	GGTCTAAACTACGAATGTTAAATAAG	*lola-R* R	CCTGGGACTTGTTCTCTCGTTTCAG
lola-I F	CTAATTTGTAGCTCCAAGCAGC	*lola-S* F	ATTACCGTGGATAGGAAGTACAATC
lola-I R	GTTGGTTTTCTTAGGTTTTTATGTG	*lola-S* R	CGTTTACTGTATGGATAATAACCGCTAC
lola-J F	GAATTCGCGCCCATTAAATGTGCATG	*lola-T* F	GAGATTCAGCGCAGTTTCCAGCG
lola-J R	CTCCAGCAAACAGTCGTCCAGTTC	*lola-T* R	GTCGATCGGTGAAGACCACGTG

CDS cloning oligos

Name	Sequence (5'-3')
Tbh CDS F (with NotI site)	ATGCGCGGCCGCCTGCTTAAAATTCCGCTGCAGC
Tbh CDS R (with AscI site)	ATGCGGCGCGCCATAGATGCACTCCCCCAGC
lola-A CDS F (with NotI site)	ATGCGCGGCCGCCATGGATGACGATCAGCAGTTTTG
lola-A CDS R (with AscI site)	ATGCGGCGCGCCTATTATCGATTTCAGAGGCAACAAAC
lola-H CDS F (with NotI site)	ATGCGCGGCCGCCATGGATGACGATCAGCAGTTTTG
lola-H CDS R (with AscI site)	ATGCGGCGCGCCTGCGGTGGCCTCCCATTTGGTG
lola-O CDS F (with NotI site)	ATGCGCGGCCGCCATGGATGACGATCAGCAGTTTTG
lola-O CDS R (with AscI site)	ATGCGGCGCGCCTCGATGTTGGTGGGTGCG
lola-F CDS F (with NotI site)	ATGCGCGGCCGCCATGGATGACGATCAGCAGTTTTG
lola-F CDS R (with AscI site)	ATGCGGCGCGCCGTTGTTGTTATAAGCAAATGGCATAG

DamID cloning oligos

Name	Sequence (5'-3')
lola-O CDS F (with BglII site)	ATGCGCGGCCGCGAATGGATGACGATCAGCAGTTTTG
lola-O CDS R (with XbaI site)	ATGCTCTAGATCATCGATGTTGGTGGGTGC

In-situ hybridization oligos

Name	Sequence (5'-3')
lola-F in situ probe F	ACCTGAAGTACGACTACAAGCA
lola-F in situ probe R	GTTGTTGTTATAAGCAAATGGCATAG
futsch in situ probe F	CTACTGGGGCCACCCAAGC
futsch in situ probe R	GAAGCTCATCATCGGATGTAATG
Sp6	ATTTAGGTGACACTATAGAA

qPCR oligos

Name	Sequence (5'-3')
Tdc2 qPCR F	GTGGACTTTGCCAACGAGTT
Tdc2 qPCR R	ATCTTCGGATCGCTGACCAT
Tbh qPCR F	ACAATGTACGTGGTTTGGGC
Tbh qPCR R	AGTATCTTGTCGGCCCGTAG
slit qPCR F	GGTTACGCGAACAGCGGAC
slit qPCR R	CGTGACGTGCAGATCAAGG
spire qPCR F	GCTTCTGGGTGCAGGTGATC
spire qPCR R	GATGTCGCCCATGAGTATTTC
robo qPCR F	CTTTTCTCGTCGTGAAGGATTC
robo qPCR R	GCAGTGGAAAGTGG TGTCTG
futsch qPCR F	GCTTCCAGACCAGCTTCC
futsch qPCR R	GGTCTGGAAGCTTCCTTGG
Bacc qPCR F	CGAGGGCGACAGTGAAATC
Bacc qPCR R	GATCGTCCGAGCCGGAAC
Rpl15 qPCR R	AGGATGCACTTATGGCAAGC
Rpl15 qPCR F	GCGCAATCCAATACGAGTTC

RESULTS

4. Results

4.1 CRISPR/Cas9-induced *lola* isoform-specific knock-out

In order to functionally characterize individual *lola* isoforms *in vivo*, we sought to generate knock-out (KO) flies for each isoform using the recently established CRISPR/Cas9 system (Jinek *et al.*, 2012). The CRISPR/Cas system relies on an adaptive antiviral defence mechanism used by bacteria to induce double-strand breaks in the genome of invading organisms (Ishino Y., Shinagawa H., Makino K., Amemura M., 1988). CRISPR, which stands for *clustered regularly interspaced short palindromic repeats*, acts together with an RNA-guided endonuclease, the Cas protein, to target and cleave foreign DNA. With a recent breakthrough in genome engineering the now widely used CRISPR/Cas9 system was established, which allows to sequence-specifically target and modify genomic regions in various organisms (Cong *et al.*, 2013; Mali *et al.*, 2013). Here, Cas9 recognizes a guide RNA (gRNA), whose spacer region is homologous to the genomic region of interest, thereby binds and unfolds the genomic DNA. Consequently, the Cas9 protein induces double-strand breaks surrounding the so-called protospacer adjacent motif (PAM), a Cas9-specific *NGG* sequence, inducing non-homologous end joining that is typically accompanied by nucleotide substitutions. To successfully manipulate the *Drosophila* genome, transgenic flies expressing the desired gRNA are generated and crossed with flies encoding a germline-specific Cas9 protein (Kondo and Ueda, 2013). The F1 generation is thus crossed further and screened by PCR for the existence of specific mutations.

To generate KO flies for all Lola splice variants, two gRNAs were designed to target the isoform-specific C-terminal exon (**Figure 5A**). By the use of two distinct gRNAs spanning the ZF domain we aimed to generate loss-of-function mutations for individual isoforms lacking a functional C-terminal motif. For this purpose, both gRNAs were cloned into one destination vector (pBFv-u6.2B) and integrated into the genome by microinjection and PhiC31-mediated attB/attP recombination (Keravala and Calos, 2008). After the establishment of transgenic gRNA-

expressing lines, these flies were crossed with flies expressing Cas9 in the germline.

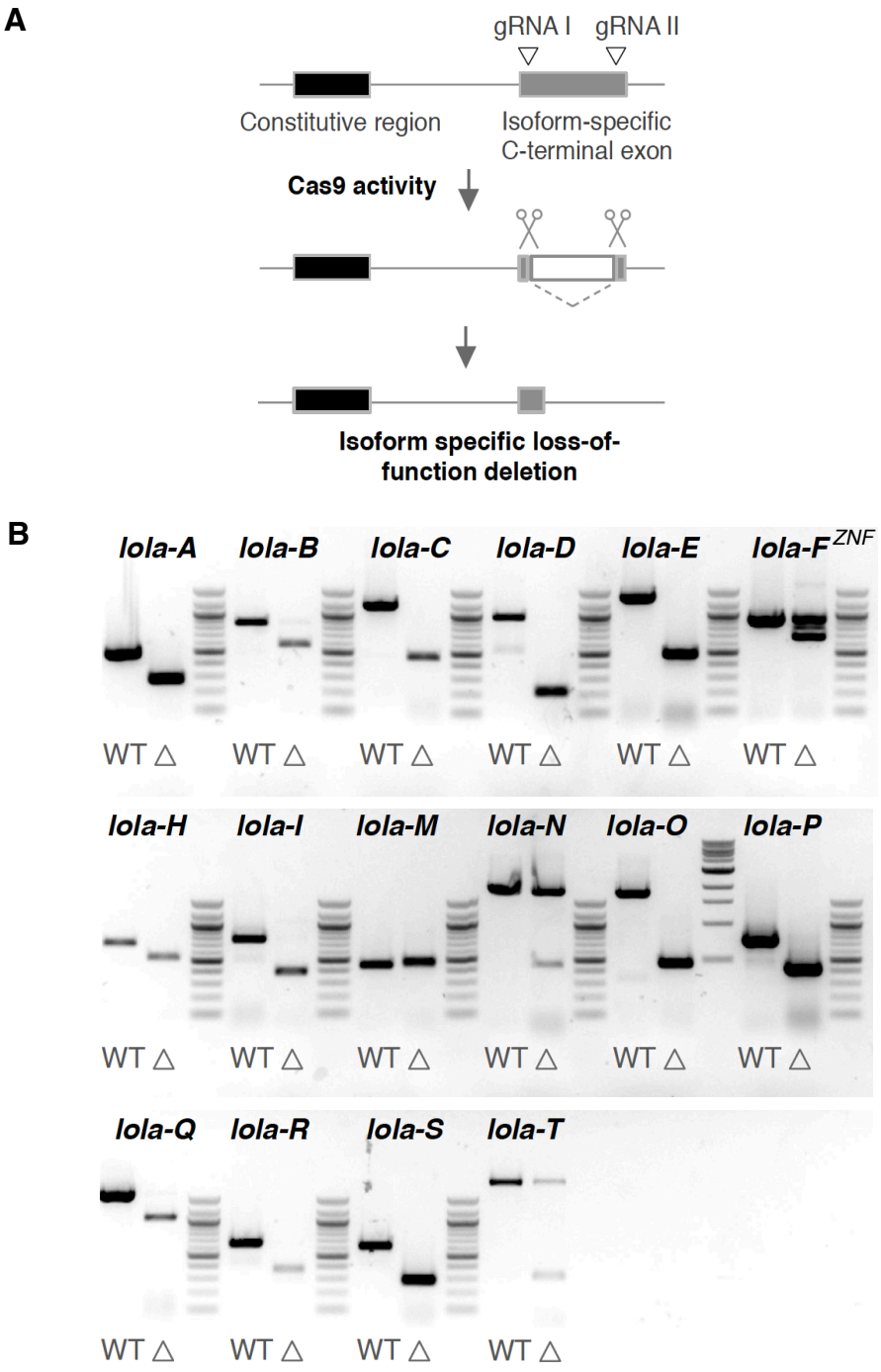

Figure 5: CRISPR/Cas9 approach to systematically mutate each Lola isoform.

(A) Two gRNAs were designed to target the isoform-specific C-terminal exon, resulting in double-strand breaks and a subsequent loss-of-function deletion for respective isoforms upon Cas9 activity. **(B)** Gel analyses of established *lola* mutants. Agarose gel shows amplicons of respective genomic regions in wild type (WT, left lane) and CRISPR/Cas9 induced *lola* isoform-specific mutant flies (Δ, right lane). Mutation in Lola-M resulted in partial nucleotide duplications. Mutants for *lola-G, -J, -K*, and *–L* bear a frameshift and are not displayed. Lethal alleles are heterozygous and show both the mutant and the wild type allele.

Genomic DNA of F1-generation flies was isolated and screened for specific modifications by PCR using primers spanning the flanking sequences targeted by both gRNAs. In most cases, Cas9 activity resulted in a deletion of the sequence flanked by the two Cas9-target sites. In the subsequent PCR, those deletion mutations were identified based on the smaller PCR amplicon size compared to the wildtypic control (**Figure 5B**). Obtained DNA fragments were subsequently gel-purified and sequenced at *GATC biotech*.

Deletion mutations were obtained for 16 of the targeted C-terminal exons, resulting in loss-of-function mutation for the respective Lola isoform. Additionally, perturbation of exon *lola-M* led to a partial duplication comprising 74 nucleotides, subsequently disrupting the triplet code and changing the encoded amino acid sequence. Likewise, indels-induced frameshift mutations were obtained for isoforms *lola-F*^{Stop}, *lola-K*, *lola-L* and *lola-G* (**Figure 6**). Finally, mutations targeting *lola-J* deleted 21 nucleotides within the isoform-specific ZF motif, leading to the depletion of one conserved Cys residue (**Figure 8**).

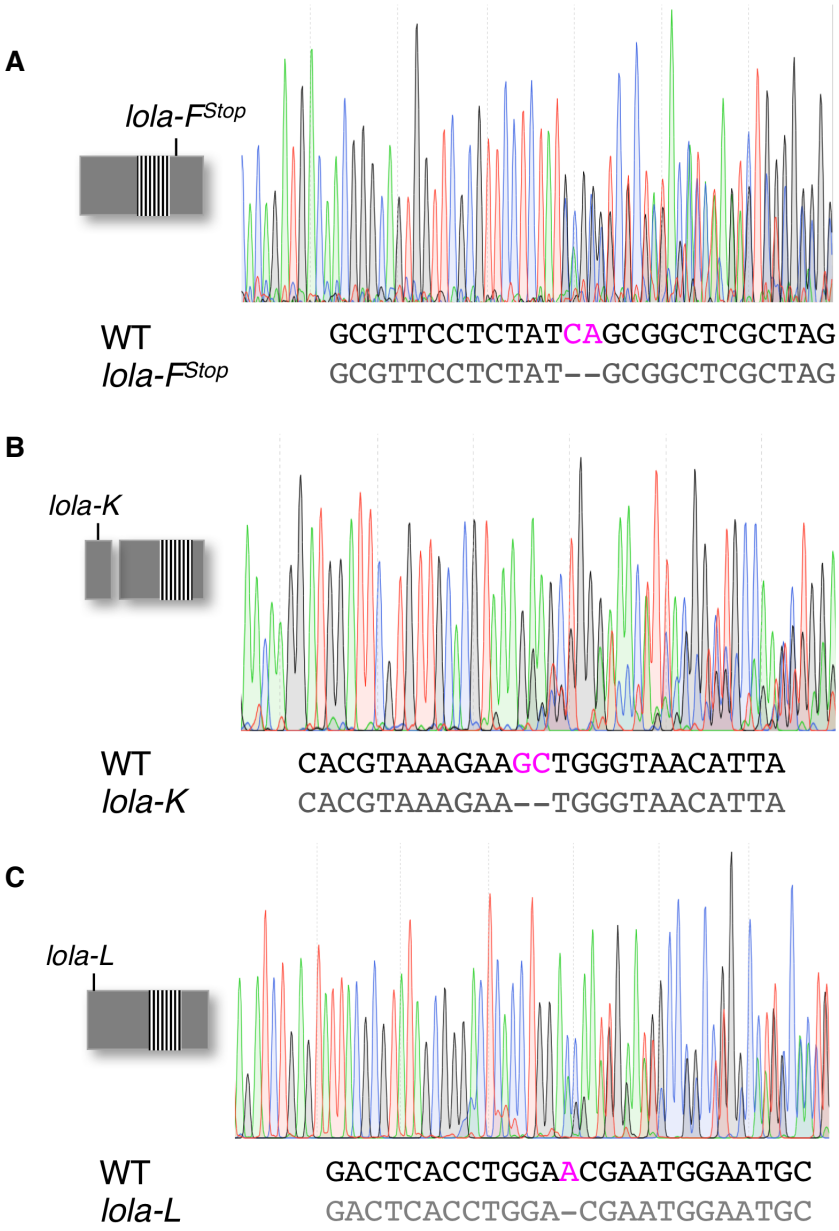

Figure 6: Chromatograms of heterozygous *lola* mutations inducing a frameshift.

PCR amplified genomic regions spanning the desired mutation for *lola-F*^{stop} **(A)**, *lola-K* **(B)** and *lola-L* **(C)** were sequenced at *GATC Biotech*. Deleted nucleotides are highlighted in pink and mutation position is indicated on the corresponding scheme. The denoted nucleotide deletions result in double-layered chromatograms downstream of the mutation position.

4.2 *lola* mutants display diverse phenotypes

Our targeted CRISPR/Cas9 screen generated KO fly lines for all 20 described *lola* isoforms, with eight isoform-specific mutants displaying phenotypes at different developmental stages. Isoforms Lola-F, Lola- K, Lola-L, Lola-N, and Lola-T are essential during early development, as mutations targeting these isoforms result in late embryonic or early larval lethality (**Table 3**). In contrast, depletion of Lola-A, Lola-H and Lola-O lead to distinct phenotypes specifically in adult flies, suggesting imago-related roles for these splice variants. With the exception of Lola-A and –H, the observed phenotypes were exclusive for evolutionary conserved isoforms, raising the question about the relevance of non-conserved ones (see **Table 3**).

Isoform	ZF conservation	Physiological function	Reference	Stage of survival of mutant flies
Lola-A	-	Locomotion control	**This study**	Adult fly
Lola-E	82%	-		Adult fly
Lola-F	81%	Axon guidance	**This study**	1st instar larva
		Nb proliferation	Wissel et al., 2016	
Lola-H	44%	Locomotion control	**This study**	Adult fly
Lola-I	87%	-		Adult fly
Lola-K	90%	ISNb development	Goeke et al., 2003	1st instar larva
		GSC maintenance	Davies et al., 2013	
Lola-L	94%	ISNb development	Goeke et al., 2003	1st instar larva
		GSC maintenance	Davies et al., 2013	
		Nb proliferation	Wissel et al., 2016	
Lola-N	74%	Neuronal maintenance	Southall et al., 2014	1st instar larva
Lola-O	88%	Octopamine synthesis	**This study**	Adult fly (shortened lifespan)
Lola-T	90%	Gonadal development	Davies et al., 2013	1st instar larva

Table 3: Summary of Lola isoforms with phylogenetically conserved ZF motifs.
Stage of survival of KO flies and isoform-specific function is indicated. ZF identity between *D. melanogaster* and *A. Gambiae* was obtained from Goeke et al., 2003.

4.2.1 Proof of principle experiments validate previously identified isoform-specific functions

Lola-B, a non-conserved Lola isoform, was previously reported to play a critical role in Nb differentiation. Knock-down (KD) of Lola-B using RNA interference (RNAi) impaired Nb proliferation, resulting in larval brains of reduced size accompanied by decreased numbers of both neurons and Nbs (Neumüller *et al.*, 2011). In contrast, our *lola-B* mutant allele did not recapitulate this phenotype (**Figure 7**). In the absence of Lola-B activity, third instar larval brains appear as wild type with respect to brain diameter (243.13 µm for control and 240.0 µm for *lola-B* mutant brains, p>0.6; n=8) and Nb number (84.5 for control vs. 80.5 for *lola-B* mutant brains, p>0.6; n=8), suggesting that the effect observed upon *lola-B* KD was due to RNAi off-target activity.

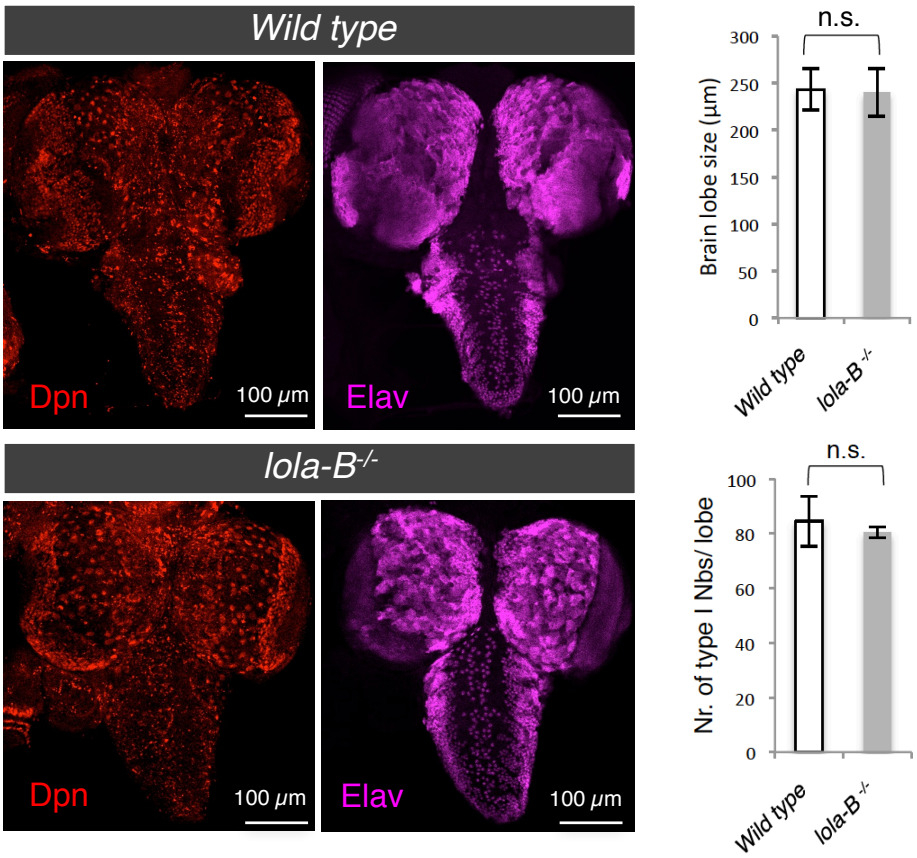

Figure 7: *lola-B* deficient 3rd instar larval brains appear normal.

(Left) Larval CNS was immunostained for the Nb-specific marker Deadpan (Dpn, red) and the neuronal transcription factor Elav (magenta). (Right) Brain lobe size was measured and the number of Nbs was counted (n=8). Data are represented as average±SD and statistical significance was tested using ANOVA one-way t-test.

Another non-conserved isoform is Lola-J, which was very recently identified to play a role in axon guidance (Peng *et al.*, 2016). Lola-J was shown to mediate its function by physically interacting and repressing PKG in neuronal cells. This interaction occurs via specific binding of PKG to Lola-J C-terminal domain. *lola-J* KO embryos revealed significant ISNb growth and guidance defects. Remarkably, heterozygous loss of Lola-J is sufficient to display this phenotype. As impairment of ISNb development is typically accompanied by embryonic or larval lethality (Crowner *et al.*, 2003; Goeke *et al.*, 2003; Bao *et al.*, 2007; Carrasco-Rando *et al.*, 2016) it is surprising that no obvious lethality was observed for heterozygous mutants.

Peng *et al.* induced a 1bp-deletion and a subsequent frameshift mutation upstream of the ZF motif. In contrast *lola-J* mutant flies obtained in our study bear a 21-nucleotide deletion within the isoform-specific C-terminal ZF motif, thus depleting the second conserved Cys residue of the C_2HC motif (**Figure 8**). Despite the continuity of the triplet code downstream of the *lola-J* deletion mutation, perturbation of conserved ZF residues might impair binding specificity of the ZF motif. However, in contrast to the findings by Peng and colleagues (2016), homozygous *lola-J* KO flies generated in our study revealed no obvious phenotype at any stage of development. Thus, this result indicates that our mutation is not sufficient to alter Lola-J function, suggesting that the zinc finger motif is dispensable for its function.

Figure 8: Scheme of the CRISPR/Cas9 induced mutation targeting *lola-J*.

Genomic DNA was isolated from homozygous mutant adult flies and sequenced at *GATC Biotech*. The nucleotide sequence is displayed as reverse complement. The induced ola-J mutation comprises a deletion of 21 nucleotides and hence 7 amino acids (pink) in the C-terminal ZF domain.

The isoform Lola-N was proposed to play a regulatory role in maintaining the differentiation state of postmitotic neurons (Southall *et al.*, 2014). While a *lola-N* mutant allele has not been generated in the study of Southall and colleagues, tumour formations in the adult brain arising from $lola^{E76}$ null mutant clones were rescued by ectopic neuronal Lola-N cDNA expression. To analyse these findings further, our *lola-N* CRISPR allele was recombined with FRT42D sites and MARCM clones were generated in the adult brain (**Figure 9**). In contrast to previous conclusions, *lola-N* mutant MARCM clones were non-proliferative and thus indistinguishable from control clones. Hence, these findings suggest that Lola-N fulfils its tumour suppressor function in coordination with other Lola isoform(s).

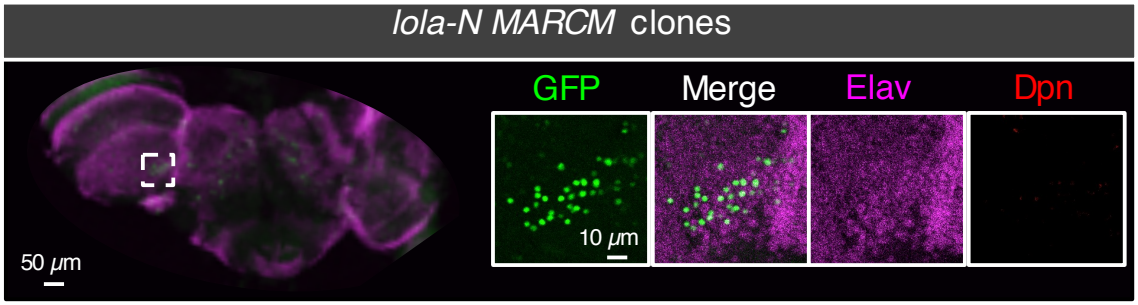

Figure 9: *lola-N* mutant MARCM clones in the *Drosophila* adult brain.

Anti-GFP (green) immunostaining was performed to identify GFP-positive MARCM clones. Neuronal cells (anti-Elav; magenta) in the adult brain deficient for Lola-N appear wildtypic with respect to the expression of the neuronal marker Elav and the Nb marker Dpn (red).

In contrast to the aforementioned examples we could recapitulate previously identified specific *lola* functions for few isoforms. Peripheral ISNb development was analysed in embryos deficient for *lola-K* and *lola-L*, respectively. Both isoforms have been reported to play non-redundant roles in the peripheral nervous system (PNS) by regulating ISNb axon growth (Goeke *et al.*, 2003). Anti-Fasciclin 2 (Fas2) immunostaining on mutant alleles obtained in our CRISPR/Cas9 screen could reproduce these previously described defects (**Figure 10A**). More precisely, individual depletion of *lola-K* and *lola-L* led to embryonic lethality accompanied by stalling of ISNb axon extension and impaired NMJ formation in the developing embryo.

Furthermore, previous studies identified a role for Lola in gonadal development during *Drosophila* embryogenesis (Erin L. Davies *et al.*, 2013). Only recently this gonad-specific function was assigned to the splice variant Lola-T (Erin L Davies *et al.*, 2013), a highly conserved isoform that shares a strong homology (92 %) to Lola-K (Goeke *et al.*, 2003). Similar to the loss of all Lola isoforms, the absence of Lola-T activity perturbs germ cell migration and gonad compaction, a phenotype that was recapitulated with our *lola-T* mutant allele (**Figure 10B**). Indeed, Anti-Vasa immunostaining on *lola* null and *lola-T* mutant embryos displayed dispersed germ cells und uncompacted gonads, thus verifying the previously characterised Lola-T function in gonadal development.

In conclusion, our obtained *lola* alleles could reproduce in most cases previously reported isoform-specific Lola functions. In few instances however, phenotypes could not be reproduced, likely due to previous off-target activity or to redundant functions among different Lola isoforms.

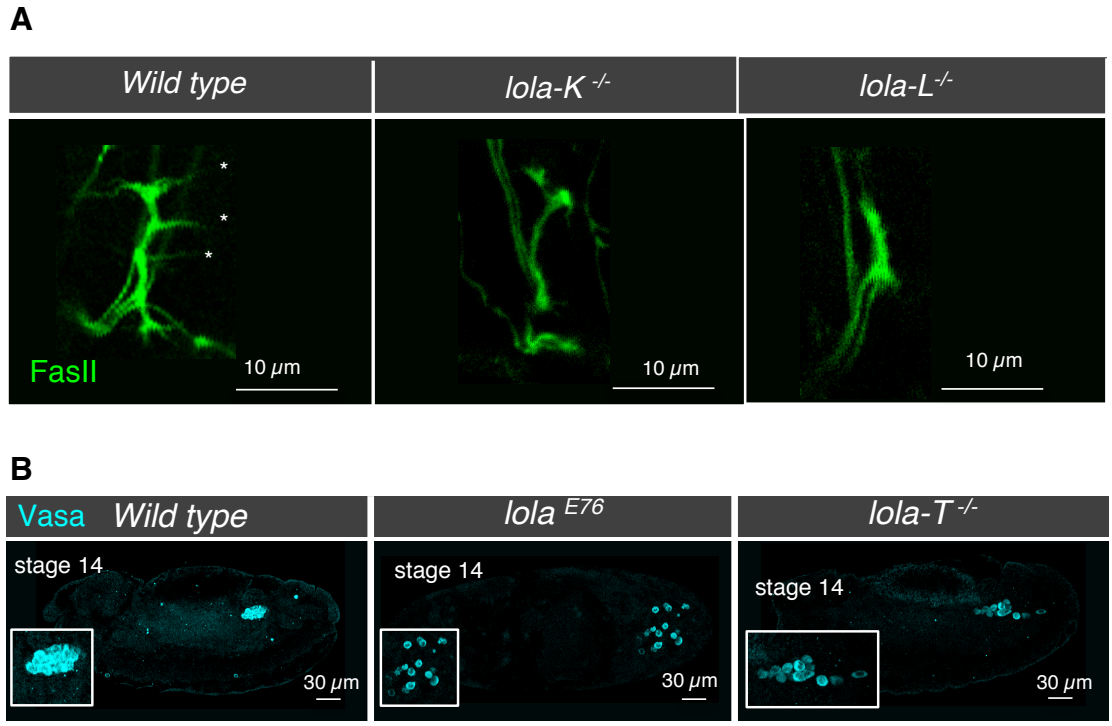

Figure 10: Proof of principle experiments to validate the CRISPR/Cas9-mediated *lola* KO screen.

(A) Anti-Fas2 staining (green) visualizes the peripheral ISNb motor nerve on stage 16 embryos. ISNb development is disrupted in both *lola-K* and *lola-L* mutant embryos. NMJs are highlighted by an asterisk. **(B)** Gonad formation is disrupted in both *lola-T* and *lola*^{E76} null mutant embryos, confirming previously described functions for Lola-T in gonadal development. Anti-Vasa staining (blue) visualizes germ cells on stage 14 embryos (lateral view).

4.3 Lola-A and Lola-H regulate locomotion in opposite directions

In order to address locomotive abilities of *lola* mutant alleles obtained in our study, climbing assays were systematically performed for all homozygous isoform-specific *lola* mutants. Using this assay, we found that individual mutation of the non-conserved isoforms *lola-A* and *-H* produced viable flies with peculiarities in their locomotion behaviour. Depletion of *lola-A* increased climbing speed of adult flies, leading to a state of hyperactivity (**Figure 11A**). In contrast,

lola-H KO flies showed impaired locomotion that is accompanied by clumsiness, as demonstrated by the inability of climbing (**Figure 11B**). To rule out off-target activity as a result of the CRISPR/Cas9 system, both fly lines were recombined with an artificial bacterial genomic construct (BAC), encoding the entire *lola* locus. Importantly, locomotion abnormalities observed for both *lola* mutants were restored to wildtype levels upon recombination with the *lola* BAC, thus restricting the induced mutation to the *lola* genomic region. While further investigations will be required to uncover the precise mechanism underlying locomotion control of these isoforms, our findings suggest an essential but opposing physiological function for Lola-A and Lola-H in regulating fly locomotion.

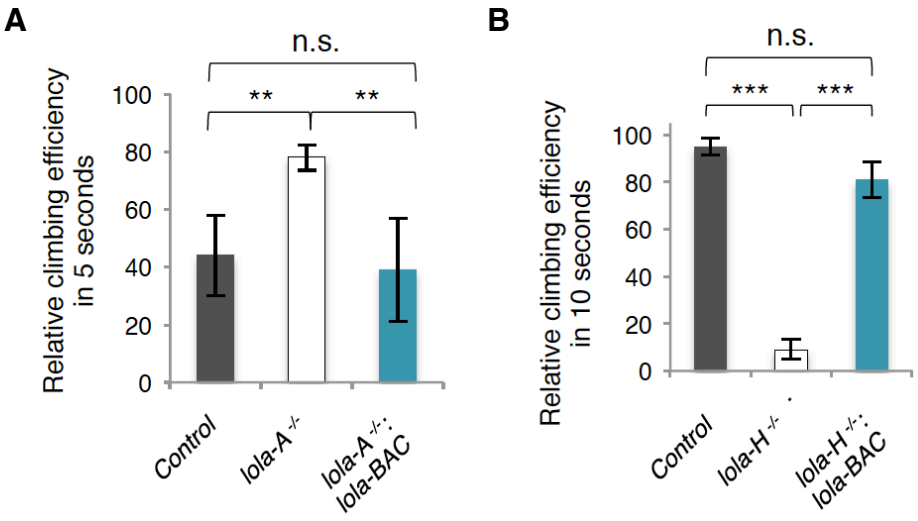

Figure 11: *lola-A* and *lola-H* mutant flies reveal locomotion abnormalities in opposing directions.

(A) *lola-A* mutant adult males are hyperactive, whereas *lola-H* **(B)** mutant flies display impaired locomotive abilities. Both phenotypes are restored to control levels by recombination with a *lola* BAC. Measurement intervals were 5 seconds for *lola-A* KO males and 10 seconds for *lola-H* KO males. Climbing assay were performed in five technical and three biological replicates. Statistical analysis was performed using ANOVA one-way t-test. **p-value<0.01, *** p-value<0.001. Error bars represent ±SD.

4.4 Lola-F regulates axon guidance processes at the embryonic ventral midline by activating numerous axon guidance genes

Among essential Lola isoforms is Lola-F, a nuclear protein encoding a highly conserved ZF motif (Goeke *et al.*, 2003; Zhang *et al.*, 2003). Lola-F was first discovered as an interactor of the chromosome kinase JIL-1 during embryonic development (Zhang *et al.*, 2003), implying a regulatory role for this splice variant during embryogenesis. Very recently it has been shown that Lola-F acts redundantly in combination with Lola-L to regulate larval Nb development (Wissel *et al.*, 2016).

Altogether, these findings indicate that Lola-F is involved in essential processes during embryonic and larval development. While initial approaches have been made in uncovering its role in the larval CNS, a physiological function for Lola-F in embryos has not yet been described.

4.4.1 Lola-F is required during embryonic development

In the absence of Lola-F activity, the vast majority of embryos failed to hatch as first instar larvae. A small percentage of so-called escapers managed to shed their embryonic chorion layer by hatching, however they subsequently failed to move and died within the next several hours during first instar larval stage. The initial *lola-F*^{Stop} allele we obtained using the CRISPR/Cas9 screen carried a 2bp-deletion and a subsequent frameshift downstream of the ZF motif, resulting in a premature stop codon (**Figure 12A**). In order to address the function to Lola-F C-terminal isoform-specific ZF, we generated a second *lola-F*^{ZNF} allele that specifically lacks the entire ZF domain. We were able to confirm embryonic lethality for this second *lola-F* allele.

Lola-F, also named Lola zf5 in a previous report (2003), is a 79,3 kDa protein that migrates as a 105-kDa protein on SDS-page. This knowledge allowed us to precisely detect Lola-F by immunoblotting using an anti-Lola antibody that recognizes the constitutive N-terminus shared by all Lola proteins (**Figure 12B**). The specific depletion of Lola-F was confirmed for both alleles using protein lysates from

homozygous mutant embryos. Importantly, the overall levels of other isoforms remained largely unchanged, suggesting that depletion of Lola-F does not or only mildly affect the expression of other Lola isoforms. In addition, immunoblotting using the Lola-F specific anti-Lola zf5 antibody (Zhang *et al.*, 2003) confirmed its depletion in *lola-F*^{Stop} embryos. The Lola zf5 antibody reacts to the immunogen sequence amino acid (aa) 427-748, whereas the 2 bp-deletion generated in the *lola-F*^{Stop} allele occurs at aa 550. The immunogen sequence is hence reduced by 198 aa and thus likely limits the immunoreaction between antibody and antigen (Zhang *et al.*, 2003). In order to further validate our mutant alleles, an anti-Lola zf5 immunostaining was performed on homozygous *lola-F*^{Stop} and control embryos (**Figure 12C**). We found that Lola-F was enriched in the developing nervous system while the staining was absent in mutant embryos. These results suggested that Lola-F might be involved in nervous-system related functions in embryos.

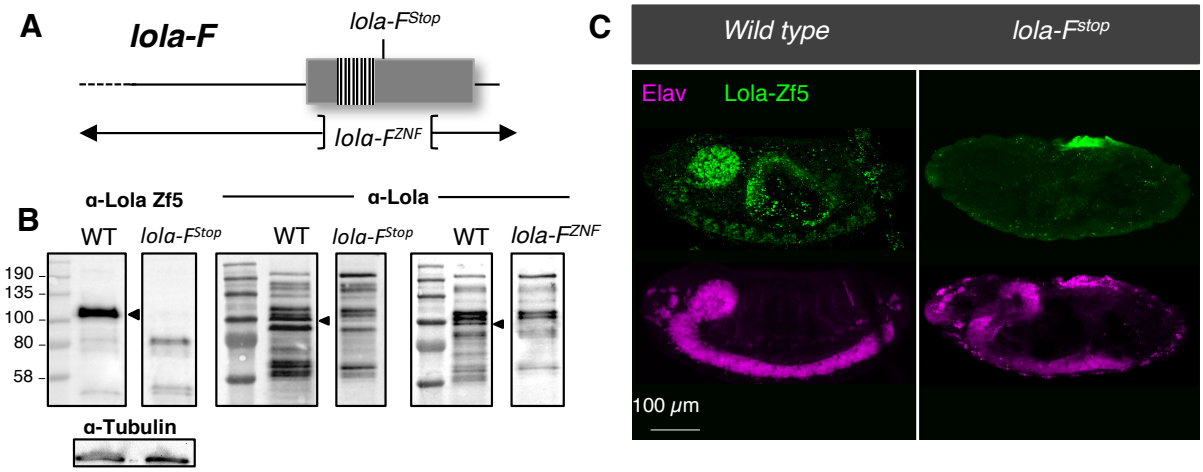

Figure 12: Validation of *lola-F* specific alleles.

(A) Scheme of *lola-F* specific genomic region. *lola-F*^{Stop} bears a 2-bp deletion resulting in a premature stop codon downstream of the ZF motif, while *lola-F*^{ZNF} lacks the entire ZF motif. **(B)** Immunoblotting using anti-Lola zf5 and anti-Lola antibodies on control and *lola-F* mutant lysates. Arrowheads depict the band specific for Lola-F. Anti-Tubulin was used as a loading control. **(C)** Immunostaining using the anti-Lola zf5 antibody (green). Control embryos display Lola-F protein in the nervous system (anti-Elav; magenta) and no immunofluorescence is detected in *lola-F*^{Stop} embryos. Lateral view on stage 13/14 embryos.

4.4.2 *lola-F* is expressed in neurons and neural stem cells of the developing nervous system

In order to characterize the physiological role of Lola-F during embryonic development, *in-situ* hybridizations were performed at different developmental stages. Expression analyses revealed significant enrichment of *lola-F* mRNA in the developing embryonic nervous system (**Figure 13A**). Importantly, the hybridization signal was lost in *lola-F*^{ZNF} mutant embryos, confirming the specificity of the *lola-F* probe. More precisely, early embryos (stages 10/11) displayed *lola-F* mRNA accumulation in the ventral nerve cord (VNC) and the embryonic brain at similar levels. Interestingly, subsequent embryonic development restricted *lola-F* mRNA expression to the brain lobes, while majority of the signal was lost in the VNC. Deeper analysis by fluorescent *in-situ* hybridization revealed a localization of *lola-F* mRNA to both Nbs and differentiated neurons during embryonic stages 10 to 13/14 (**Figure 13B**). However, as embryonic development proceeds, *lola-F* mRNA expression becomes restricted to Nbs of the central brain, where it was maintained at high levels until at least third instar larval stages (**Figure 13C**).

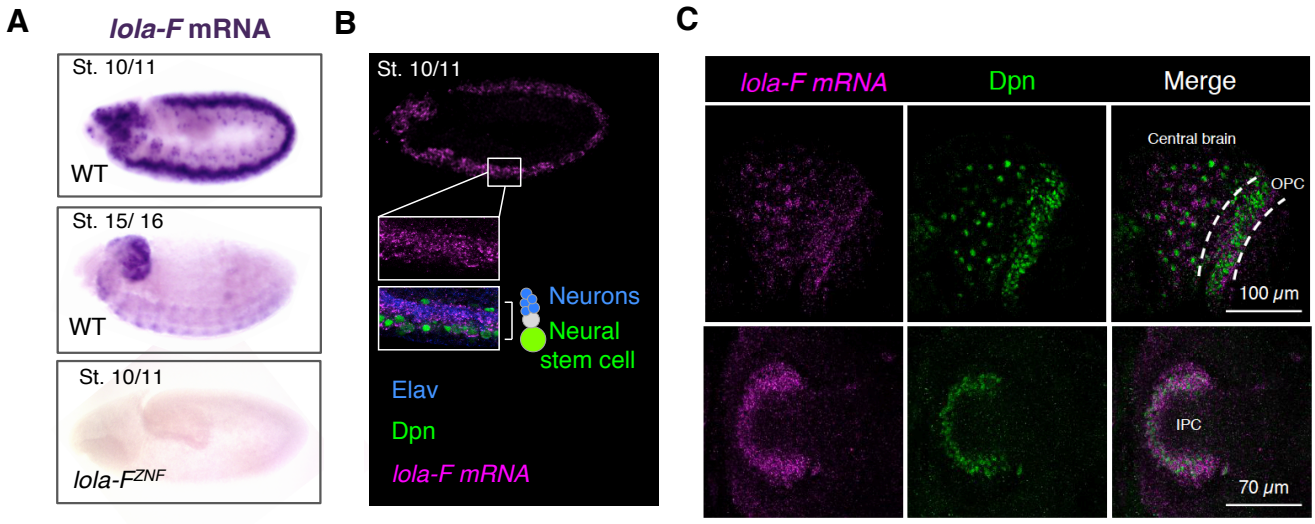

Figure 13: *lola-F* mRNA is enriched in the embryonic and larval CNS.

(A) *In-situ* hybridization using a *lola-F* probe. *lola-F* mRNA (magenta) is enriched in the embryonic nervous system and absent in *lola-F*^{ZNF} mutant embryos. **(B)** *lola-F* mRNA co-localizes with both the neuronal marker Elav (blue) and Nb marker Dpn (green; lateral view, stage 10/11). **(C)** *lola-F* mRNA is present in Nbs (anti-Dpn, green) of the central brain and the larval optic lobe, where it shows a strong enrichment in Nbs of the outer proliferation center (OPC) and inner proliferation center (IPC).

4.4.3 Depletion of Lola-F affects axon guidance along the embryonic ventral midline

To address our hypothesis that Lola-F might play an important role during CNS development, a systematic screen was performed to uncover potential nervous system abnormalities in the absence of Lola-F activity. For this purpose, control, *lola-F* and $lola^{E76}$ null mutant embryos were immunostained for different neural markers (**Figure 14**). The loss of all Lola isoforms was previously shown to strongly impair motorneuron axonal growth and pathfinding along the ventral midline (Crowner *et al.*, 2002; Goeke *et al.*, 2003). We could recapitulate this phenotype by performing an anti-Fas2 immunostaining on $lola^{E76}$ null mutant embryos. More precisely, $lola^{E76}$ embryos (stage 15/16) displayed stalled growth of motor axons accompanied by ventral midline crossings in majority of the embryonic hemisegments. Interestingly, a comparable phenotype was observed in the absence of *lola-F*. *lola-F* mutant embryos revealed axonal midline crossing events in most of the hemisegments. However, in contrast to the $lola^{E76}$ null allele, *lola-F* mutant embryos contained motor-axon bundles of increased thickness and length, indicating that axon growth is not as severely impaired in comparison to the loss of all *lola* isoforms.

In conclusion, our data indicate that Lola-F regulates axonal growth and guidance along the embryonic ventral midline, a function for which *lola* was first named by Giniger and colleagues in 1994.

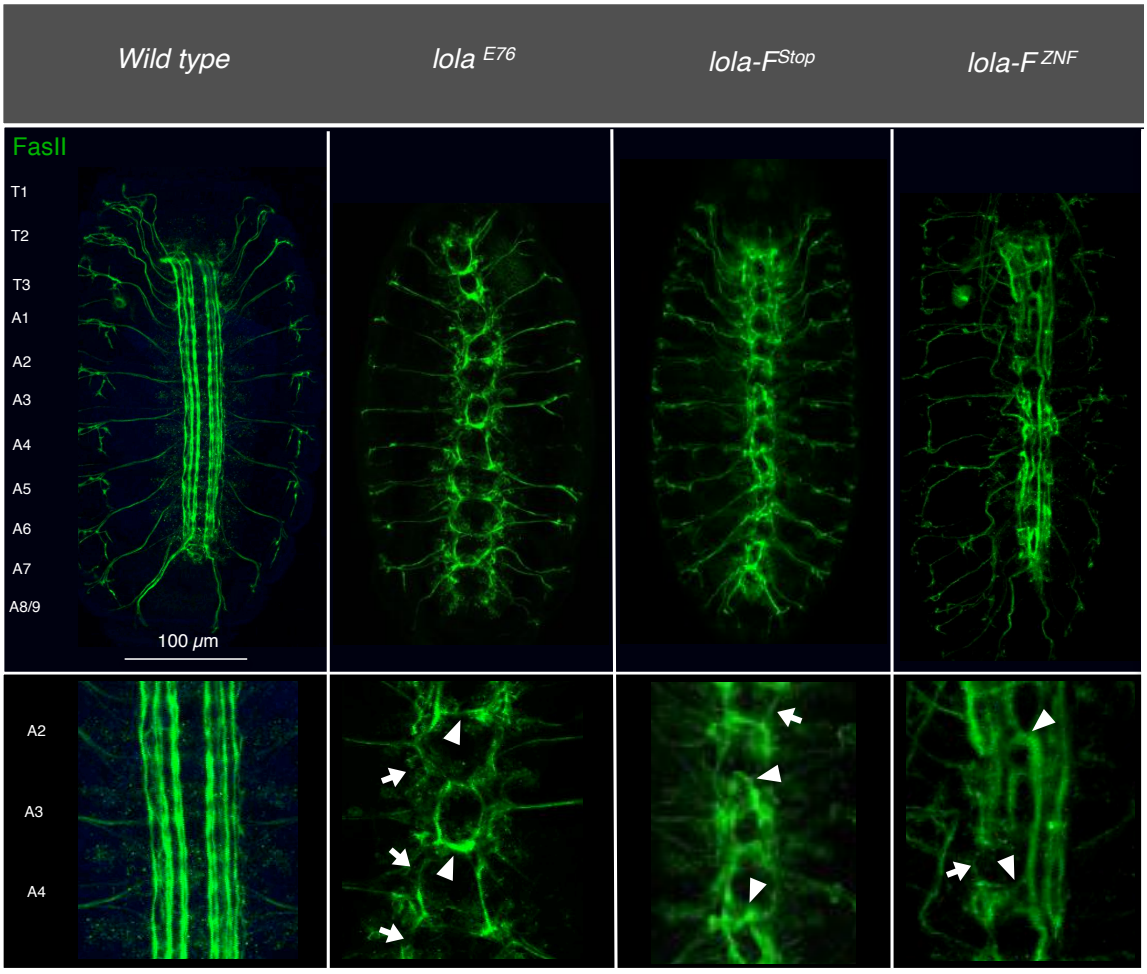

Figure 14: Lola-F regulates axon guidance during embryonic development.

(A) Immunostaining of the VNC using an anti-Fas2 antibody. Axonal pathfinding is disrupted in *lola-F* mutant embryos, similar to the defects observed for *lola*^{E76} null mutants. In comparison to *lola-F* mutants, *lola*^{E76} null mutants show more severe axon growth defects (arrows). Axonal midline crossings (arrowheads) are observed in the absence of all Lola isoforms, similar to the defects found in *lola-F* mutants. Ventral view on stage 15/16 embryos. Anterior is top.

4.4.4 Establishment of neural identity is unaffected in the absence of Lola-F

Defects in axon guidance may arise either from defects in the guidance system itself or can be an indirect consequence of alterations in neural identity (Younossi-Hartenstein and Hartenstein, 1993). To test the nature of the axonal guidance defects observed upon depletion of Lola-F, the number of neurons, Nbs and glial cells was analysed (**Figures 15A-C**). I found that the absolute number of all three cell-types was unaltered in *lola-F*^{Stop} embryos, implying that neuronal identity is unaffected. It is noteworthy, however, that glial cell arrangement was strongly disrupted in the absence of Lola-F activity (**Figure 15B**). Evidences from recent years suggest that axon guidance cues similarly regulate glial cell migrations in the developing nervous system. For instance, the well-characterized and conserved axon guidance gene *Netrin* was shown to build guidance cues for longitudinal axons during embryonic nervous system development (Harris, Sabatelli and Seeger, 1996). Intriguingly, the loss of Netrins likewise impaired glial cell arrangement along the embryonic ventral midline (von Hilchen *et al.*, 2010), suggesting that impairment of axonal pathfinding will likely also affect glial cell migration.

In conclusion, the depletion of Lola-F has no effect on the establishment of neural identity. It however leads to glial cell rearrangement along the ventral midline, most likely as an indirect consequence of impaired axonal guidance.

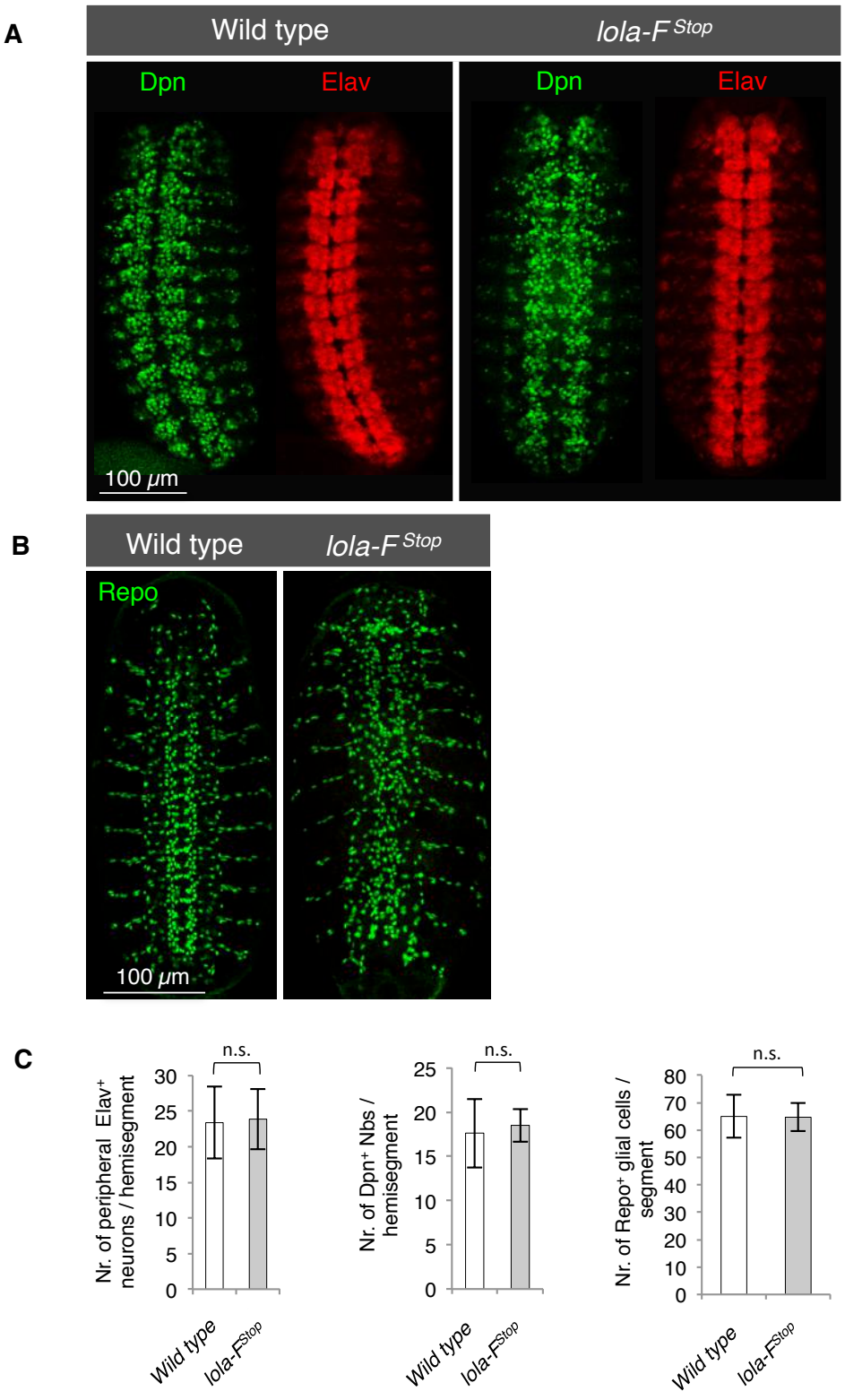

Figure 15: Neural identities are properly established in *lola-F* mutant embryos.

(A) *lola-F*^{Stop} mutant embryos show no defect in the number of neurons (anti-Elav, red) quantified in **(C)** (stage 13/14 embryos, ventral view; n=8, p-value 0.84) and Nbs (anti-Dpn, green; n=7, p-value 0.93). ANOVA one-way t-test was performed. Data represents average±SD. **(B)** Glial cell arrangement is perturbed in *lola-F*^{Stop} mutants while the number of glial cells (anti-Repo; green) shows no aberration from control embryos as quantified in (C) (stage 13/14 embryos, ventral view; p-value 0.57). ANOVA one-way t-test was performed. Data are represented as average of eight analysed segments ±SD.

4.4.5 Lola-F is required in neurons to regulate axonal pathfinding along the embryonic ventral midline

Previous applications of the CRISPR/Cas9 system in *Drosophila* have led to numerous off-target events that need to be evaluated carefully (unpublished data from the Roignant group, IMB Mainz). To this end, *trans*-heterozygous flies were generated by recombining both *lola-F* alleles with a deficiency line that lacks the entire *lola* locus. These *trans*-heterozygous combinations gave indistinguishable phenotypes for both alleles, confirming that the axon guidance phenotype is *lola* specific. Moreover, expression of a *lola* BAC was sufficient to rescue the axonal guidance defects and also lethality of both alleles (data not shown), confirming an essential role for Lola-F in the process of embryonic axonal guidance along the ventral midline.

We thereafter aimed to identify the cell-type specific requirement for Lola-F by generating a transgenic line expressing Lola-F under the control of UAS promoter. Ectopic neuronal Lola-F cDNA expression using *elav*-GAL4 rescued the axonal guidance defects observed in *lola-F* mutant embryos (**Figure 16**). In contrast, ectopic expression of other Lola isoforms (Lola-H, Lola-O) was not sufficient to restore proper axon guidance cues, confirming a Lola-F specific neuronal role in axonal pathfinding. Intriguingly, ectopic neuronal Lola-F cDNA expression using *Elav*-GAL4 in a *lola-F* mutant background did not rescue lethality that occurs during first instar larval stages. This data suggests that 1) Lola-F plays an axon guidance independent function in cell-type(s) other than neurons, or 2) neuronal ectopic Lola-F expression is lethal at post-embryonic stages. Our *in-situ* hybridization assays revealed a strong neuronal *lola-F* mRNA enrichment at early embryonic development (stages 10-13), which was subsequently reduced towards the end of embryogenesis (stages 15-17). Hence, these findings support our second hypothesis, suggesting that Lola-F expression must be tightly regulated. In accordance with this, ectopic neuronal Lola-F levels in a wild type background induced mild axon crossing defects, similar to what has been observed in the absence of Lola-F activity.

Taken together, our findings suggest that Lola-F levels require a fine-tuned regulation in order to properly fulfil its function in regulating axonal pathfinding along the embryonic ventral midline.

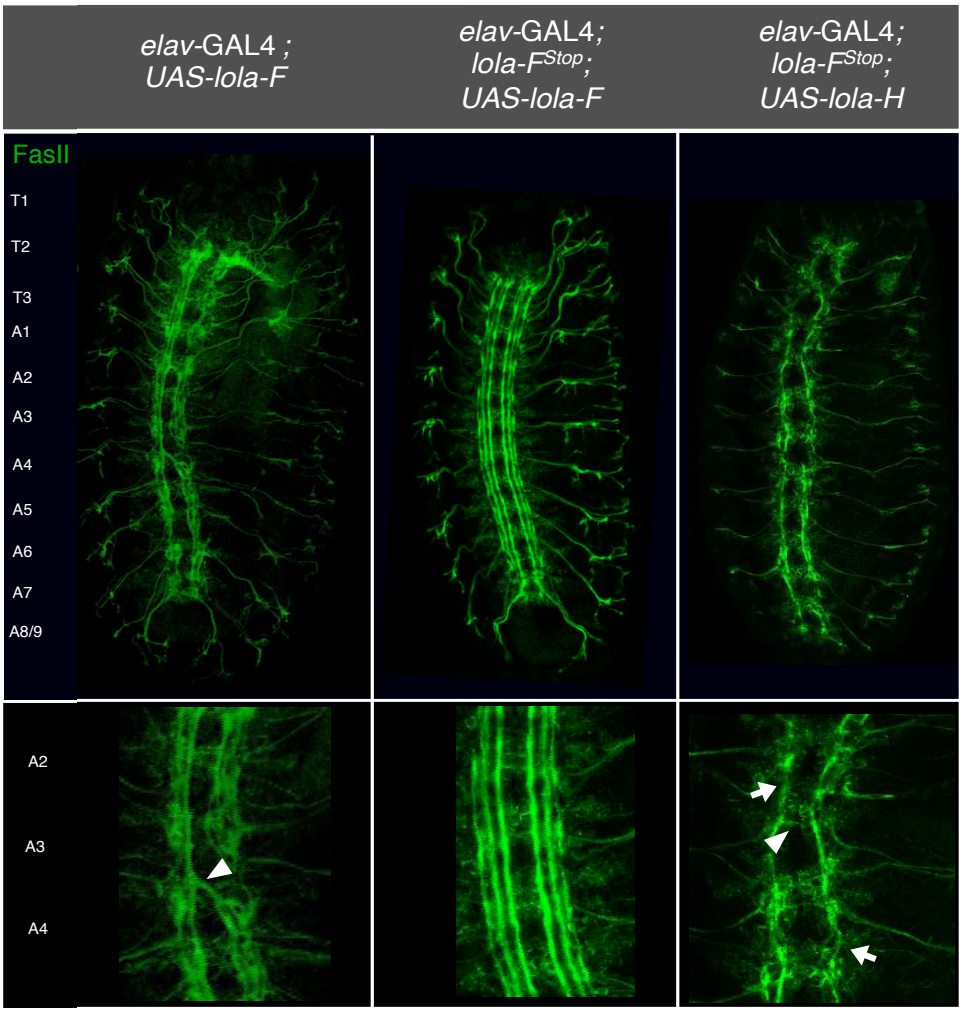

Figure 16: Lola-F regulates embryonic axonal guidance.

(A) Immunostaining of the VNC using an anti-Fas2 antibody on stage 15/16 embryos (ventral view; anterior is top). Neuronal ectopic Lola-F expression in a wild type background induces axonal midline crossing (arrowhead). Axon guidance defects in *lola-F*^{Stop} embryos are restored to wild type levels upon ectopic neuronal Lola-F cDNA expression. Neuronal ectopic Lola-H expression has no profound effect on axonal midline crossing and axon stalling (arrows) in *lola-F*^{Stop} embryos.

4.4.6 Majority of Lola isoforms is expressed in neurons during embryonic development

We next wondered whether other isoforms that are essential during embryonic development were also involved in regulating neuronal processes. To this end, transcriptome analysis was performed on FACS-sorted neurons to identify *lola* isoforms expressed specifically in these cells. For this purpose, neuronal UAS-mCherry expression was induced by *elav*-GAL4 and embryos were processed at stage 15/16 (13-16 hours after embryo laying (AEL)). Neuronal cells were subsequently FACS sorted and subjected to RNA-sequencing. Similar to previous findings by *in situ* hybridizations (Goeke *et al.*, 2003), we found that most isoforms were expressed in neurons at this developmental stage (**Figure 17**). More precisely, the most expressed isoforms were Lola-A, -F, -H, -K and –N. In contrast, isoforms Lola-J, -M, -O, -P and –B were barely detectable. The strong neuronal *lola-F* expression confirms our *in situ* hybridization data and supports our finding that Lola-F primarily acts in neurons to regulate motor-axon guidance during embryonic development. In accordance with the previously identified function for Lola-N in repressing Nb genes in neurons (Southall *et al.*, 2014), this splice variant showed the strongest neuronal expression together with Lola-H. Interestingly, our CRISPR/Cas9 screen identified a potential role for Lola-H in regulating locomotion behavior. Based on the FACS data, we predict that Lola-H carries this role specifically in neurons, where it likely regulates processes responsible for *Drosophila* locomotion. Further experiments will be required to identify the precise physiological function of Lola-H in neuronal cells.

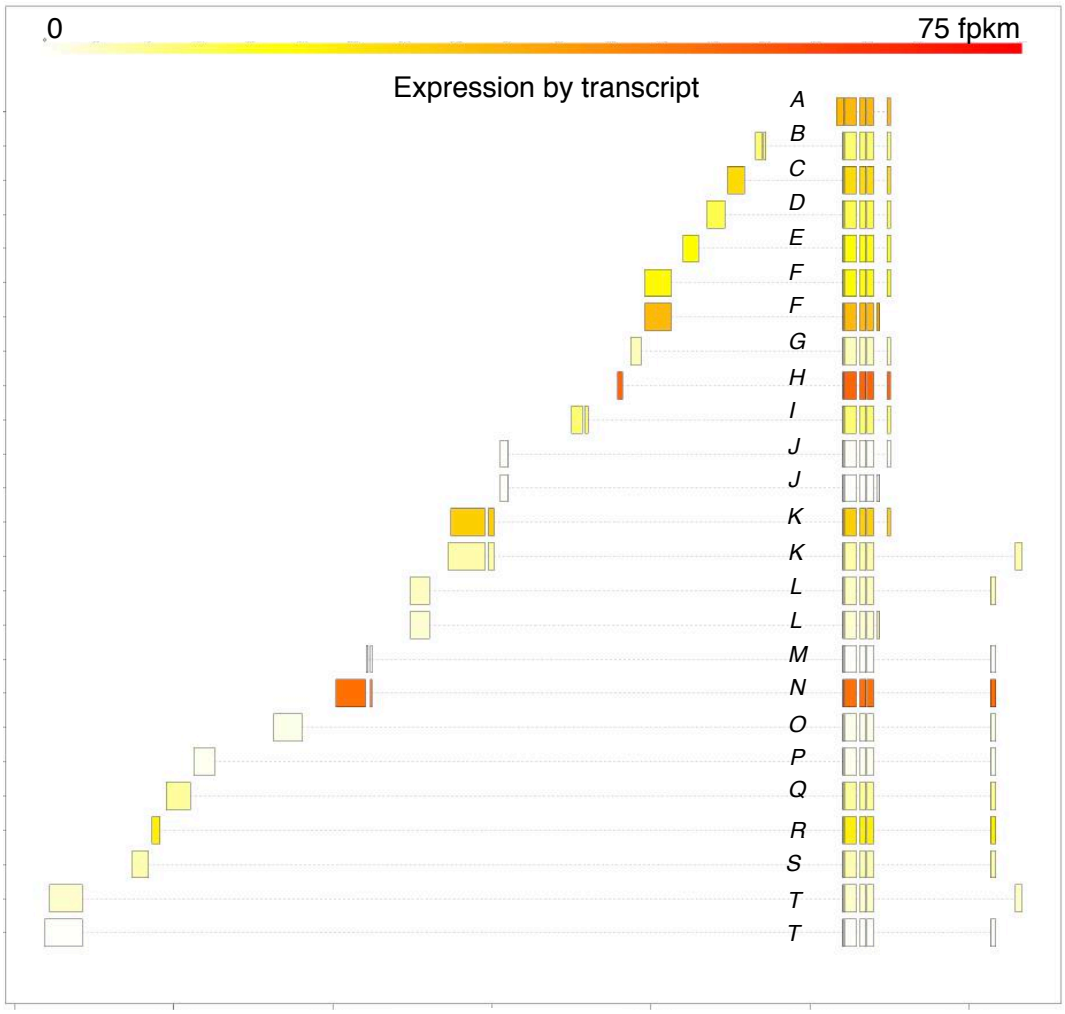

Figure 17: *Iola* isoform expression in FACS-sorted neurons.

Transcriptome analysis was performed on FACS-sorted neurons 13-16 hr AEL in order to identify the neuronal expression of individual *Iola* isoforms. Neuronal mCherry expression was induced by *elav*-GAL4 and neurons were FACS sorted based on mCherry expression. The average of seven biological replicates is shown. The 5'-UTR is on the right, C-terminal exons are left.

4.4.7 None of the remaining neuronal Lola isoforms is essential for axonal guidance in the VNC

Our FACS data revealed a high to moderate neuronal expression of the isoforms Lola-K, Lola-L and Lola-N. To analyze whether these essential splice variants might regulate axonal guidance, anti-Fas2 staining was performed on homozygous mutant embryos. Remarkably, none of the essential Lola isoforms appear to be required for axonal pathfinding along the VNC (**Figure 18A**). Only minor proportions of *lola-K* mutants occasionally displayed crossing defects, so-called 'wiggles', between the hemisegments A5 and A6 (**Figure 18B**).

Previous studies reported a non-redundant role for the isoforms Lola-K and Lola-L in regulating muscle innervation by the peripheral ISNb (Goeke *et al.*, 2003). As described previously (see 4.2), our obtained CRISPR mutant alleles could recapitulate the hitherto described phenotype in ISNb aberration for *lola-K* and *lola-L* mutant embryos. Remarkably, a similar phenotype was observed for *lola-F* mutants (**Figure 18C**). Depletion of Lola-F lead to stalled ISNb axon growth with a subsequent failure to form NMJs with surrounding muscles, suggesting that this splice variant is likewise involved in peripheral ISNb development.

In summary, our findings provide evidences that Lola-F is the major isoform that regulates axonal pathfinding in the embryonic VNC. Moreover, Lola-F is further required in peripheral ISNb development, a process that is also regulated by the isoforms Lola-K and Lola-L in a non-redundant manner.

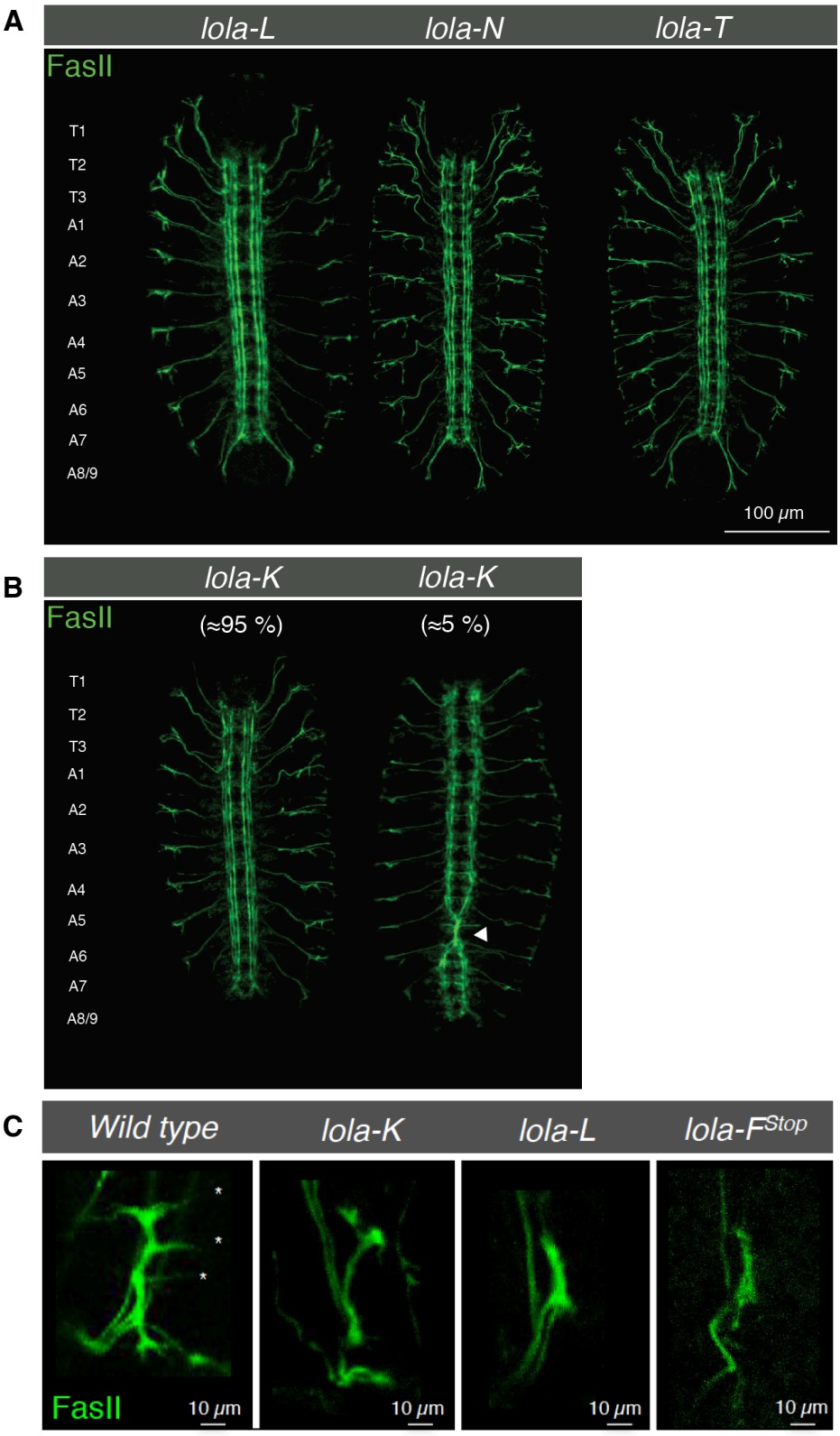

Figure 18: The remaining lethal *lola* alleles display a wildtypic VNC.

(A) Immunostaining of the VNC using an anti-Fas2 antibody (green) on lethal alleles (ventral view, stage 15/16). (**B**) Minor proportions of *lola-K* mutants exhibit 'wiggles' of axonal tracts (right, arrowhead), while majority of homozygous embryos reveal a wildtypic VNC (left). (**C**) Peripheral ISNb development is disrupted in *lola-K* and *lola-L* mutant embryos (lateral view, stage 16). Similarly, *lola-F*^{Stop} mutant embryos display ISNb axon stalling and a failure to form NMJs (anti-Fas2). NMJs are highlighted by an asterisk.

4.4.8 Lola-F positively regulates several axon guidance genes

Previous studies identified the repulsive ligand Slit and its receptor Robo as targets of Lola in its axonal guidance function during embryonic neurogenesis (Crowner et al., 2002). Lola positively regulates Slit and Robo levels, which repels axons away from the midline and subsequently prevents axonal midline crossings. In contrast, Lola was shown to repress the actin nucleation factor Spire, which has earlier been described to regulate motor axon growth (Gates et al., 2011). The combinational effect of Lola on Slit/Robo and Spire levels is believed to account for the severe defects on axon growth and guidance observed in the absence of all Lola isoforms. Microarray analysis using *lola* null mutant RNA extracts revealed, however, that expression of these factors was only mildly affected, suggesting that other factors might account for the severity of the phenotype.

To get further insights into the mechanism by which Lola controls axonal pathfinding we took advantage of our specific *lola-F*^{Stop} allele to perform a transcriptome analysis at embryonic stage 15 (13+2 AEL), when majority of axon growth and guidance events is taking place. In addition, samples from *lola*^{E76} null mutant embryos were included to compare the identity of affected genes with the one derived from the depletion of Lola-F only. Transcriptome analysis revealed that 465 genes and 586 genes were significantly up-, and down-regulated, respectively, in *lola-F* mutant embryos (**Figure 19A;** adjusted P-value <0.01). GO term analysis identified enrichment for genes involved in neuronal development and axon guidance processes specifically for down-regulated genes (**Figures 19C**), emphasizing the role of Lola-F in regulating embryonic axogenesis. Affected down-regulated genes involve the well-described axon guidance genes *Netrin-B*, *futsch*, *Dscam1* and *Cadherin-N*. Furthermore, among down-regulated genes, 217 (37%) were also found reduced in the absence of all Lola isoforms, including the previously described targets *slit* and *robo1* (**Figures 19A-B**). However, in contrast to the *lola*^{E76} null mutant, the absence of Lola-F activity has no significant effect on *spire* expression, indicating that other Lola isoforms must control its level (**Figure 19B**). The unaltered *spire* expression in *lola-F* mutants might account for the milder phenotype with regard to axon growth compared to the loss of all Lola isoforms. Moreover, potential antagonistic isoform-

specific Lola functions might nullify each other's effect, which would explain that only a subset of genes that are affected in the *lola-F* mutant is also misregulated upon the complete loss of Lola.

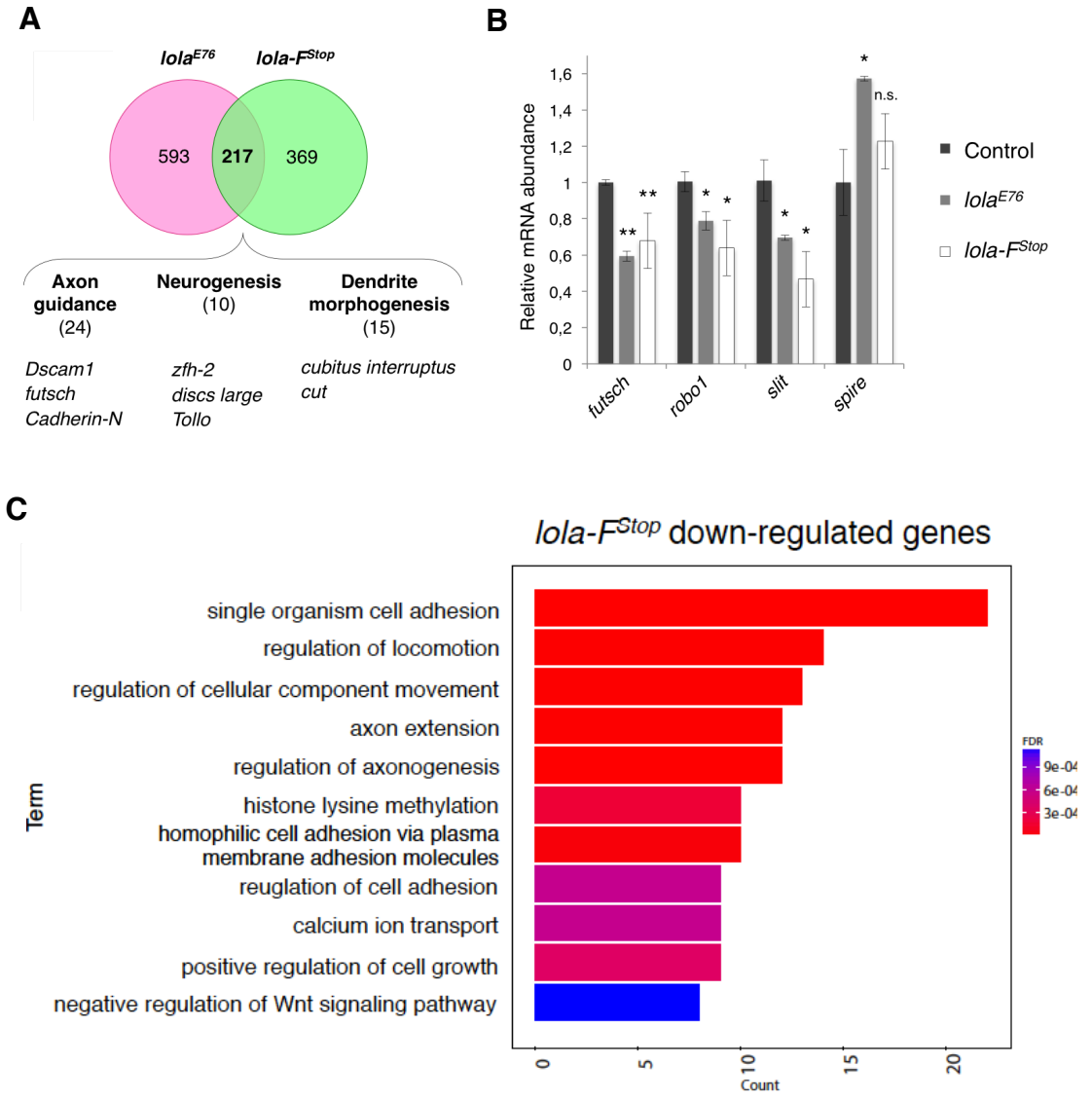

Figure 19: Lola-F positively regulates axon guidance genes.

(A) Transcriptome analysis of mutant RNA extracted from *lola-F*^{Stop} and *lola*^{E76} null mutant embryos (13-15 hr AEL) reveals 217 commonly down-regulated genes. Highlighted are examples of shared target genes involved in axon guidance, neurogenesis and dendrite morphogenesis. **(B)** qRT-PCR for selected genes on *lola*^{E76} and *lola-F*^{Stop} mutant RNA extracted from stage 15 embryos. ANOVA t-test was performed to test statistical significance. *** p<0.001, **p<0.01; *p<0.05. Data are represented as median ±SD **(C, D)** Significant GO terms (adjusted *P* value < 0.05) of differentially expressed genes in *lola-F*^{Stop} mutant embryos. Analysis was performed by Nastasja Kreim (IMB core facility) using the Bioconductor package of GOstats. **(C)** Down-regulated genes in *lola-F*^{Stop} embryos reveal enrichment for axon extension and regulation of axogenesis.

4.4.9 Futsch is a key target in Lola-F-mediated axonal guidance

Among the top 15 down-regulated genes that are common in both *lola* null and *lola-F* mutants was *futsch*, a well characterized and conserved axon-guidance gene. The axonal defects observed for *lola-F* KO embryos mimic the previously characterized *futsch*^{P158}mutant phenotype (Hummel et al., 2000). Depletion of Futsch lead to stalling of the peripheral ISNb motornerve and a subsequent failure to form NMJs, similar to what we observed in the absence of isoforms Lola-F, -K and –L (see 4.3.7). Most importantly, *futsch*^{P158} mutant embryos revealed defects in motor axon guidance at the ventral midline, reminiscent to *lola-F* mutants (Hummel et al., 2000). We confirmed the reduction in *futsch* transcript levels upon depletion of Lola-F by qRT-PCR (**Figures 19B, 20A**) and *in-situ* hybridization (**Figure 20B**). In addition, immunostaining on *lola-F*^{Stop} embryos using the Futsch-specific antibody anti-22C10 showed a reduced fluorescent intensity on peripheral axons, indicating a decrease of Futsch protein in the absence of Lola-F activity (**Figure 20C**).

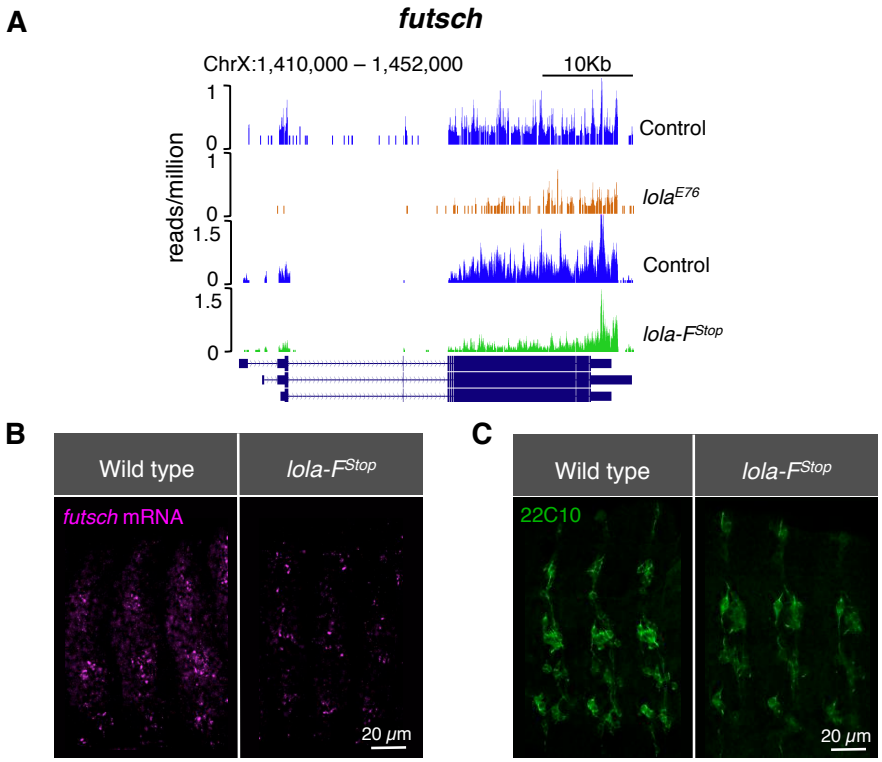

Figure 20: *futsch* levels are reduced in the absence of Lola-F activity.

(A) PolyA-selected mRNA sequencing tracks of the *futsch* locus. Transcriptome analysis was performed on RNA isolated from embryos 13+2 hr AEL. **(B)** *In-situ* hybridization using a *futsch*-specific probe shows decreased mRNA levels in *lola-F*^{Stop} mutant embryos (stage 15/16, lateral view on peripheral neurons; anterior is left; three hemisegments are shown). **(C)** Futsch protein levels were

reduced in the absence of Lola-F activity. Anti-22C10 immunostaining was performed on stage 15/16 embryos to detect Futsch protein levels. Ventral view is reminiscent to (B).

To examine whether the effect on Futsch in the absence of Lola-F contributes to the observed phenotype of axonal midline crossing we tested whether restoring its levels in neurons could rescue the observed axonal defects. To this end, a commercially available UAS-Futsch line was recombined with the neuronal *elav*-GAL4 driver line. Ectopic neuronal Futsch expression increased fluorescent intensity of an anti-22C10 immunostaining (**Figure 21A**). In addition, Futsch levels were restored to wild type levels in embryos deficient for *lola-F*. Remarkably, this ectopic Futsch expression was sufficient to partially restore both axonal guidance in the VNC and ISNb development in the PNS (**Figures 21B-C**). In control embryos (*elav*-GAL4, UAS-*futsch;* stage 15/16) no midline crossing events were observed. In contrast, *lola-F* mutants exhibited axonal midline crossings in the vast majority of hemisegments (9 midline crossings/embryo in *lola-F*^{Stop} embryos; 4.5 midline crossings/embryo in *lola-F*^{ZNF} embryos; n=9), which were significantly reduced upon ectopic neuronal *futsch* expression (2.5 midline crossings/embryo for *lola-F*^{Stop}, n=9; p-value<0.001; 1.9 midline crossings/embryo for *lola-F*^{ZNF}, n=9; p-value<0.01). A similar restoring effect was observed regarding peripheral ISNb development. In wild type, the ISNb connects with surrounding muscles via three NMJs. In the absence of Lola-F activity, however, ISNb growth was stalled and NMJs were not formed properly (0.8 NMJs/hemisegment; p-value<0.001 compared to 2.5 NMJs of control embryos; n=5). Supplying ectopic *futsch* partially restored ISNb axon growth and NMJ formation of *lola-F*^{Stop} mutants (1.8 NMJs/hemisegment, n=5; p-value<0.05 compared to *lola-F*^{Stop}).

In conclusion, these findings demonstrate that Lola-F regulates axonal pathfinding by positively regulating the expression of numerous axon guidance genes during embryogenesis. One key target gene in this process is *futsch*, which encodes a microtubule associated protein that was previously identified to regulate axonal guidance in the *Drosophila* CNS.

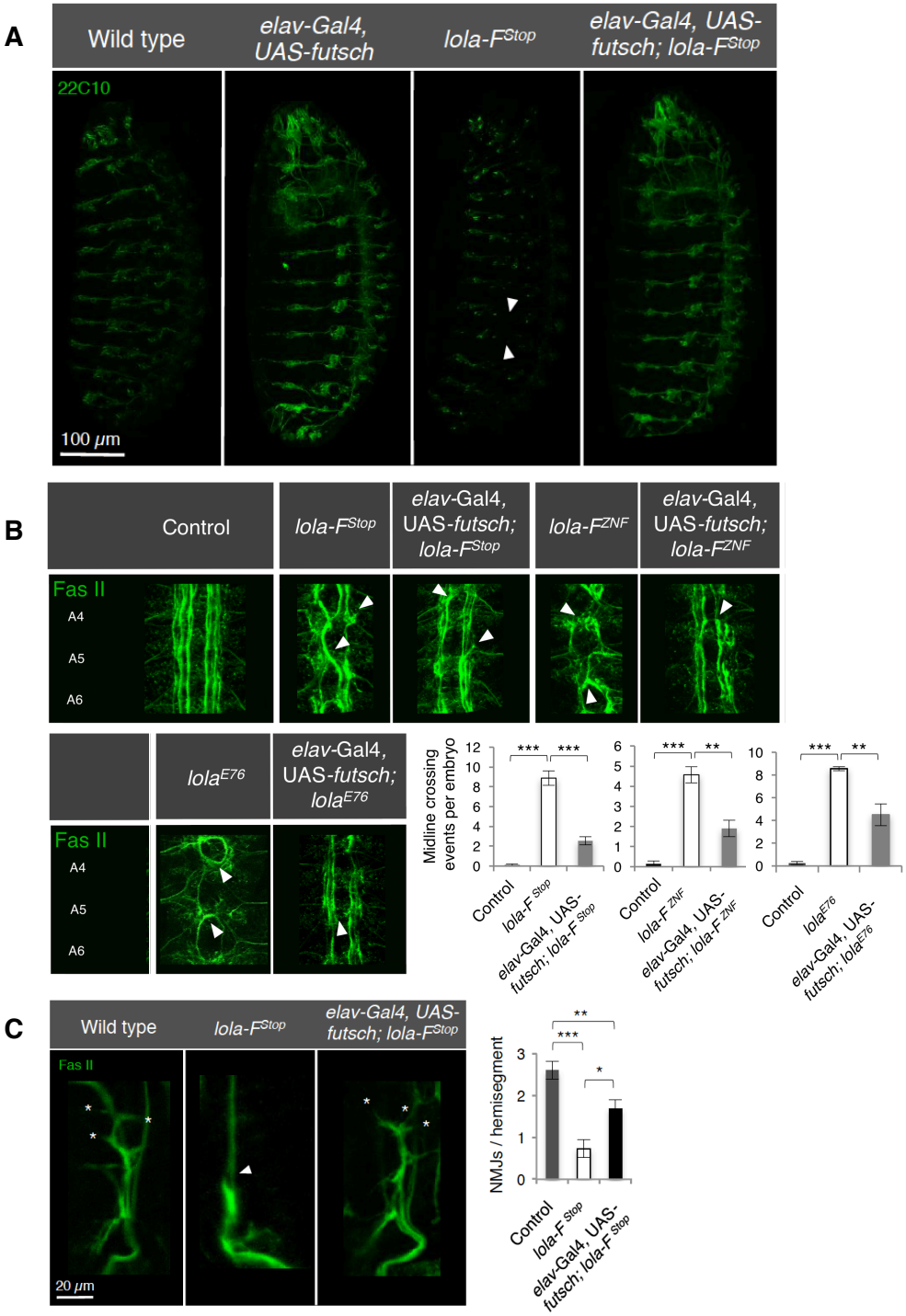

Figure 21: Ectopic Futsch levels partially rescue axonal midline crossing of *lola-F* mutant embryos.

(**A**) Futsch overexpression increases fluorescent intensity of an anti-22C10 immunostaining. *lola-F*^{Stop} mutants reveal decreased Futsch protein levels and defective peripheral axon tracts (arrowheads), which are restored upon ectopic neuronal Futsch expression. Laser settings were unchanged between imaging. Lateral view on stage 15/16 embryos, anterior is top. **(B,** left**)** Immunostaing of the VNC using an anti-Fas2 antibody to analyse midline-crossing events. Ectopic neuronal Futsch expression partially rescues axonal midline crossing of *lola-F*^{Stop} and *lola-F*^{ZNF} embryos. Ventral view on stage 15/16 embryos; anterior is up; three segments are shown **(B**, right) Quantification of midline-crossing events. Nine embryos were analysed and tested for significance using ANOVA one-way t-test. ***p-value<0.001. Data are represented as average

±SEM. **(C**, left**)** ISNb development is impaired upon Lola-F depletion (arrow) and is partially rescued by neuronal ectopic Futsch expression. NMJs are marked by asterisk. Lateral view on stage 15/16 embryos; anterior is left. **(C**, right) Quantification of NMJs formed per hemisegment. Fifteen NMJs were analysed in 5 embryos and tested for significance using ANOVA one-way t-test. ***p-value <0.001, **p-value<0.01, *p-value<0.05 Data are represented as as average ±SEM.

4.4.10 Ectopic neuronal Lola-F expression has no effect on Futsch levels

Depletion of Futsch was previously shown to alter axonal pathfinding along the embryonic ventral midline (Hummel *et al.*, 2000b). Our findings support a model in which Lola-F controls embryonic axon guidance in the VNC by positively regulating *futsch*. To address whether Lola-F directly activates *futsch* transcription, we analyzed its levels after ectopic neuronal Lola-F cDNA expression (**Figures 22A-B**). We found that elevated Lola-F doses had no effect on *futsch* levels, indicating that Lola-F alone is not sufficient to transcriptionally activate *futsch* expression. Furthermore, in contrast to the axonal defects observed in the absence of Futsch activity, neuronal overexpression of *futsch* did not impair growth and guidance of motor axons along the ventral midline (**Figure 22C**).

Previous findings suggest that a splice variant of the BTB-ZF protein Tramtrack (Ttk) negatively regulates *futsch* transcription (Giesen *et al.*, 1997; Hummel *et al.*, 2000b). To test whether the reduced *futsch* levels observed in the absence of Lola-F activity was indirectly mediated by upregulation of Ttk levels, *ttk* expression was analysed in *lola-F*^{Stop} embryos (**Figure 22D**). A mild down-regulation of both *ttk* isoforms was observed, suggesting that impaired axon guidance upon Lola-F depletion is not mediated by a change in Ttk levels.

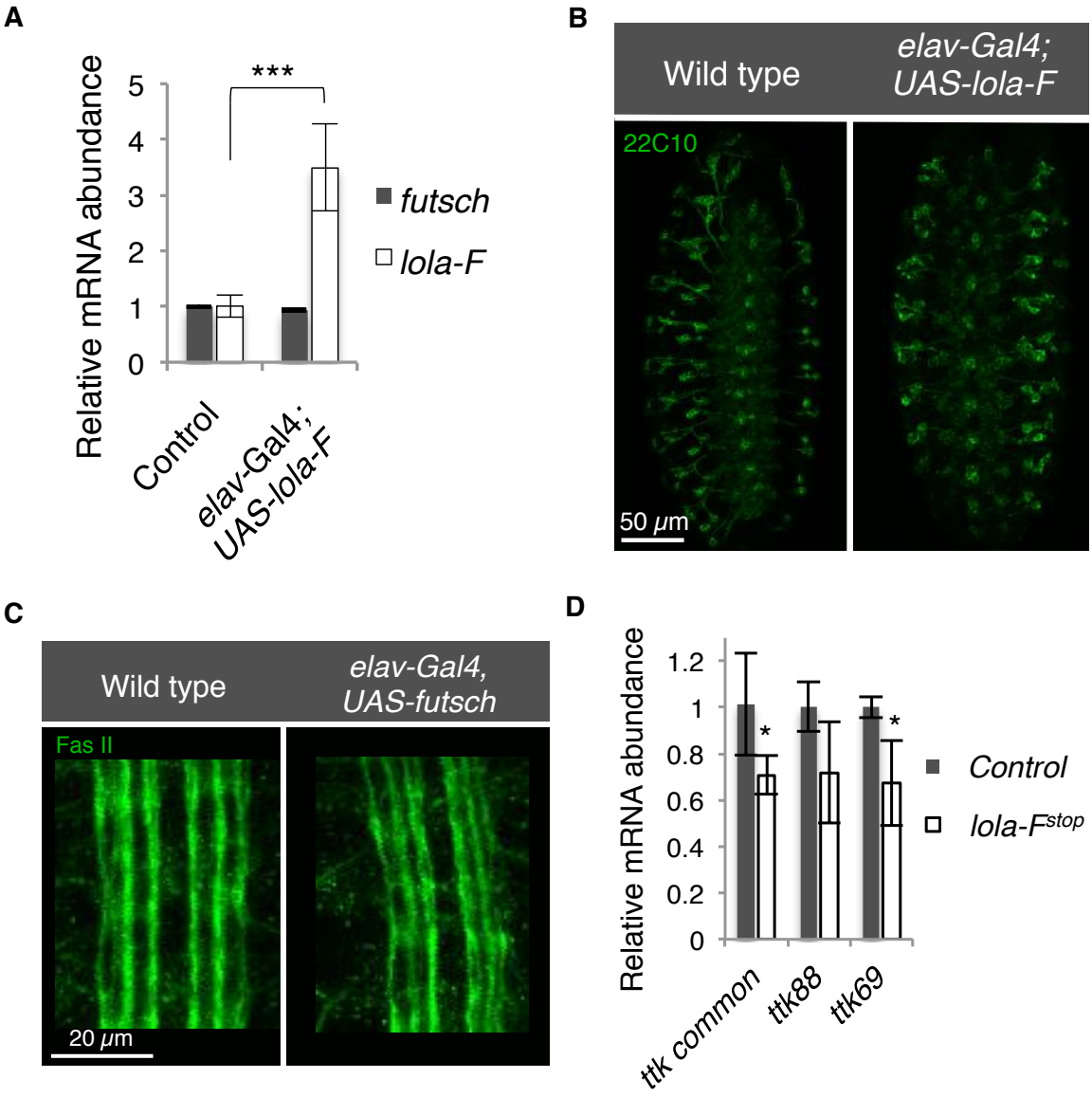

Figure 22: Ectopic neuronal Lola-F cDNA expression has no effect on Futsch levels.

(A) qRT-PCR was performed on RNA extract isolated from embryos 13+2 hr AEL. Ectopic neuronal Lola-F cDNA expression is unable to elevate *futsch* transcript levels. Data are represented as average ±SD; ***p-value<0.001. **(B)** Anti-22C10 immunostaining on stage 15/16 embryos to monitor Futsch protein levels. Ventral view, anterior is top. Laser settings were unchanged between recordings. **(B)** Ectopic neuronal Futsch expression does not affect axon guidance of motorneurons (anti-Fas2) along the ventral midline. Ventral view on stage 15/16 embryos, anterior is top. Three segments are shown. **(D)** Ttk levels are moderately downregulated in the absence of Lola-F activity. qRT-PCR was performed to track *ttk* expression in *lola-F*^{Stop} embryos 13+2 hr AEL. Data are represented as average ±SD; * p-value<0.05.

4.4.11 The loss of Lola-F has no effect on larval brain development

The observation that *lola-F* mRNA is strongly enriched in larval Nbs prompted us to ask whether Lola-F might play a specific function during larval brain development, distinct from its role in embryonic axon guidance. To this end, *lola-F*^{Stop} and control flies were recombined with FRT42D sites, which were subsequently used to generate MARCM clones in the third instar larval brain. In order to specifically generate *lola-F* mutant in Nbs, MARCM clones were induced in freshly hatched first instar larvae, at the time when Nbs start to divide and generate many progeny cells (Truman, Taylor and Awad, 1993). Surprisingly, Nb-specific MARCM clones for both *lola-F* alleles appeared indistinguishable from control clones (**Figure 23A**). Quantification of the total cell number per clone revealed no difference for any given Nb lineage (**Figures 23B-C**; p-value>0.2 for Nb type I lineages; p-value>0.9 for Nb type II lineages), suggesting that the loss of Lola-F alone is not sufficient to impair neuronal development in the larval brain. Meanwhile, a study was published in which combinational depletion of Lola-F and Lola-L by RNAi-mediated KD resulted in over-proliferation of Type II Nbs in the larval central brain (Wissel et al., 2016). In accordance with our data, individual KD of either of these two isoforms had no effect on Nb proliferation, suggesting that Lola-F and Lola-L act redundantly in controlling self-renewal of Type II Nbs in the central brain. While further research is necessary to understand how these two isoforms regulate Nb development, these findings emphasize the complexity of Lola isoforms, which are acting either individually or redundantly to regulate distinct physiological functions in a cell-type specific manner.

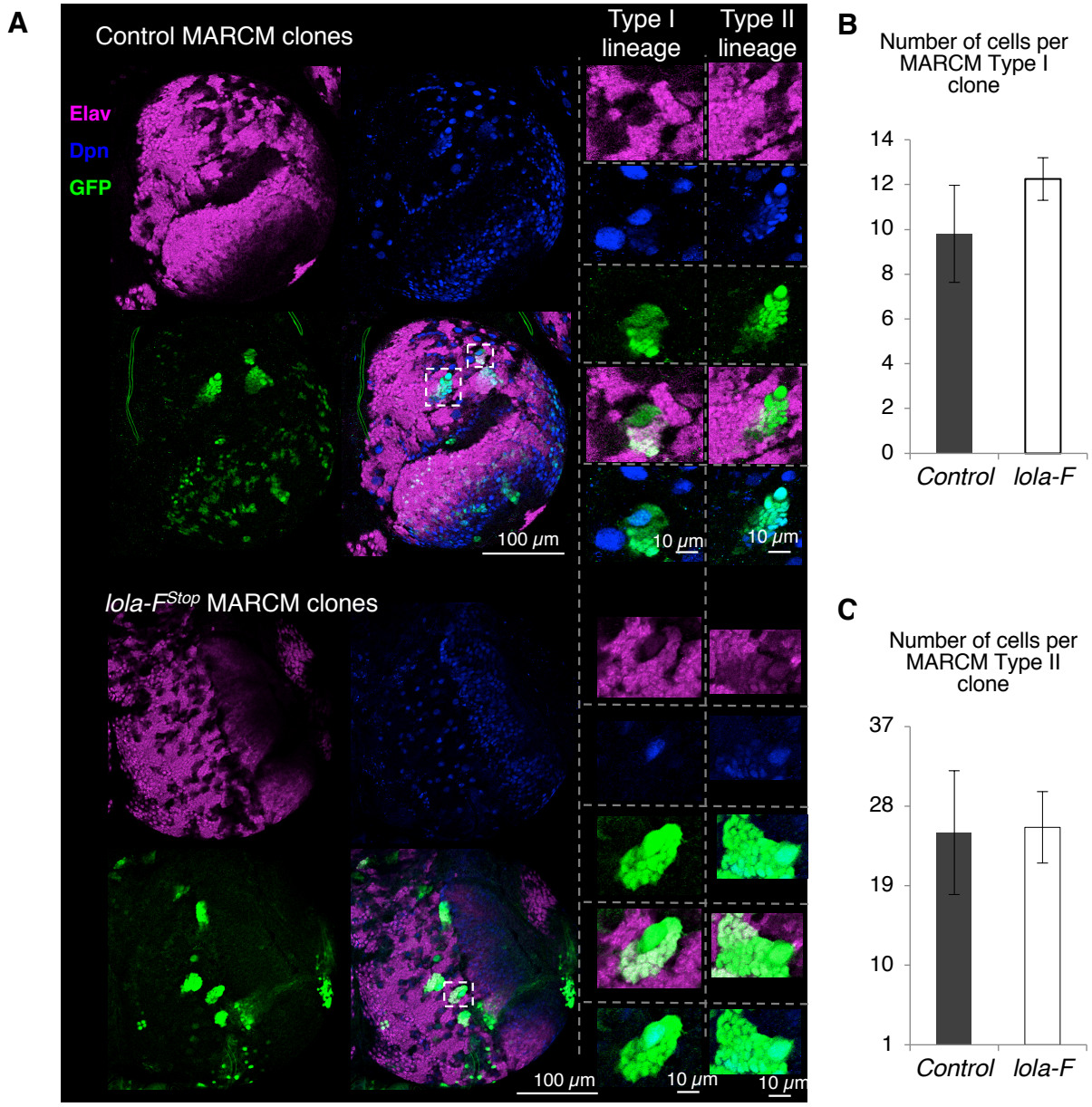

Figure 23: *lola-F* mutant MARCM clones in third instar larval brains show wildtypic characteristics.

(A) Control and *lola-F*^{Stop} MARCM clones in the larval brain are indistinguishable. Type I and Type II clones contain one Dpn positive Nb (blue) and several Elav positive neurons (magenta). Type II clones in addition contain several Dpn positive cells of smaller size. **(B)** Quantification of the total number of cells in Type I clones for the control and the *lola-F*^{Stop} allele. Four clones were analysed and tested for significance using ANOVA two-way test ($p>0.2$). Data are represented as average ±SEM. **(C)** The total number of cells in Type II clones for control and *lola-F*^{Stop} MARCM clones. Three clones were analysed and significance was tested using ANOVA two-way test ($p>0.9$). Data are represented as average ±SEM.

4.4.12 Conclusion: Lola-F is the main isoform involved in axonal guidance along the embryonic VNC

The loss of Lola-F activity severely disrupts the *Drosophila* VNC and leads to lethality by the end of embryogenesis. Expression of *lola-F* mRNA must be tightly regulated as ectopic Lola-F levels in neurons impaired axonal pathfinding along the embryonic ventral midline. Among the target genes regulated by Lola-F are well described axon-guidance genes, such as *Dscam1*, *Slit/Robo*, *Netrin-B* and *futsch*. The latter one was not previously identified as a key Lola target. The phenotype observed in the absence of Lola-F is similar to the complete loss of all Lola isoforms. Nevertheless, axon extension is less severely affected in *lola-F* mutant embryos. Lola was proposed to regulate axon growth by negative regulation of the actin-nucleation Spire (Gates, Kannan and Giniger, 2011). However, the absence of Lola-F does not alter Spire expression, thus potentially explaining the milder phenotype on axon growth. It will be interesting to address which Lola isoform(s) control Spire expression.

In conclusion, our findings identify Lola-F as a novel, previously uncharacterized isoform that acts as a critical regulator of axonal guidance processes along the embryonic ventral midline by activating numerous axon guidance genes.

4.5 The splice variant Lola-O regulates neurotransmitter biogenesis in *Drosophila*

Our systematic CRISPR/Cas9-mediated KO screen revealed a complex phenotype for adult flies bearing a mutation in the highly conserved isoform Lola-O. This splice variant has not been previously characterized. Hence, the following section will focus on the detailed physiological and molecular analysis of this isoform.

4.5.1 CRISPR/Cas9 induced mutations targeting Lola-O

The *lola-O* specific mutant allele lacks majority of its isoform-specific C-terminal exon, including the entire ZF domain (**Figure 24A**). In order to validate the genomic deletion, qRT-PCR and RNA-sequencing were performed using RNA extracts isolated from control and *lola-O* KO embryos (22+2 hours AEL; **Figures 24B-C**). For qRT-PCR, the forward primer spans the N-terminal common region, while the reverse primer was designed to anneal within the deleted C-terminal region. In contrast to control, no amplification was obtained with extract from the *lola-O* mutant sample. Similarly, the RNA sequencing data revealed no read within the expected mutant genomic region, confirming that the molecular deletion within the Lola-O C-terminal exon. Moreover, expression levels of other Lola isoforms remained virtually unchanged, suggesting that the loss of Lola-O activity does not affect expression of other *lola* isoforms.

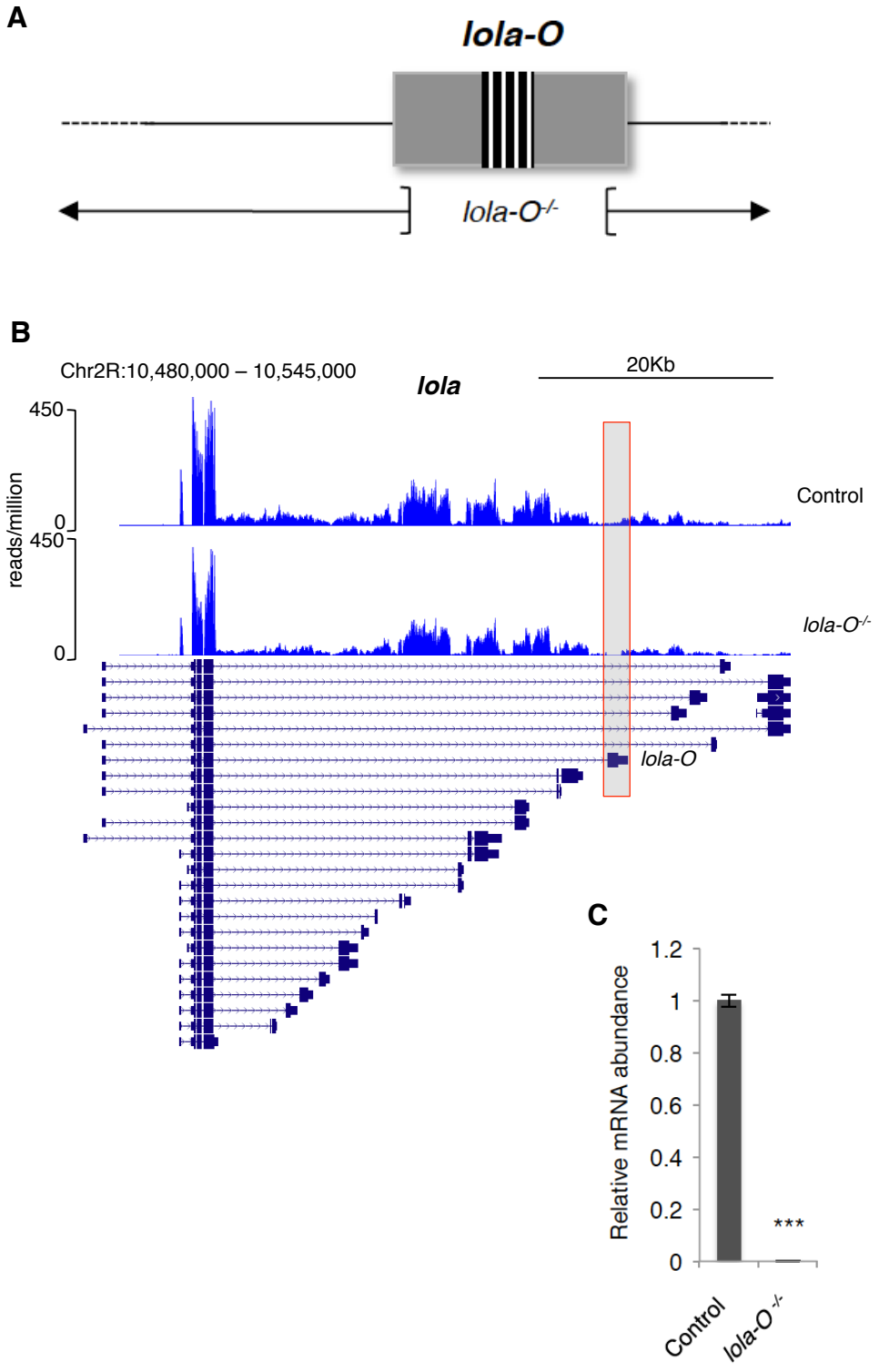

Figure 24: The *lola-O* mutation depletes the entire ZF domain.

(A) Scheme of the *lola-O* genomic region and the obtained genomic deletion, in which the entire Lola-O specific ZF motif is deleted. (B) Poly-A selected RNA-seq track for the *lola* locus. The *lola-O* specific deletion is confirmed by the absence of read within the Lola-O C-terminal exon (red box). *lola-O* mutant RNA extract was isolated from 22+2 hr old embryos. (C) qRT-PCR on *lola-O* mutant RNA extract validates the absence of *lola-O* mRNA levels. The reverse primer anneals within the deleted region. ***p-value<0.001 Data are represented as median ±SD.

4.5.2 *lola-O* mutant flies display a strong degeneration phenotype

Depletion of *lola-O* gives rise to homozygous viable adult flies that display numerous abnormalities, including severely impaired longevity and premature death. Typically, *Drosophila* flies live up to an average of 81 days, while *lola-O* KO flies had a maximum lifespan of 21 days under the same conditions (**Figure 25A**). Lifespan assays of control flies revealed an average half-life of 58 days, a time point at which 50 % of flies are alive. In contrast, the half-life of *lola-O* KO flies is 11 days (p-value$<$0.001, vs. control flies). In addition, locomotion assays indicated significantly impaired locomotive abilities of flies lacking *lola-O* (**Figure 25B**; 38 % efficient climbing of *lola-O* KO flies vs. 98 % of control flies; p-value$<$0.001). Interestingly, specifically *lola-O* mutant females exhibited cuticle malformation on the abdomen and suffered from partial sterility with reduced egg laying rates (**Figures 25E V; 25B-C;** 1.8 eggs/hour/female for control females vs. 0.5 eggs/hour/female for *lola-O* KO females; p-value$<$0.001). Both males and females also frequently formed melanotic masses, so-called pseudotumours, which occurred predominantly on abdomen and limbs, leading to the loss of the affected appendage (**Figures 25D, 25E II-IV**). Melanotic tumours are typically non-proliferative and are believed to arise as an immune-response mediated by encapsulation of hemocytes (Minakhina and Steward, 2006). These melanotic masses were not only seen on *lola-O* deficient adult flies, but were also occasionally present in third instar larvae, yet with reduced frequency (**Figure 25E I**). All these phenotypes were also observed on *trans*-heterozygous flies that carry a *lola* deficiency allele, and were rescued by recombination with a Lola BAC, thus demonstrating that they arise due to the lack of Lola-O and ruling out any off-target events.

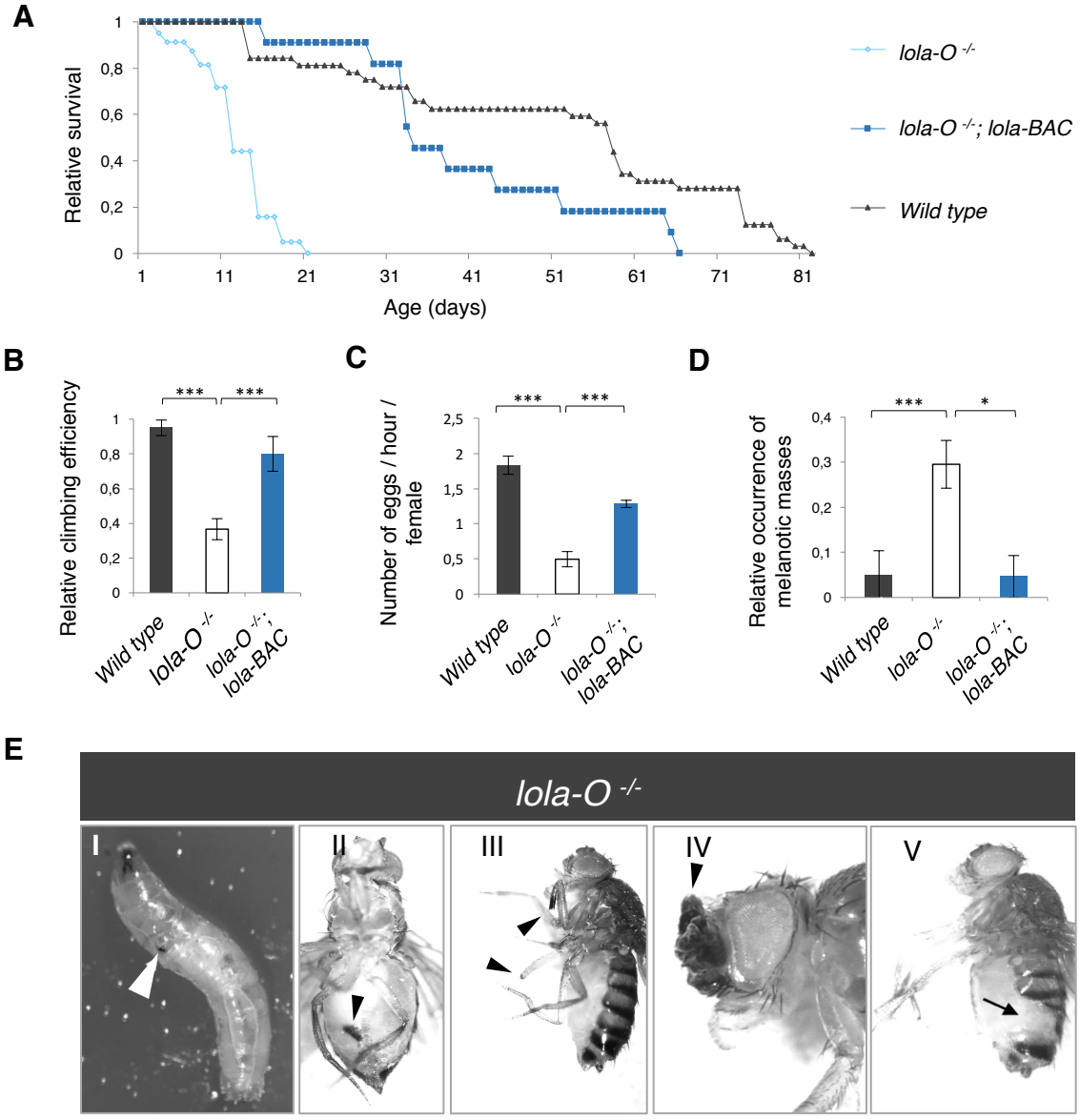

Figure 25: Depletion of Lola-O induces degeneration in adult flies.

(A) Survival curve of adult *Drosophila*. Flies lacking *lola-O* display significantly impaired longevity **(B)** Locomotion abilities are impaired compared to control flies. Climbing assay was performed in two replicates, data is shown as average ±SEM. ***p-value <0.0001. (**C**) *lola-O* mutant female flies reveal reduced fertility as seen on the reduced number of eggs laid. Data are represented as average ±SEM and significance was tested using one-way ANOVA. ***p-value <0.001. **(D)** Quantification of melanotic masses. Phenotypic penetrance of melanotic mass formation is reduced to control levels by recombination with a *lola* genomic construct. 10 flies were examined in four replicates at 11 days of age. Statistical analysis was performed using ANOVA one-way t-test. ***p-value <0.001, **p-value<0.01. Data are represented as average ±SEM. **(E)** Depletion of *lola-O* induces formation of melanotic masses (arrowheads) in both adults (II-IV) and larvae (I), eventually leading to the loss of affected limbs of adult flies (III). Females deficient for *lola-O* show cuticle malformation (arrow) (V).

4.5.3 Lola-O mediates its activity through a neuronal function

In order to characterize the physiological function of Lola-O, we first aimed to identify its cell-type specific expression pattern during *Drosophila* development. Fluorescent *in-situ* hybridization revealed accumulation of *lola-O* mRNA in the embryonic nervous system, suggesting that Lola-O might overtake crucial regulatory functions in the developing CNS (**Figure 26A**). To test this hypothesis, transgenic flies expressing *lola-O* under a UAS promoter were generated and recombined with different tissue-specific driver lines. Ectopic ubiquitous of Lola-O using *Tubulin*-GAL4 was sufficient to partially restore the lifespan and reduced phenotypic penetrance of *lola-O* KO flies (**Figure 26B**). Likewise, ectopic neuronal (*elav*-GAL4) expression of Lola-O could improve all previously described phenotypes observed in the absence of Lola-O activity (**Figures 26C-D**). In contrast, glial-specific (*repo*-GAL4) expression had no profound effect and failed to restore longevity (**Figure 26E**).

Taken together, these findings indicate that Lola-O's function is dedicated to the neuronal cell type.

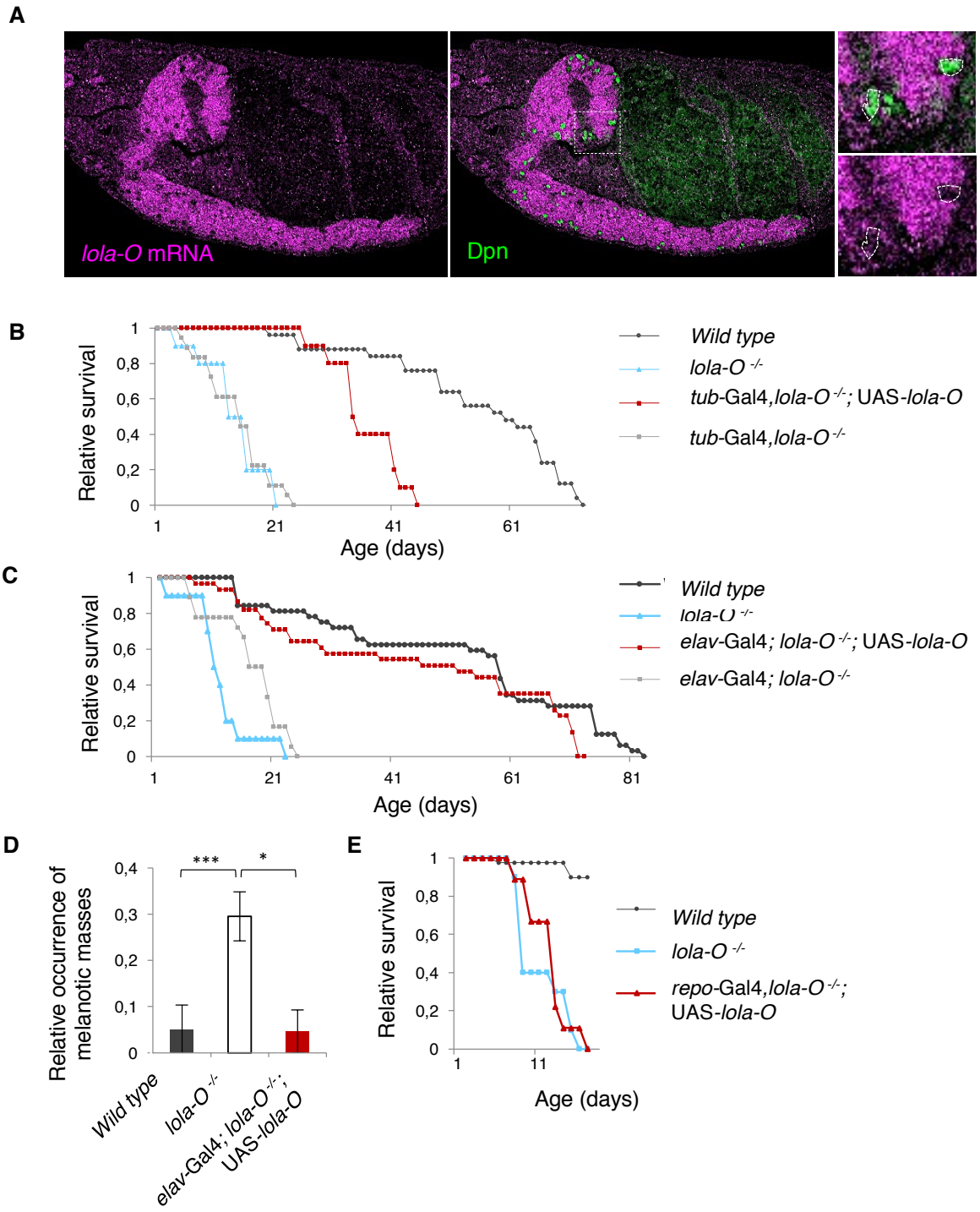

Figure 26: Lola-O is required in neurons to regulate various physiological processes.

(A) Fluorescent *in-situ* hybridization shows accumulation of *lola-O* mRNA in the embryonic nervous system, where it does not co-localize with Dpn-positive Nbs. **(B)** Ubiquitous ectopic expression of Lola-O cDNA (*Tub*-GAL4) elongates the lifespan of *lola-O* mutants by 2-fold. *lola-O* KO flies recombined with the driver line serve as a control. **(C)** Ectopic neuronal expression of Lola-O (*elav*-GAL4) restores wildtypic longevity of *lola-O* mutants. **(D)** Melanotic tumour formation is limited to control levels by driving Lola-O cDNA expression in neurons. 10 flies were examined in four replicates at 11 days after hatching. Statistical analysis was performed using ANOVA one-way t-test. ***p-value <0.001, *p-value<0.05. Data are represented as average ±SEM. (E) *repo*-GAL4 driven glial-cell specific Lola-O cDNA expression has no positive effect on premature lethality of *lola-O* KO flies.

4.5.4 Lola-O is expressed in a subset of neuronal cells

In order to obtain further insights into Lola-O function we seek to address its localization in third instar larval brains, when formation of melanotic masses was first observed. *In-situ* hybridization on larval CNS using a *lola-O* specific probe was not successful in detecting *lola-O* mRNA at this particular developmental stage, suggesting that Lola-O is expressed at very low levels in third instar larval brains. To overcome this problem we took advantage of a fly line carrying a *lola*-BAC encoding a Lola-O-GFP fusion protein (Venken *et al.*, 2009). Immunostaining using an anti-GFP antibody confirmed our findings that Lola-O is generally expressed at a very low level in the larval brain and additional antigen-retrieval steps were required to improve immunoreactivity (**Figure 27A**; see methods). Interestingly, the observed Lola-O-GFP expression was refined to only a subset of neuronal cells, which includes the midline and lateral midline of the ventral ganglion and few groups of cells in the central brain. In order to reveal the identity of these cells, flies carrying a UAS-GFP transgene reporter were recombined with flies expressing GAL4 under the control of various neuronal promoters and the resulting GFP signal was subsequently compared with the observed Lola-O-GFP expression pattern. We found that GFP expression driven by the *Tdc2*-GAL4 driver was reminiscent to the expression of Lola-O-GFP, in particular along the ventral midline and the central brain (**Figure 27B**).

Therefore, these findings strongly suggest that expression of the splice variant Lola-O is limited to Tdc2-positive neurons in the larval brain.

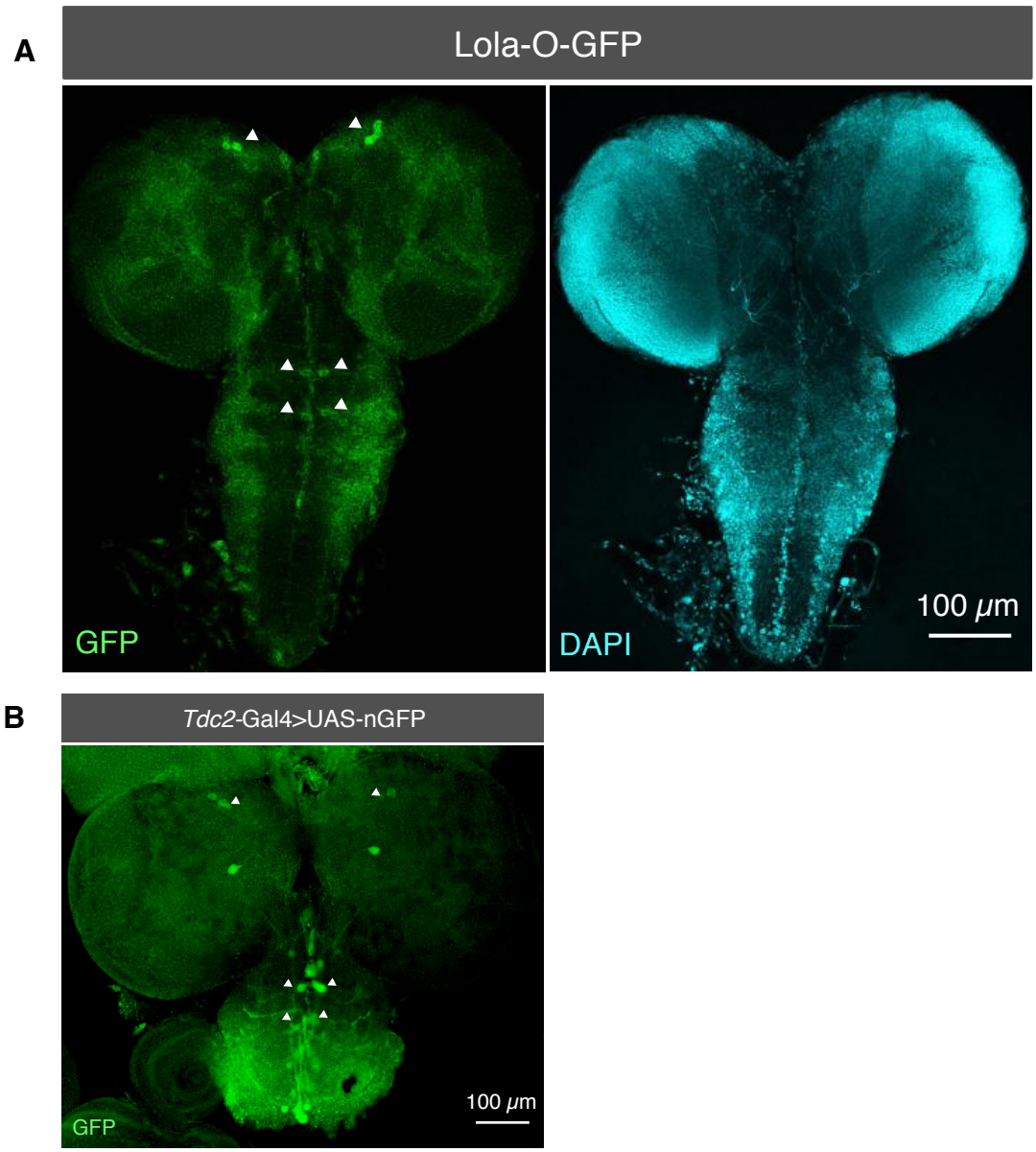

Figure 27: Lola-O is expressed in a specific subset of cells in the third instar larval brain.

(A) Lola-O-GFP immunostaining using an anti-GFP antibody shows Lola-O enrichment in a subset of cells in the central brain and along the ventral midline (arrowheads). (**B**) UAS-GFP expression driven by *Tdc2*-GAL4 is visualized by an anti-GFP antibody. Tdc2-positive cells are present in the VNC along the midline and in a subset of cells in the central brain (arrowheads), reminiscent to the Lola-O-GFP expression pattern.

4.5.5 Octopamine is involved in various physiological functions

Tdc2 stands for *Tyrosine-decarboxylase 2* and encodes a key enzyme of the octopamine-synthesis pathway. The monoamine octopamine is homologous to the human norepinephrine and acts as a neurotransmitter, neuromodulator and neurohormone in invertebrates. Its physiological function includes the regulation of ovulation, aggression behaviour, locomotion and lifespan (Monastirioti, Linn and White, 1996; Stathakis *et al.*, 1999; Zhou, Rao and Rao, 2008; Sembulingam and Sembulingam, 2012; Yang *et al.*, 2015a; Li *et al.*, 2016). Octopamine synthesis acts on the amino acid tyrosine, which is modified into the intermediate compound tyramine by the enzyme Tyrosine-decarboxylase 2 (Tdc2). Subsequently, the Tyramine-ß-hydroxylase (TBH) hydrolyses tyramine to form the neurotransmitter octopamine (Barron, Søvik and Cornish, 2010). Interestingly, flies deficient for TBH (*Tbh*^{nM18}), which thus fail to produce octopamine, display a phenotype similar to the defects observed for *lola-O* KO flies, including impaired longevity, sterility and formation of melanotic masses (**Figures 28A-B**; Li et al., 2016; Monastirioti et al., 1996).

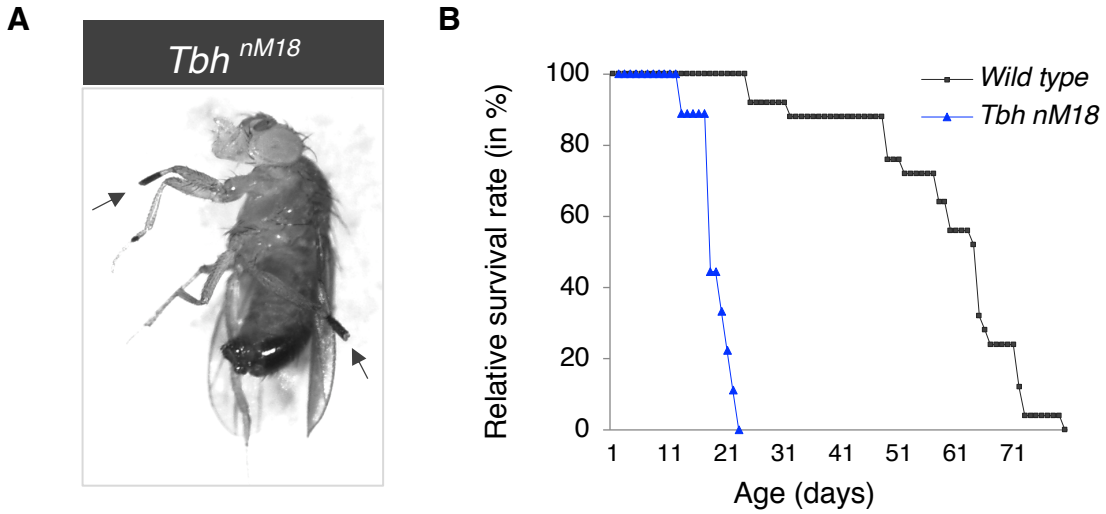

Figure 28: *Tbh* deficient flies display a phenotype reminiscent to *lola-O* mutants.

(A) Melanotic masses are frequently formed in the absence of TBH, leading to the loss of affected limbs (arrows). **(B)** *Tbh*^{nM18} flies reveal impaired longevity compared to control flies. The average of two biological replicates is shown.

4.5.6 *lola-O* is specifically expressed in octopaminergic neurons in the larval brain

To confirm the expression of Lola-O-GFP in octopaminergic neurons, larval brains were co-immunostained for anti-GFP and an antibody that recognizes the enzyme TBH, which was shown to be a faithful marker of octopaminergic neurons (Selcho et al., 2012). Remarkably, TBH and Lola-O-GFP co-localized in a cluster of dorso-medial cells in the larval central brain and along the midline in the VNC, thus confirming our first observation that Lola-O expression is restricted to octopaminergic neurons (**Figure 29A**). Nevertheless, single cells lateral of the midline were, however, only positive for Lola-O-GFP, implying potential Lola-O functions independent of its role in octopaminergic neurons. Besides, Lola-O-GFP displayed a strong accumulation in the third instar larval ring gland, an organ that controls metabolism-related functions through ecdysone signalling and insulin production (**Figure 29B;** Ou et al., 2016). As TBH expression was not detectable in the ring gland, an octopamine-independent role for Lola-O in this tissue is possible.

Altogether, the co-localization of Lola-O-GFP and TBH in the larval brain demonstrates that expression of this splice variant is highly specific to octopaminergic neurons. These findings suggest that Lola-O function is likely linked to the octopaminergic pathway.

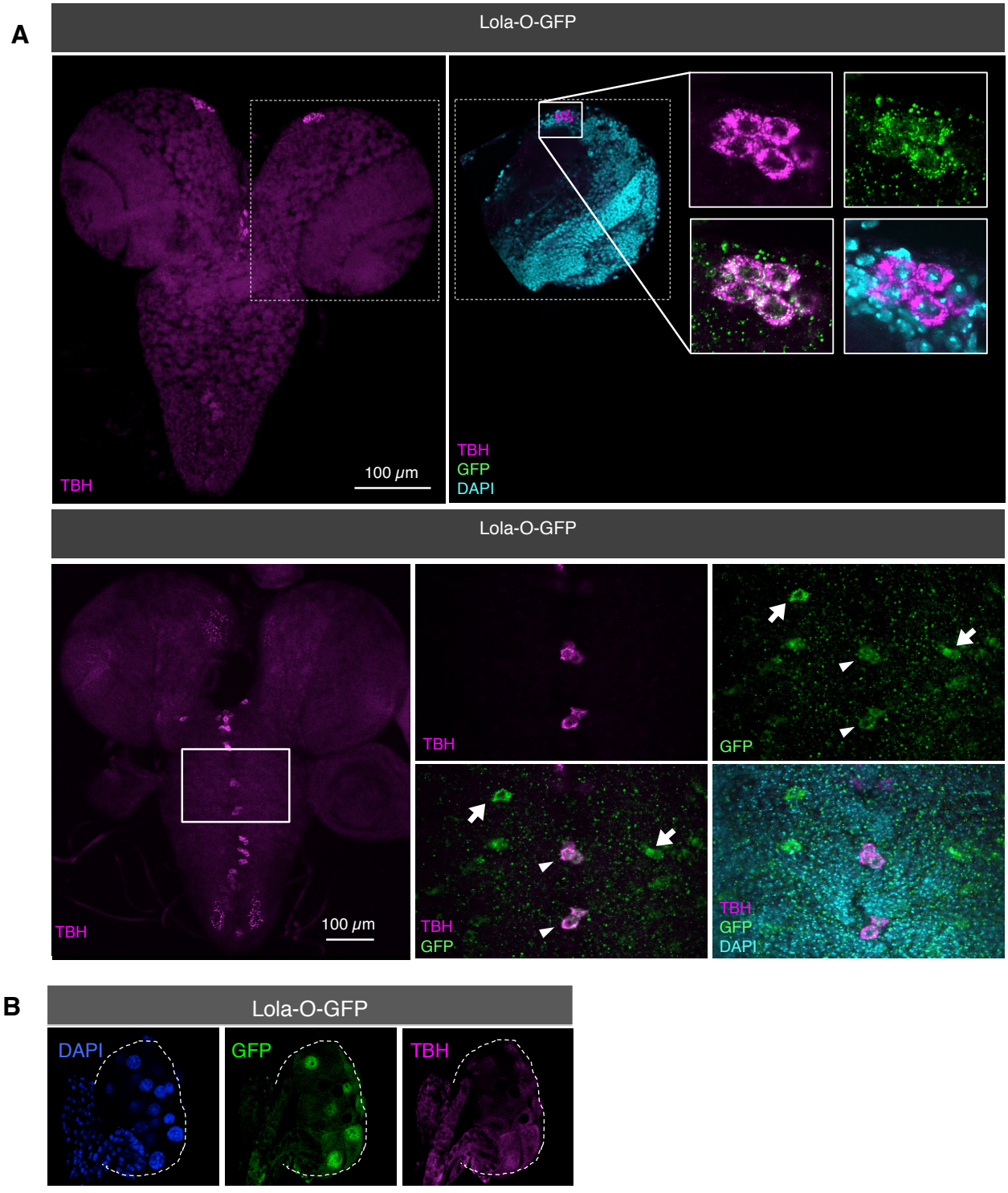

Figure 29: Lola-O localizes to TBH-positive octopaminergic cells.

(A) Lola-O-GFP (anti-GFP, green) and TBH (pink) co-localize in the larval central brain and in cells along the midline of the VNC (arrowheads). Individual Lola-O positive cells at the lateral midline show no TBH immunoreactivity (arrows). **(B)** Lola-O-GFP is highly abundant in nuclei of the third instar larval ring gland, where no TBH immunoreactivity is detectable.

4.5.7 Depletion of Lola-O is partially rescued by ectopic octopamine

Perturbation of octopamine levels leads to phenotypes reminiscent to the loss of Lola-O, suggesting that *lola-O* deficient flies may suffer from altered octopamine levels. To examine whether Lola-O has an essential function in the octopaminergic pathway, a drug-feeding assay was performed to test whether ectopic octopamine could complement the loss of Lola-O. To this end, control and *lola-O* KO flies were supplied with octopamine- and tyrosine-enriched food. Previous studies showed that feeding octopamine and tyrosine needs to be strictly controlled in order to prevent premature lethality (Crocker and Sehgal, 2008). Both compounds were therefore supplied in sex-specific concentrations of 5 mg/ml for males and 7.5 mg/ml for females. Interestingly, ectopic octopamine was sufficient to elongate the half-life of *lola-O* KO flies by 2-fold (**Figures 30A-B;** 11 days +/- 2.6 versus 21 days +/- 3.6, p-value <0.5). In contrast, feeding tyrosine had no effect on survival. Similarly, feeding octopamine to Tbh^{nM18} mutant flies rescued the lifespan to a comparable extent (**Figure 30C**). Octopamine was also fed to wildtype flies, which showed no substantial effect on longevity. Furthermore, octopamine-enriched food improved locomotion abilities of *lola-O* mutants (**Figure 30D**; 61,5 % locomotion ability on octopamine food vs. 39,0 % on control food, p-value<0.05) and reduced the occurrence of melanotic masses close to wild type levels (**Figure 30E**; 9,9 % on octopamine food vs. 30,1 % on control food; p-value<0.05).

Collectively, our results strongly suggest that the phenotypic defects observed in *lola-O* mutant flies likely result from reduced levels of octopamine.

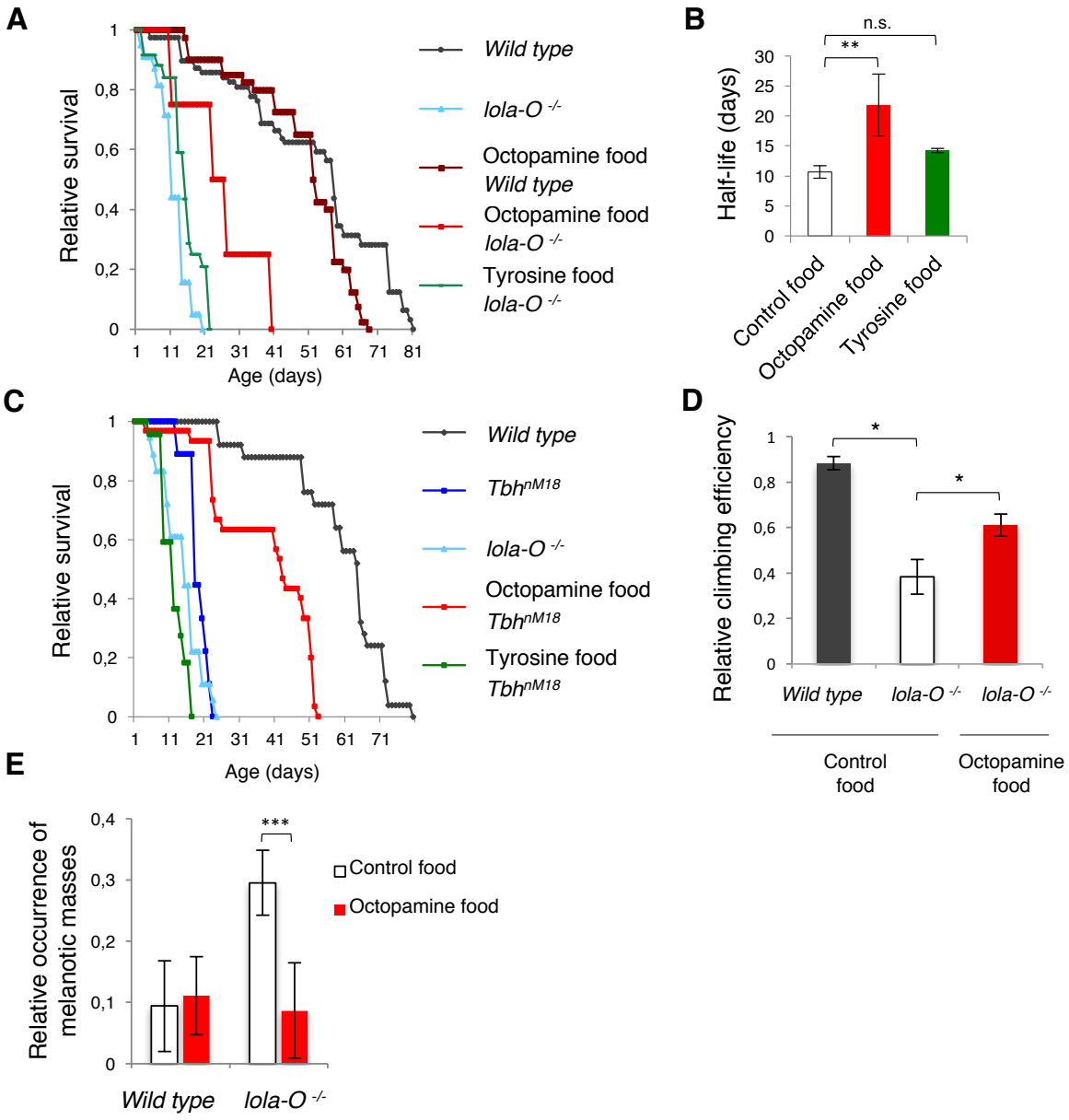

Figure 30: Ectopic octopamine partially rescues the phenotype associated with the loss of Lola-O.

(A) Drug-feeding assay for *lola-O* mutants. Rearing *lola-O* mutant flies on octopamine-enriched food elongates longevity by 2-fold while tyrosine feeding has no effect on survival. The average of three biological replicates is shown. **(B)** Quantification of the half-life deduced from (A). Feeding octopamine to *lola-O* mutants increases the half-life from 10.6 days to 21.8 days. ANOVA t-test was applied, ***p-value<0.001. Data are represented as average of three biological replicates ±SD. **(C)** Drug feeding assay for Tbh^{nM18} mutant flies. Octopamine feeding enhances lifespan for Tbh^{nM18} flies by 2-fold. In contrast, tyrosine-enriched food reveals no positive effect on survival. **(D)** Relative climbing efficiency is enhanced by feeding octopamine to *lola-O* mutants. Three days old male flies were used for locomotion quantification. ANOVA one-way t-test was performed to test statistical significance, ***p-value<0.001, **p-value<0.01. Data are represented as average ±SD. (E) Occurrence of melanotic masses is reduced upon feeding octopamine to *lola-O* KO flies. Freshly hatched males and females were separated and analysed for melanotic masses at 11 days of age. ANOVA one-way t-test was applied, p-value <0.001. Data are represented as average of four biological replicates ±SEM.

4.5.8 Expressing *lola-O* cDNA in octopaminergic neurons rescues most of *lola-O* mutant defects

The precise localization of Lola-O in octopaminergic cells prompt us to hypothesize that Lola-O might fulfil its function within this precise subset of neuronal cells. Therefore, we reasoned that ectopic Lola-O expression in octopaminergic neurons should be sufficient to rescue the defects observed with its loss and to restore wildtypic behaviour. In order to test this hypothesis, a *Tdc2*-GAL4 driver line was used and crossed with UAS-Lola-O. *Tdc2*-GAL4 has previously been shown to be a truthful marker for octopamine-producing cells, allowing to restrict Lola-O cDNA expression to this neuronal subset of cells (Yarali and Gerber, 2010). Remarkably, ectopic Lola-O expression in octopaminergic neurons completely restored the defects associated with its loss, including survival (**Figure 31A;** 45 days for *lola-O* rescue flies vs. 12 days of *lola-O* mutant flies), climbing ability (**Figure 31B**; 91 % for *lola-O* rescue flies vs. 38 % of *lola-O* mutant flies; p-value$<$0.001), appearance of melanotic tumours (**Figure 31C;** 4 % for *lola-O* rescue flies vs. 34 % for *lola-O* mutants; p-value$<$0.01) and fertility of female flies (**Figure 31D;** 1.2 eggs/hour for *lola-O* rescue flies vs. 0.4 eggs/hour for *lola-O* KO females; p-value$<$0.01).

Altogether, these findings demonstrate that the primary activity of Lola-O is restricted to octopaminergic neurons in the adult *Drosophila* brain. The loss of Lola-O within those specialized neuronal cells is accompanied by neurodegenerative defects leading to various phenotypes in adult flies, reminiscent to the consequences of perturbed octopamine levels. Finally, our findings indicate that Lola-O might regulate the octopamine synthesis pathway in *Drosophila*.

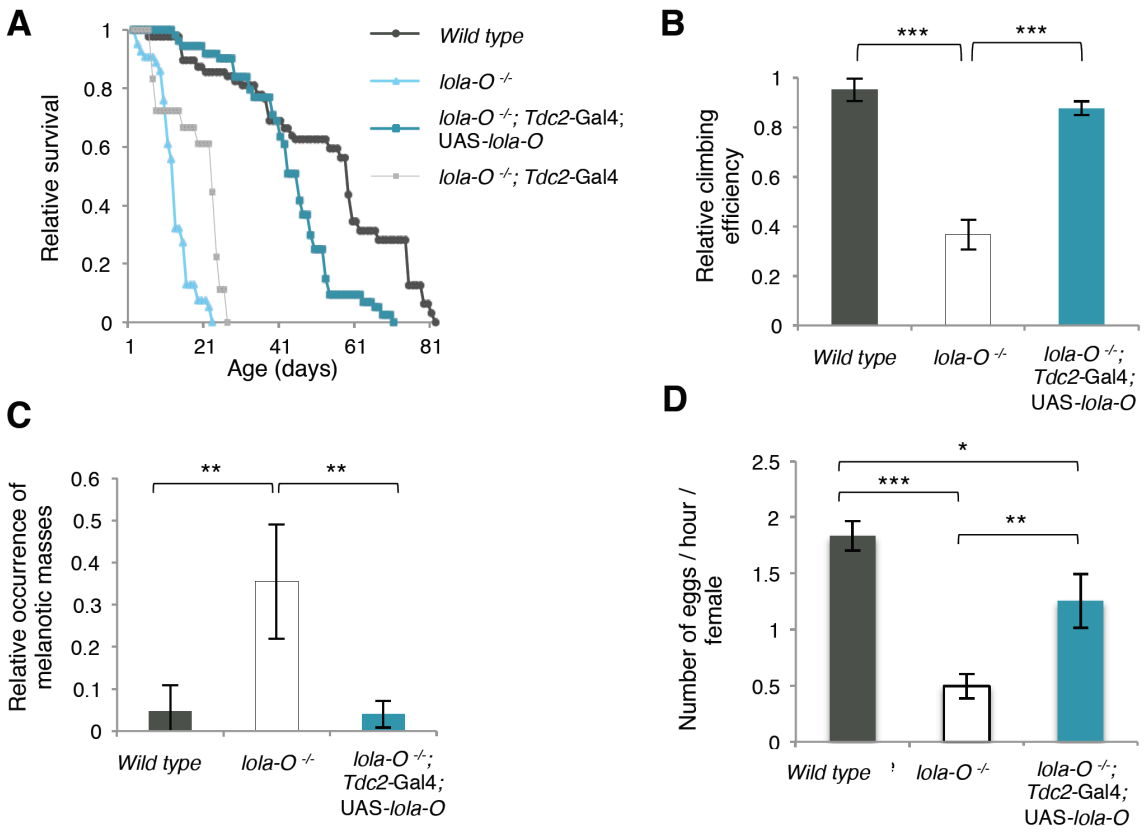

Figure 31: Lola-O activity is required in octopaminergic cells.

Ectopic *lola-O* expression using *Tdc2*-GAL4 restores survival **(A),** climbing efficiency **(B)**, occurrence of melanotic masses **(C),** and fertility. (A) The average of three biological replicates is shown. (B) Three days old flies were used for locomotion quantification ANOVA one-way t-test was performed to test statistical significance. ***p-value<0.001. Data are represented as average ±SD. (C) Four biological replicates comprising 10 flies each were analysed at 8 days of age. ANOVA one-way t-test was performed to test statistical significance. **p-value<0.01. Data are represented as average ±SEM. **(D)** Average number of eggs laid for three days. ANOVA one-way t-test was performed to test statistical significance. ***p-value<0.001, **p-value<0.002, *p-value<0.05. Data are represented as average ±SD.

4.5.9 Depletion of Lola-O affects expression of genes involved in neurogenesis and metabolism

In order to characterize the function of Lola-O in more details we aimed to identify the transcriptional network regulated by Lola-O. For this purpose, a transcriptome analysis was performed using RNA extracted from stage 17 mutant embryos (22+2 hours AEL). In the absence of Lola-O activity, 1151 genes and 1116 genes were up- and down-regulated, respectively. GO-term analysis revealed the strongest enrichment for up-regulated genes involved in neurogenesis (**Figure 32B;** 103 genes, p-value 1.4E-14), supporting our findings that Lola-O activity is predominantly required in the nervous system. In contrast, down-regulated genes were mainly involved in metabolic-related processes, such as the regulation of glucose metabolism (**Figure 32A**; 37 genes, p-value 7.8E-5) and chitin metabolic processes (30 genes, p-value<8.5E-5). Chitin synthesis was shown to be essential for proper cuticle development and pigmentation, a process that is likely dysregulated in the absence of Lola-O and could potentially explain the cuticle deformity observed in *lola-O* mutant female flies (Moussian *et al.*, 2005). Furthermore, down-regulated genes revealed an enrichment for genes involved in behavioural response to ethanol (15 genes, p-value<1.2E-4) and determination of lifespan (27 genes, p-value 1.0E-3). Both enriched terms are typically affected upon altered octopamine levels (Chen *et al.*, 2013; Li *et al.*, 2016), which is in accordance with our findings that Lola-O regulates octopamine synthesis in *Drosophila*.

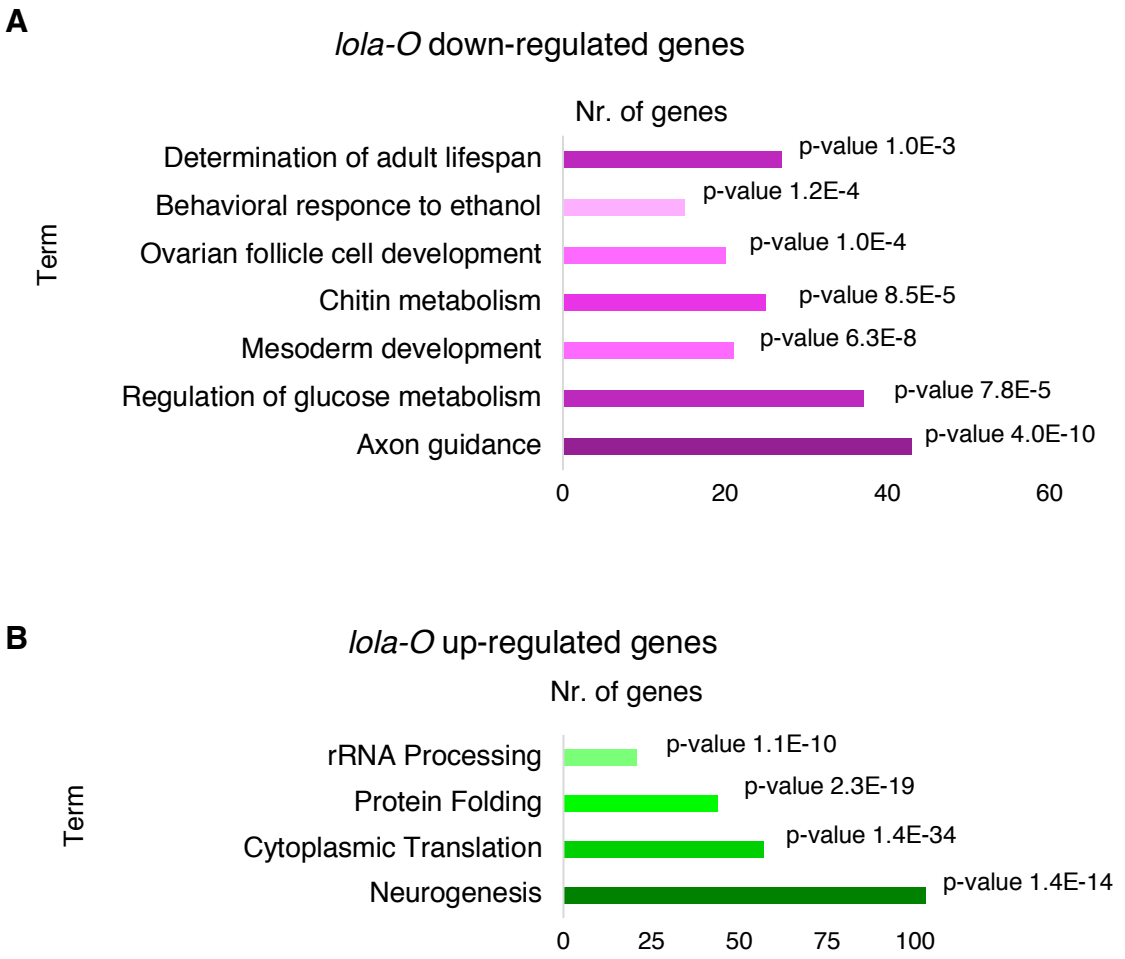

Figure 32: GO-term analysis for differentially regulated genes in *lola-O* mutant embryos.

(A) Down-regulated genes in *lola-O* mutant embryos reveal enrichment for regulation of glucose metabolism and determination of adult lifespan. **(B)** Up-regulated transcripts are predominantly involved in neurogenesis related processes. GO-term analysis was performed with DAVID Bioinformatics Resources 6.8 (National Institute of Allergy and Infectious Diseases, NIH); The category GOTERM_BP_DIRECT was selected.

4.5.10 *Tbh* levels are reduced in the absence of Lola-O activity

Based on our previous finding that depletion of *lola-O* is compensated by supplementing ectopic octopamine, we aimed to determine whether and how Lola-O functions in the octopamine signalling pathway. For this purpose, we focused our further analysis on genes that were known to be involved in octopamine synthesis.

In *Drosophila*, octopamine is synthesized via the activity of the two enzymes Tdc2 and TBH. Overall, *Tdc2* and *Tbh* are expressed at low level in in embryos based on our RNA sequencing data, potentially explaining why we failed to detect changes in expression of these genes in our transcriptome data. To overcome this problem, control and *lola-O* mutant RNAs were isolated from adult heads, where octopaminergic neurons are predominantly present, to enrich for transcripts involved in the octopamine pathway. *Tdc2* and *Tbh* levels were subsequently analysed using qRT-PCR to test whether Lola-O might control their expression *in vivo*. Intriguingly, while *Tdc2* expression was unaffected in *lola-O* mutants, *Tbh* mRNA levels were significantly reduced (**Figure 33A**). Similar results were observed in a *trans*-heterozygous combination in which *lola-O* mutants were crossed with a *lola* deficiency line.. Besides, immunostaining on third instar larval brains displayed reduced TBH immunoreactivity in brains of *lola-O* mutant larvae, confirming the down-regulation of TBH also at the protein level (**Figure 33B**). In comparison to control larvae, Tbh^{nM18} mutant larval brains showed no TBH immunoreactivity, validating the specificity of the TBH immunostaining.

In conclusion, these findings indicate that Lola-O expression in octopaminergic neurons is required to maintain proper levels of TBH, a key enzyme in the octopamine pathway that is necessary to synthesize octopamine from the intermediate compound tyramine.

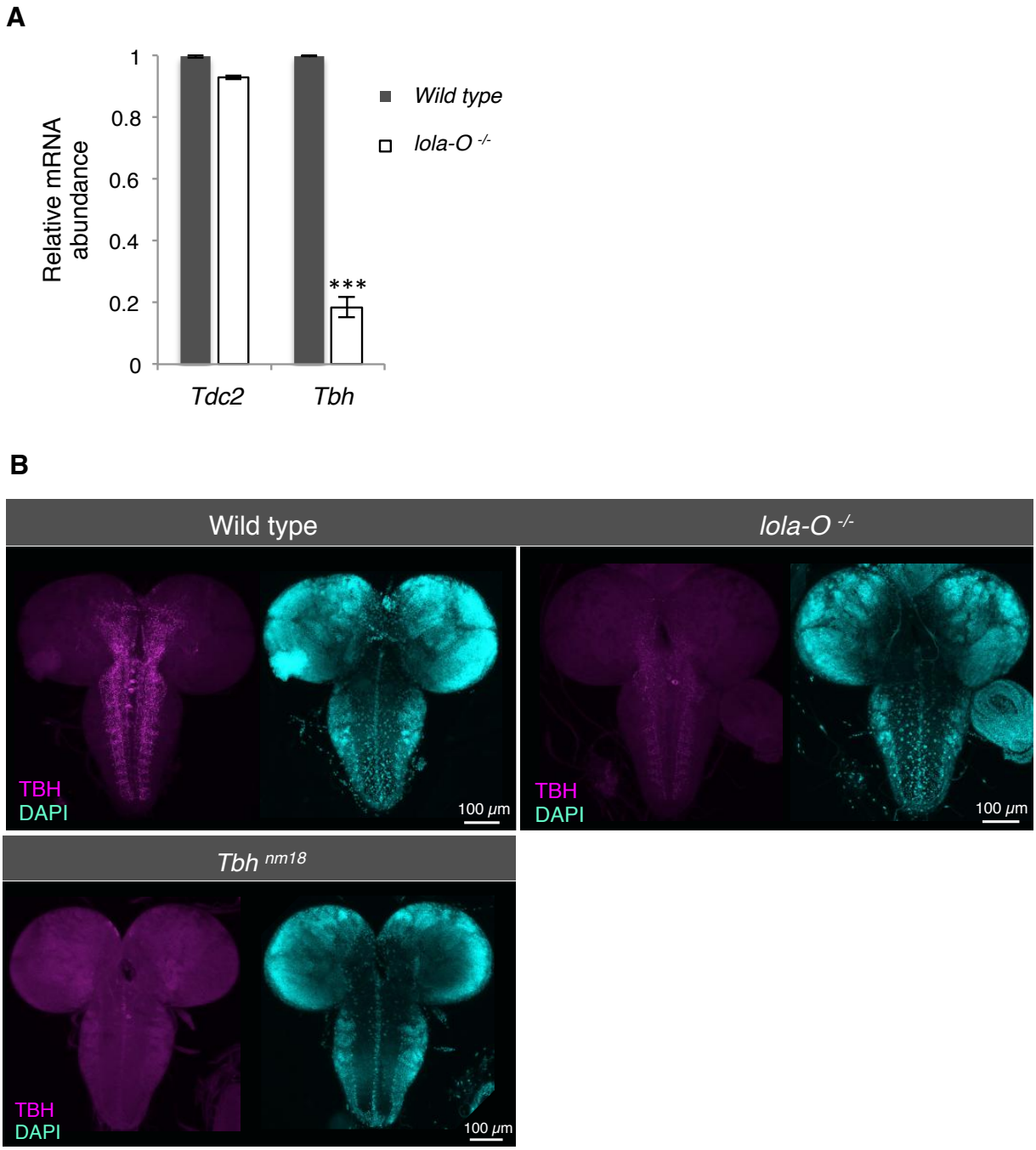

Figure 33: *lola-O* mutants have reduced TBH levels.

(A) qRT-PCR on mutant RNA extract isolated from freshly hatched adult male heads. ANOVA one-way t-test was performed. ***p-value<0.001. Data are represented as median ±SD. **(B)** Third instar larval brains of different genotypes were stained for TBH (purple) and DAPI (cyan). *lola-O* mutant larval brains show reduced TBH immunoreactivity compared to control brains. Immunoreactivity for TBH is diminished in *Tbh*^{nM18} mutant larval brains. Laser power was unchanged between scans to allow direct comparisons.

4.5.11 Lola-O regulates the octopamine pathway via regulation of *Tbh*

Given the reduced abundance of TBH in *lola-O* mutants, we wondered whether ectopic expression of *Tbh* cDNA would be sufficient to restore longevity and phenotypic penetrance of these flies. For this purpose, transgenic flies were generated with integrated *Tbh* under the control of a UAS-promoter. Interestingly, ectopic neuronal (*elav*-GAL4) TBH expression was sufficient to partially restore longevity and to significantly decrease the occurrence of pseudotumors in *lola-O* mutant flies (**Figures 34 A-B**; 5 % in control flies vs. 31 % in *lola-O* mutant flies; p-value<0.001; vs. 15 % in rescue flies; p-value<0.01 vs. *lola-O* mutants). These findings therefore identify *Tbh* as a key target of Lola-O in regulating octopamine synthesis.

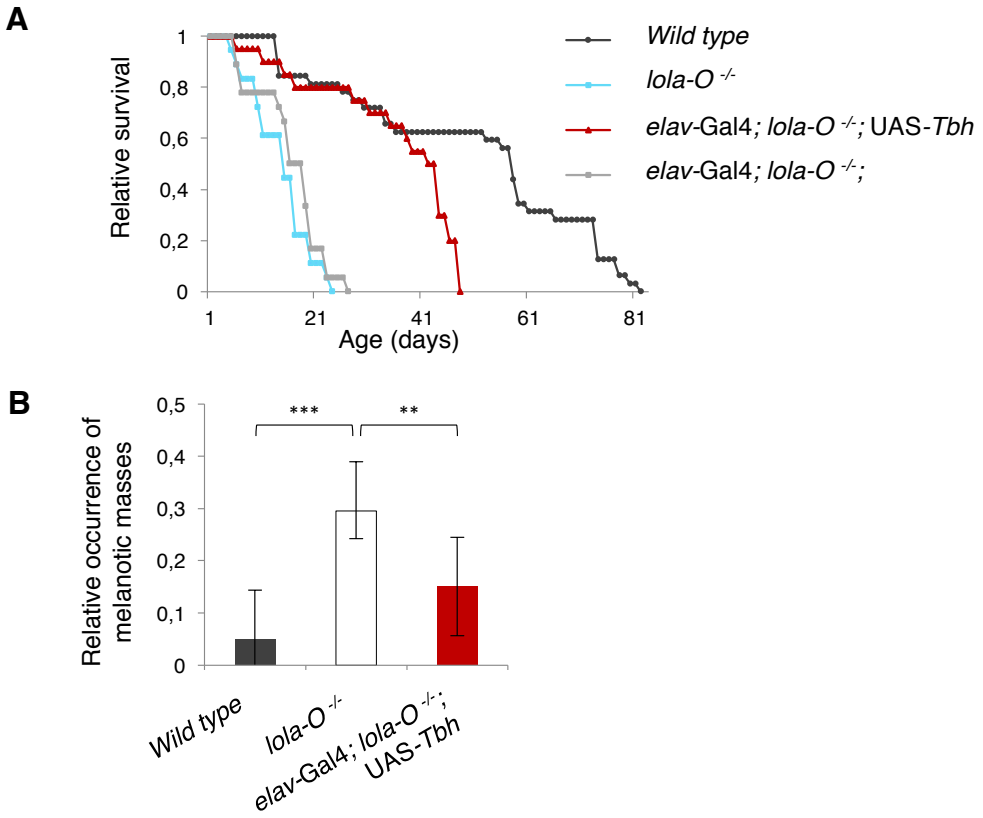

Figure 34: Ectopic neuronal *Tbh* expression is sufficient to partially rescue the defects associated with the loss of Lola-O.

(A) Ectopic neuronal *Tbh* expression using *elav*-GAL4 partially restores wildtypic longevity **(B)** and occurrence of melanotic masses of *lola-O* KO flies; ***p-value<0.001, **p-value<0.01; Data are represented as average±SEM. ANOVA one-way t-test was performed to test for statistical significance. The average of two biological replicates is shown in (A).

4.5.12 Lola-O regulates *Tbh* levels indirectly

To address whether *Tbh* is directly regulated by Lola-O, we aimed to identify Lola-O genome-wide binding sites specifically in octopamienrgic neurons. For this purpose, we took advantage of the recently established targeted DamID (TaDa) approach, which allows the identification of direct target genes in a cell-type specific manner (Southall et al., 2013). To this end, the *lola-O* CDS was cloned into *pUASTattB-LT3-NDam* to allow the targeted, low-level, expression of N-terminally tagged Dam-Lola-O. In order to identify direct target genes, neuronal Dam-Lola-O expression was induced in embryos using the driver line *Tdc2*-GAL4 and embryos were processed at stage 17 (22+2 hours AEL), just before larval hatching (Marshall et al., 2016). This corresponds to the developmental time window in which *lola-O* mRNA was detected in the entire embryonic CNS, as revealed by fluorescent *in situ* hybridization experiments. The same experiment was conducted in parallel for Dam-RNA Pol II, to identify transcriptionally active genes in octopaminergic neurons. We found 1449 genes bound by Pol II and 7327 by Lola-O, while 905 were shared between Lola-O and Pol II (**Figure 35A**; FDR of <0.01). When comparing those transcriptionally active target genes for Lola-O with our transcriptome data we found an overlap of 32.7 % with differentially expressed genes (296) in *lola-O* mutants of the same developmental stage. While *Tbh* was not among the Lola-O direct targets, we identified the gene *Bacc*, which encodes a previously identified repressor of *Tbh* (Chen *et al.*, 2013), as directly bound and repressed by Lola-O (**Figures 35B-D**). To validate the up-regulation of *Bacc* levels in the absence of Lola-O, RT-qPCR was performed on RNA extracted from stage 17 embryos (22+2 hours AEL; **Figure 35C**). Depletion of Lola-O elevated *Bacc* transcript levels by 1.6-fold compared to control embryos. While this increase is rather mild and therefore might appear not relevant, previous studies showed that heterozygous loss of *Bacc* was sufficient to up-regulate *Tbh* levels, hence leading to elevated octopamine levels accompanied by increased ethanol sensitivity (Chen *et al.*, 2013). Hence it seems that the dosage of Bacc must be tightly regulated in order to control TBH synthesis and accurate octopamine abundance.

In conclusion, our results support a model in which Lola-O regulates TBH levels indirectly, possibly via negative regulation of *Bacc* expression.

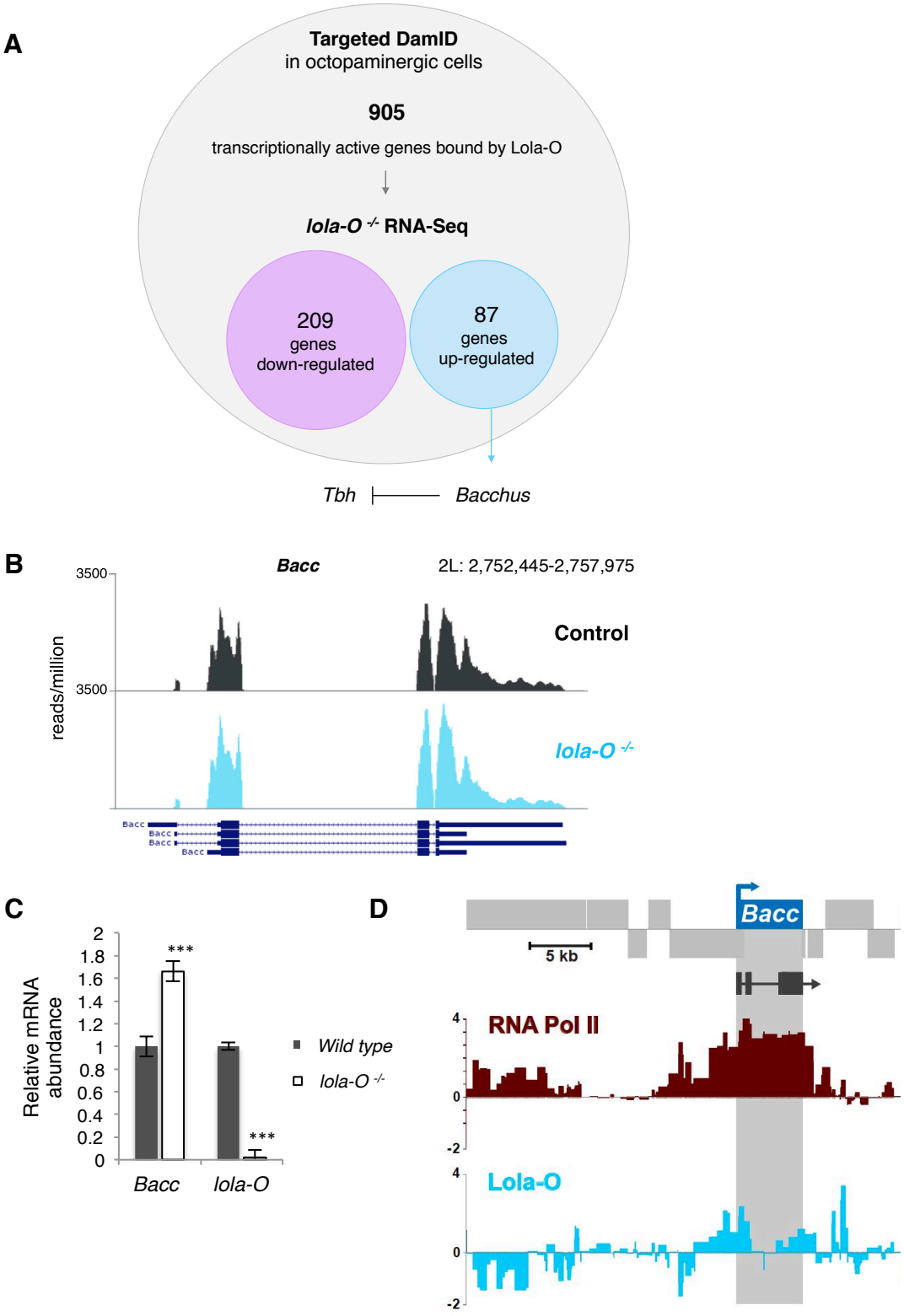

Figure 35: Lola-O directly binds and positively regulates *Bacchus*.

(A) Transcriptional network regulated by Lola-O. 905 direct target genes were commonly found for Dam-Lola-O and Dam-Pol II. Among them, 296 genes overlap with differentially expressed genes in the absence of Lola-O activity. *Bacc*, which is one of the up-regulated direct target genes, encodes a previously reported repressor of *Tbh*. Data was obtained from embryos 20-22 hr AEL. **(B)** Poly-A selected RNA-seq track of the *Bacc* locus. RNA was extracted from 22+2 hr old embryos. **(C)** RT-qPCR validates the up-regulated *Bacc* levels in the absence of Lola-O. RNA from 22+2 hr old embryos was used for analysis. (**D**) TaDa for Lola-O in octopaminergic neurons shows the binding at the *Bacc* locus. TaDa experiment was performed using genomic DNA from 22+2 hr old embryos. Vertical bards show log2fold Dam-only enrichment over Dam-Lola-O and Dam-Pol II, respectively. Grey box highlights the *Bacc* locus.

4.5.13 Conclusion: Lola-O regulates octopamine synthesis via indirect regulation of the enzyme TBH

The loss of Lola-O activity results in various physiological defects including female sterility, cuticle deformity, impaired locomotion, formation of pseudotumours and premature death. This highly conserved Lola splice variant is specifically expressed in octopaminergic neurons in the larval brain. Within these specialized cells, Lola-O controls production of the neurotransmitter octopamine. A key target in this process is *Tbh*, which encodes an enzymatic component of the octopamine synthesis pathway. Depletion of Lola-O leads to reduced *Tbh* levels, resulting in failure to synthesize octopamine.

The findings obtained in our study suggest a model in which Lola-O indirectly regulates *Tbh* levels by directly binding and repressing the gene *Bacc,* which encodes a previously identified repressor of *Tbh.*

DISCUSSION

5. Discussion

This study describes for the first time a comprehensive functional characterization of the different Lola isoforms *in vivo*. Using the CRISPR/Cas9 approach, I generated mutants for every *lola* isoform. We found that depletion of Lola-F mimics the characteristic axonal guidance phenotype that is observed in the absence of all Lola isoforms. Lola-F positively regulates the expression of several well characterized axon-guidance genes and thus acts as a critical regulator of axonal pathfinding along the embryonic ventral midline. Furthermore, a novel function for Lola was identified in neurotransmitter control. The splice variant Lola-O regulates the synthesis of the monoamine octopamine and thus prevents neurodegeneration.

5.1 CRISPR/Cas9 mediated KO to analyse physiological functions *in vivo*

In addition to revealing novel Lola functions, this study demonstrates that the recently developed CRISPR/Cas9 system enables the precise genomic manipulation of individual splice variants and is thus a powerful tool to uncover isoform-specific functions *in vivo*. One important benefit over the widely used RNAi-mediated KD is the permanent and sequence-specific modification of the genome, which thus enables the validation of potential off-target mutations (e.g. via rescue with expression of the corresponding cDNA or by crossing with a second allele or a deficiency that covers the locus). Previous studies demonstrated substantial off-target activity in RNAi experiment in *Drosophila*, underlining the importance to carefully evaluate the specificity of a desired gene manipulation (Seinen *et al.*, 2011). Likewise, studies using RNAi to analyse individual Lola functions in the *Drosophila* brain gave contradictory results (Neumüller *et al.*, 2011; Southall *et al.*, 2014). While Neumüller and colleagues observed tumour formations in the central brain when *lola* was knocked down by RNAi, a more recent study could not recapitulate this phenotype using two different *lola* null mutant alleles (Southall *et al.*, 2014). Moreover, a previously KD of Lola-B was

shown to strongly impair Nb development, resulting in reduced brain size. In contrast, our *lola-B* mutant allele did not recapitulate this phenotype, suggesting that the observed effect on larval brain development was likely a result of off-target activity.

It is noteworthy, however, that our study also generated numerous off-target activities that were likely induced by the CRISPR/Cas9 system (data not shown). Careful validations of induced genome manipulations are therefore recommended in order to analyse the specificity of the Cas9-induced mutation.

5.2 Lola-F regulates axonal pathfinding along the embryonic ventral midline

Lola is amongst the most complex loci in *Drosophila*, encoding for 20 different protein via the alternative splicing of different C-terminal exons. The loss of all Lola isoforms was shown to result in pleiotropic effects throughout the *Drosophila* life cycle, thus making it difficult to analyse Lola functions in the absence of isoform-specific mutant alleles. Lola was first described to regulate axon guidance in the CNS and PNS of *Drosophila* embryos by mildly regulating the expression of numerous axon guidance genes (Crowner *et al.*, 2002; Goeke *et al.*, 2003; Gates, Kannan and Giniger, 2011; Peng *et al.*, 2016). Until our study, it has remained unclear whether the regulating function on axonal pathfinding depends on one specific Lola isoform or whether it is the combinational activity of multiple ones. We identified Lola-F as the main isoform required in this early nervous system dependent process. Similar to the loss of all Lola isoforms, the absence of this highly conserved splice variant strongly impairs axonal pathfinding of motorneurons along the embryonic midline and impairs growth of the peripheral ISNb. Transcriptome analysis of RNA extract isolated from *lola-F* mutant embryos revealed only slight changes on the expression of axon guidance genes, similar to what has been observed in the absence of all Lola isoforms (Gates, Kannan and Giniger, 2011).

How exactly Lola exerts its function in the regulation of axonal guidance is yet to be determined. However, several key targets have been identified. For instance, Lola was shown to regulate the expression of the midline repellent Slit and its axonal receptor Robo (Crowner *et al.*, 2002). Embryonic axon guidance relies on Slit expression in the midline cells of the VNC, which subsequently repels longitudinal axons away from the ventral midline and thus prevents axonal midline crossing (Bhat, Gaziova and Krishnan, 2007). In the absence of Lola activity, both Slit and Robo levels are drastically reduced and hence axon tracts are disorganized. In the PNS, Lola regulates axonal growth and NMJ formation of the peripheral ISNb via reducing the expression of the actin nucleation factor Spire (Gates, Kannan and Giniger, 2011). Our study identified Lola-F as a positive regulator of both *slit* and *robo* levels, suggesting that axonal midline crossing observed in the absence of Lola-F activity mainly arises from altered levels of these axon guidance factors. In contrast, *Spire* expression was unaffected in embryos deficient for Lola-F, implying that other isoforms must control its levels. Moreover, the highly conserved and well-characterized axon guidance gene *futsch* was identified as another key target of Lola-F in regulating axonal guidance. Depletion of the microtubule-associated protein Futsch results in an axon guidance phenotype reminiscent to the loss of Lola (Hummel *et al.*, 2000b). Futsch levels are slightly reduced in the absence of Lola-F activity, while ectopic neuronal Futsch expression is capable of partially restoring axonal pathfinding along the ventral midline. In vertebrates, heterozygous mutation of the Futsch homologue MAP1B leads to a drastic reduction of brain size in mice, suggesting that Futsch levels require a fine-tuned regulation (Edelmann *et al.*, 1996). Interestingly, Futsch expression was shown to be repressed by a splice variant of Ttk (Giesen *et al.*, 1997). Similar to Lola, Ttk encodes for a BTB-ZF protein, suggesting that this class of proteins plays a concerted role in fine-tuning Futsch expression. Proteins comprising BTB-ZF domains were shown to predominantly act as transcription factors with repressive roles on gene expression (Bardwell and Treisman, 1994). However, our findings indicate that Lola-F positively regulates expression of neuronal genes, suggesting that Lola-F acts differently in comparison to other BTB proteins. Nevertheless, this positive effect may be mediated indirectly, for

instance by inhibition of a repressor protein. Additional experiments are therefore required to identify direct targets of Lola-F.

5.3 Lola might acquire novel functions by forming homo- and hetero-dimers

All Lola isoforms encode an N-terminal BTB domain that was previously shown to mediate protein homo- and hetero-dimerization. Accordingly, Lola-F was shown to complex with two other Lola isoforms in embryonic extracts, and homo-dimeric pairing between Lola isoforms was further found in a yeast-two hybrid assay (Giot *et al.*, 2003). But Lola can also interact with factors that do not contain a BTB domain. For instance Lola-J has recently been found associated to PKG via its isoform-specific ZF domain, while Lola-F was shown to interact with the chromosome kinase JIL-1 (Zhang *et al.*, 2003; Peng *et al.*, 2016).

In conclusion, Lola isoforms might acquire novel functions by forming homo- or hetero-dimers as well as by recruiting diverse co-repressors or co-activators during development. Further interactome studies followed by genetic validation will therefore be necessary to understand the full complexity of Lola function on gene expression.

5.4 Functional redundancy between Lola isoforms

Interestingly, the expression of Lola-F drops as *Drosophila* development progresses and becomes primarily restricted to Nbs in the larval brain. During my PhD, I could identify a neuronal role for Lola-F during early development. However it remained unclear whether it plays additional functions later during development. MARCM clone analysis showed no obvious defects in the larval or adult brain in the absence of Lola-F activity. In accordance with our findings, Wissel and colleagues did not identify defect on larval brain development upon

Lola-F KD. However they found that the double KD of Lola-F and Lola-L significantly elevated Nb proliferation (Wissel *et al.*, 2016). These results therefore indicate that Lola-F plays a redundant role with Lola-L in Nb development. Systematic double or triple KD/KO may reveal additional functions for Lola isoforms.

How exactly Lola-F and Lola-J contribute to Nb differentiation is yet to be determined. To understand how these two isoforms cooperate to regulate this process it will be important to identify their direct target genes.

The redundant role described for Lola-F and Lola-L is in contrast to what has been suggested for the neuronal isoform Lola-N. The absence of all Lola isoforms leads to tumour formations in the larval and adult optic lobes. As Lola N is highly enriched in postmitotic neurons and since its ectopic neuronal expression can prevent neuronal dedifferentiation of *lola* mutant clones, a model was proposed in which Lola-N is the major isoform required to prevent neuronal reprogramming (Southall *et al.*, 2014). Surprisingly, however, although our *lola-N* mutant is lethal by the end of embryogenesis, *lola-N* mutant MARCM clones do not exhibit obvious defects neither during larval nor at adult stages. Thus, from our findings we conclude that 1) the absence of Lola-N activity results in embryonic lethality, suggesting that this isoform regulates essential processes during early development, distinct from its later role in neuronal differentiation; 2) since *lola-N* mutant MARCM clones reveal wildtypic characteristics, this splice variant likely cooperates with another Lola isoform in regulating the differentiation state of neurons.

Perturbation of neural identities is usually accompanied by fatal consequences, such as under- or over-proliferation of Nbs, eventually leading to brain tumour growth. Distinct regulatory layers are therefore required to maintain integrity of brain development. For instance, studies in vertebrates identified redundant functional roles for the POU homeodomain proteins in migration and positioning of cortical neurons (Sugitani *et al.*, 2002), suggesting that similar processes might also be present in *Drosophila*. Previous transcriptome analysis of FACS sorted

larval neurons and Nbs showed that expression of Lola-F and Lola-L is highest in Nbs, while Lola-N is highly abundant in neurons together with Lola-H and Lola-K (**see Table 4**; Berger et al., 2012). Similar results were obtained in our study for FACS sorted embryonic neurons, which revealed high expression levels of the isoforms Lola-N and Lola-H (see 4.4.6; **Figure 7**). Analysing the relationship between the isoforms Lola-N, -H and –K during *Drosophila* brain development thus provide an interesting basis for future experiments to examine whether Lola-N might act redundantly with these specific isoforms to prevent neuronal dedifferentiation.

Isoform	**Neuroblast**_FPKM	**Neuron**_FPKM
Lola-A	28,51	34,13
Lola-B	58,04	61,56
Lola-C	37,06	49,95
Lola-D	33,19	54,12
Lola-E	3,15	12,25
Lola-F	163,63	74,24
Lola-G	3,64	11,24
Lola-H	49,57	287,64
Lola-I	4,22	15,44
Lola-J	0,27	1.69906e-07
Lola-K	56,49	179,59
Lola-L	66,78	46,50
Lola-M	11,39	6,78
Lola-N	25,85	227,23
Lola-O	3,83	17,96
Lola-P	6,29	22,21
Lola-Q	3,14	18,21
Lola-R	6,99	16,41
Lola-S	8,47	12,00
Lola-T	27,27	18,79

Table 4: Transcript expression of *lola* isoforms in FACS-sorted larval neurons and Nbs. The highest neuronal expression is observed for Lola-H, followed by Lola-N and Lola-K. Nbs reveal a strong expression of isoforms Lola-F and Lola-L. Data was obtained by Berger et al., 2012.

5.5 Cell-type specificity of different Lola isoforms

It is intriguing that Lola isoforms appear to have opposing functions in Nbs and differentiated neurons. While Lola-F and Lola-L were reported to be required in Nbs to regulate their proliferation (Wissel *et al.*, 2016), Lola-N is highly abundant in postmitotic neurons to maintain their differentiation state (Southall *et al.*, 2014). It will thus be interesting to analyse their respective direct targets to identify the isoform-specific consensus sequences and further characterize how these isoforms exert their specificity.

It is widely known that promoter activity can influence and determine tissue-dependent expression of individual genes, suggesting that the differential expression of Lola isoforms might be a consequence of alternative promoter activity. As *lola* is encoded by at least four promoters, it will be interesting to determine their impact on the expression levels of the different isoforms. Alternatively, splicing regulators might be differentially expressed in neurons and Nbs, promoting the expression of specific isoforms in these cell types. Additional experiments are needed to further validate how cell-type specificity is achieved for Lola isoforms.

5.6 *lola trans*-splicing is isoform specific

Expression of distinct *lola* isoforms depends not only on promoter activity but further relies on alternative splicing of C-terminal exons. *lola* splicing was previously shown to occur via *cis*- and *trans*-splicing (Goeke *et al.*, 2003; McManus *et al.*, 2010; Gao *et al.*, 2015). Intriguingly, exons Lola-A to Lola-F were reported to be processed exclusively via *cis*-splicing (McManus *et al.*, 2010). In contrast, both *cis*- and *trans*-splicing events were detected for the remaining *lola* exons (Lola-G to Lola-T) that are located further downstream. We could experimentally confirm these findings by performing interallelic complementation assays by taking advantage of our generated mutant alleles. Recombination of the lethal alleles *lola-K, -L,-N* and -*T* with $lola^{E76}$ null mutant flies gave rise to homozygous viable

offspring, confirming the *trans*-splicing of the respective isoform-specific C-terminal exon. In contrast, both our *lola-F* alleles failed to restore the lethal phenotype upon recombination with the *lola* null mutant, suggesting that *trans*-splicing does not occur for this isoform. Regardless of the precise mechanism by which *trans*-splicing is regulated and the purpose of *trans*-splicing, these results imply a potential positional dependency. As exons Lola-A to Lola-F are in close proximity to the N-terminal constitutive region, while the remaining *trans*-spliced exons are positioned further downstream, these results suggest that *trans*-splicing may facilitate the expression of isoforms whose structure would otherwise create challenges to the classical *cis*-splicing machinery.

5.6 Novel connection between Lola and octopamine synthesis

Our study identified a specific expression for Lola-O in a subset of neuronal cells, which we identified as octopaminergic neurons. The mechanisms that restrict Lola-O expression to these specialised cells are currently unknown and further experiments will be required to determine how this specificity is achieved. Moreover, we described a novel role for this splice variant in regulating the synthesis of octopamine, a homologue to the human norepinephrine that acts as neurohormone, neuromodulator and neurotransmitter (Nathanson, 1979). Its synthesis in *Drosophila* is acquired in a two-step mechanism involving the subsequent activity of two enzymatic components, TBH and Tdc2 (Monastirioti, Linn and White, 1996). Our findings support a model in which Lola-O directly binds and represses *Bacc*, which encodes a previously identified repressor of *Tbh* (Chen *et al.*, 2013). This novel role of Lola in neurotransmitter biogenesis has likely been missed due to pleiototropic effects of *lola* null mutants and the absence of specific *lola-O* alleles.

Previous studies suggested that octopamine levels require a fine-tuned regulation, as reducing its levels was shown to result in various phenotypic defects including sterility and impaired longevity (Monastirioti, Linn and White, 1996; Li *et al.*, 2016). Furthermore, excessive octopamine levels also have a lethal effect (Crocker

and Sehgal, 2008). Currently, very little is known about the dynamics underlying octopamine synthesis during the *Drosophila* life cycle. Studies on honeybees have shown that octopamine synthesis increases with age (Harris, & Woodring, 1991), which might also be the case in *Drosophila*. Furthermore, octopamine synthesis was shown to be stress-induced in the haemolymph of both locusts and cockroaches (Davenport & Evans, 1984), implying that differential concentrations of octopamine are required in response to altered environmental circumstances. Only recently it was shown that heat dependent stress conditions elevate octopamine synthesis in *Drosophila* via activity of the forkhead boxO (FOXO) transcription factor (Gruntenko et al., 2016). More precisely, the absence of FOXO leads to an increase in Tdc2 levels and a subsequent rise in octopamine metabolism. These findings offer an interesting base to examine whether TBH expression is also stress-induced in a FOXO-dependent manner and whether Lola-O contributes to this effect.

6. Graphical abstract

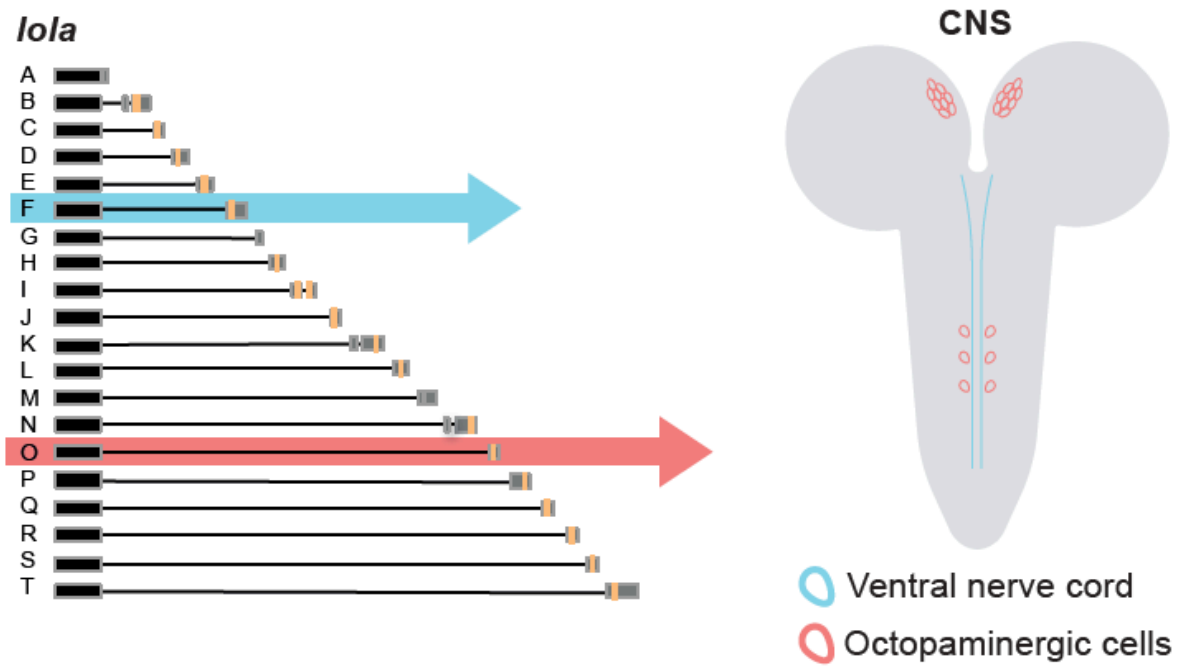

SUMMARY

7. Summary / Zusammenfassung

7.1 Summary

longitudinals lacking (lola) is one of most complex genes in *Drosophila*, encoding for 20 different protein isoforms by alternative *cis*- and *trans*-splicing. Each splice variant shares a constitutive N-terminus but contains distinct isoform-specific C-terminal exons, which for most isoforms encode a zinc finger motif. Lola acts as a transcription factor playing diverse roles *in vivo*, including axonal guidance and neuronal maintenance. Majority of previously performed studies employed loss-of-function alleles disrupting all Lola isoforms, making it difficult to decipher isoform-specific roles during development. Therefore, the physiological function of individual Lola isoforms has been poorly characterized.

My PhD project aimed to better characterize physiological functions of Lola isoforms *in vivo.* Using the recently developed CRISPR/Cas9 system, I created mutations in isoform-specific C-terminal exons and mutant alleles were generated for all 20 Lola isoforms. Phenotypic analysis revealed an opposing function for the isoforms Lola-A and Lola-H in regulating locomotion behaviour of adult flies. Furthermore, a critical role was identified for Lola-O in controlling octopamine synthesis and thus preventing neurodegeneration. This splice variant is specifically expressed in octopaminergic neurons, where it regulates the expression of the Tyramine-ß-hydroxylase, a key enzymatic component of the octopamine synthesis pathway. Lastly, I identified Lola-F as an essential factor controlling axonal pathfinding along the embryonic ventral midline. Lola-F positively regulates the expression of several axon guidance genes, including the microtubule-associated factor Futsch.

This study emphasizes the significance of the CRISPR/Cas9 system in sequence specific genome modification and its concomitant importance on the functional analysis of distinct protein isoforms. Furthermore, this work demonstrates that Lola splice variants exhibit a high functional diversity in distinct cell types, thereby underlining the importance of alternative splicing as an essential process to enhance proteome diversity.

7.2 Zusammenfassung

lola gehört zu den komplexesten Genen in *Drosophila melanogaster,* welches durch alternativem Spleißen für 20 Isoformen kodiert. Alle Lola Spleißvarianten tragen eine einheitliche N-terminale BTB-Domäne, wohingegen 17 Isoformen zusätzlich über einen spezifischen C-terminale Zinkfinger verfügen. Lola fungiert als Transkriptionsfaktor mit unterschiedlich beschriebenen Funktionen *in vivo*, wie der axonalen Wegfindung und der neuronalen Instandhaltung. Die meisten bisher durchgeführten Studien arbeiteten mit Lola Nullalelen, so dass individuelle Funktionen einzelner Isoformen weitestgehend unbekannt sind.

In der vorliegenden Arbeit wurden Lola Isoformen bezüglich ihrer molekularen Funktion charakterisiert. Durch die Anwendung des CRISPR/Cas9 Systems wurden Loss-of-Function-Mutationen für alle 20 Lola Isoformen erzeugt. Dieser Forschungsansatz ermöglichte es uns, bisher unbekannte Rollen für verschiedene Spleißvarianten zu charakterisieren. Die phänotypische Analyse mutanter Fliegen ergab gegensätzliche Funktionen der Isoformen Lola-A und Lola-H in der Fortbewegung adulter Fliegen. Außerdem konnte für die hochkonservierte Isoform Lola-O eine Rolle in der Neurotransmitterbiosynthese charakterisiert werden. Die Expression dieser Spleißvariante findet hochspezifisch in oktopaminergen Neuronen des zentralen Nervensystems statt und innerhalb dieser Zelltypen reguliert Lola-O die Expression der Tyramin-ß-Hydroxylase, ein Hauptenzym der Oktopamin-Synthese, und verhindert somit neurodegenerative Folgeerscheinungen. Zusätzlich wurde Lola-F als essentieller Faktor der axonalen Wegfindung identifiziert. Lola-F reguliert die Expression verschiedener axonaler Wegfindungsgene, wobei der Mikrotubulin-assozierten Faktor Futsch ein Schlüsselziel dieses Prozesses darstellt.

Diese Arbeit veranschaulicht die Bedeutung des CRISPR/Cas9 Systems in Bezug auf die sequenz-spezifische Modifizierung des Genoms und die damit verbundene Weitreiche bezüglich der Analyse individueller Proteinfunktionen. Lola Isoformen besitzen eine hohe funktionale Diversität in unterschiedlichen Zelltypen und die hier beschriebenen Ergebnisse veranschaulichen die Bedeutsamkeit des alternativen Spleißens als essentiellen Mechanismus zur Erweiterung der Protein-Diversität.

8. Article

Cell Reports
Article

OPEN ACCESS
CellPress

Comprehensive Characterization of the Complex *lola* Locus Reveals a Novel Role in the Octopaminergic Pathway via Tyramine Beta-Hydroxylase Regulation

Nadja Dinges,[1] Violeta Morin,[1] Nastasja Kreim,[2] Tony D. Southall,[3] and Jean-Yves Roignant[1,4,*]
[1]Laboratory of RNA Epigenetics, Institute of Molecular Biology (IMB), 55128 Mainz, Germany
[2]Bioinformatics Core Facility, Institute of Molecular Biology (IMB), 55128 Mainz, Germany
[3]Department of Life Sciences, Imperial College London, Sir Ernst Chain Building, London SW7 2AZ, UK
[4]Lead Contact
*Correspondence: j.roignant@imb-mainz.de
https://doi.org/10.1016/j.celrep.2017.11.015

SUMMARY

***Longitudinals lacking* (*lola*) is one of the most complex genes in *Drosophila melanogaster*, encoding up to 20 protein isoforms that include key transcription factors involved in axonal pathfinding and neural reprogramming. Most previous studies have employed loss-of-function alleles that disrupt *lola* common exons, making it difficult to delineate isoform-specific functions. To overcome this issue, we have generated isoform-specific mutants for all isoforms using CRISPR/Cas9. This enabled us to study specific isoforms with respect to previously characterized roles for Lola and to demonstrate a specific function for one variant in axon guidance via activation of the microtubule-associated factor Futsch. Importantly, we also reveal a role for a second variant in preventing neurodegeneration via the positive regulation of a key enzyme of the octopaminergic pathway. Thus, our comprehensive study expands the functional repertoire of Lola functions, and it adds insights into the regulatory control of neurotransmitter expression *in vivo*.**

INTRODUCTION

lola is among the most complex loci in *Drosophila*, giving rise to at least 80 different mRNA isoforms through alternative *cis*- and *trans*-splicing as well as via multiple promoter activity (Figure 1A) (Goeke et al., 2003; Horiuchi et al., 2003; Ohsako et al., 2003; Zhang et al., 2003). In total, *lola* encodes 20 known protein isoforms (Lola A–Lola T) that contain a common N-terminal BTB domain, with 17 isoforms encoding a unique zinc-finger motif in their C-terminal variable exons (Figure 1B). Lola has been shown to act as a transcription factor with regulatory roles in axon growth and guidance during embryogenesis, and it is also required for maintaining neurons in a differentiated state of the developing brain (Giniger et al., 1994; Goeke et al., 2003; Southall et al., 2014). In addition, Lola has been found to control stem cell maintenance and germ cell differentiation in the *Drosophila* testis, programmed cell death during oogenesis, and gonad formation in early embryo (Bass et al., 2007; Davies et al., 2013; Tripathy et al., 2014).

Most experiments investigating Lola function utilized loss-of-function alleles containing mutations in the N-terminal constitutive region, which affect all 20 Lola isoforms and give pleiotropic effects *in vivo* (Giniger et al., 1994; Madden et al., 1999; Crowner et al., 2002; Goeke et al., 2003; Horiuchi et al., 2003; Spletter et al., 2007; Zheng and Carthew, 2008; Gates et al., 2011; Fukui et al., 2012; Davies et al., 2013; Southall et al., 2014). Studies of specific isoform mutant alleles, which are available only for Lola-K, -J, -L, and -T, revealed functions in distinct physiological processes (Goeke et al., 2003; Bass et al., 2007; Davies et al., 2013; Tripathy et al., 2014; Peng et al., 2016). Isoforms Lola-K and Lola-L are both involved in two unrelated mechanisms, which include motor nerve development and germline stem cell maintenance in the male testis, indicating that at least some Lola isoforms control multiple functions during development (Goeke et al., 2003; Davies et al., 2013).

To functionally characterize Lola isoforms, we generated mutations using CRISPR/Cas9 for all 20 *lola* isoforms by respectively targeting the isoform-specific C terminus. Among the 20 *lola* mutant strains, five are homozygous lethal during early development while three exhibit clear defects in adult flies. We demonstrate that mutations targeting *lola-F* result in severe disruption of axonal tracts at the embryonic ventral midline. We found that Lola-F regulates the expression of several axonal guidance genes, including the microtubule-associated factor Futsch. Furthermore, flies deficient for *lola-A* and *lola-H* display severe locomotion phenotypes. Finally, *lola-O* mutant flies are viable but display a strong degeneration phenotype due to a defective octopaminergic pathway. Lola-O is specifically expressed in the subset of neurons that produce octopamine (OA) and regulates its biogenesis by controlling the expression of *Tyramine beta-hydroxylase* (*Tbh*), which encodes a key enzymatic component of this pathway. Together, our data provide a comprehensive functional characterization of Lola isoforms, revealing novel roles for previously uncharacterized isoforms.

RESULTS

CRISPR/Cas9-Induced *lola* Isoform-Specific Knockout

To comprehensively characterize Lola isoforms *in vivo*, we generated knockout (KO) flies for each isoform using the

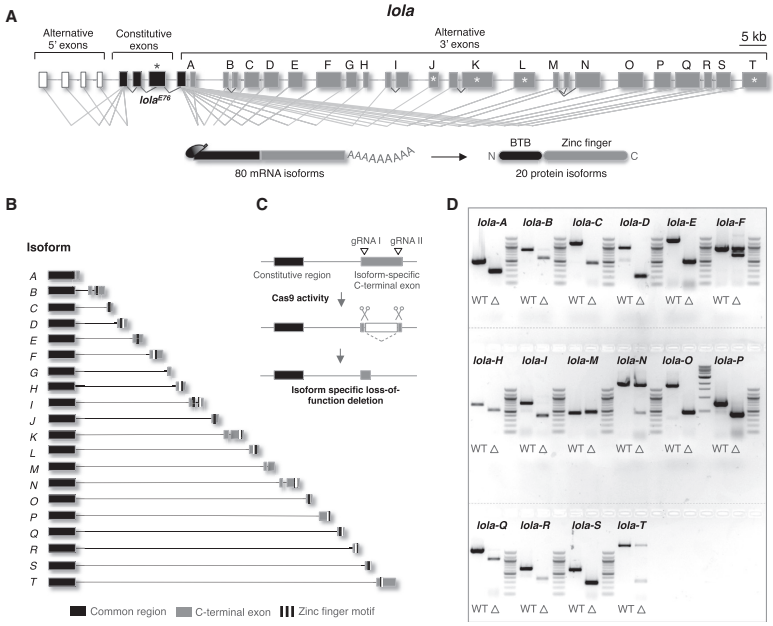

Figure 1. CRISPR/Cas9-Induced *lola* Isoform-Specific Knockout

(A) Schematic structure of the *lola* locus. *lola* comprises 32 exons including 5′ UTR exons (white boxes), constitutive exons (black), and 3′ alternative exons (gray). 80 putative transcripts encode for 20 protein isoforms, each sharing an N-terminal BTB domain but holding isoform-specific exons encoding for a C-terminal zinc-finger domain in 17 isoforms. Previously characterized mutations are marked by an asterisk.

(B) Scheme of the 20 *lola* isoforms (Lola-A–Lola-T). Stripes highlight zinc-finger motifs.

(C) CRISPR/Cas9 approach to systematically mutate each Lola isoform.

(D) Gel analyses of established *lola* mutants. Agarose gel shows amplicons of respective genomic regions in wild-type (WT, left lane) and CRISPR/Cas9-induced *lola* KO flies (Δ, right lane). Mutation in Lola-M resulted in partial duplications that disrupt the frame. Mutants for *lola-G*, *-J*, *-K*, and *-L* bear a frameshift and are not displayed. Lethal alleles are heterozygous and show both the mutant and the wild-type allele.

See also Figures S1 and S2.

CRISPR/Cas9 system. In brief, two distinct guide RNAs (gRNAs) were designed to target the isoform-specific C-terminal exon of each *lola* isoform (Figure 1C). In most cases, Cas9 activity resulted in the production of two double-strand breaks, leading to deletion of the sequence between the two Cas9 target sites and resulting in a loss-of-function mutation for the respective *lola* isoform (Figures 1D and S1).

Our targeted screen resulted in KO flies for all 20 known Lola isoforms, and mutations in 8 of these isoforms led to a clear phenotype (Table S1). Five isoform-specific mutations, including in the already described *lola-K*, *-L*, and *-T* as well as in *lola-F* and *-N*, resulted in lethality during embryonic and early larval stages. Mutations in *lola-A* and *-H* produced viable flies with impaired locomotion (Figure S2A). Interestingly, *lola-H* mutants displayed reduced locomotion, while *lola-A* mutant flies were hyperactive. Finally, *lola-O* mutants survived until adulthood, but they rapidly degenerated and died around 2 weeks after hatching. With the exception of Lola-H and -A, we found that only isoforms conserved between *D. melanogaster* and *Anopheles gambiae* play important roles during development and in adults (Table S1), raising the question of the relevance of the non-conserved Lola isoforms.

Among them, Lola-B was previously shown to play a critical role in neural stem cell (NSC) differentiation using RNAi (Neumüller et al., 2011). Upon depletion of Lola-B, NSC proliferation was shown to be drastically reduced. However, our *lola-B* KO flies did not recapitulate this phenotype, suggesting that this effect was due to off-target activity (Figure S2B). In contrast, mutations in the conserved *lola-L* and *-K* reproduced the reported defects in the innervation of ISNb motoneurons (Figure S2C), as well as the loss of *lola-T* in germ cell migration (Figure S2D). It has been reported that neurons deficient for all Lola isoforms

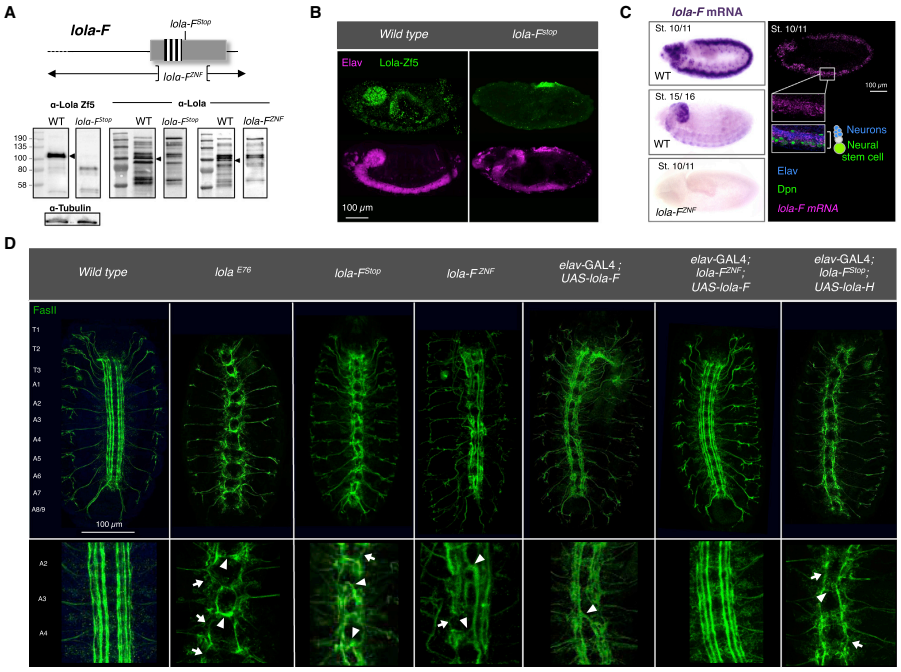

Figure 2. *lola-F* KO Embryos Display Disrupted Axonal Tracts

(A) (Top) Schematic of *lola-F* genomic region. *lola-F*^{Stop} bears a 2-bp deletion resulting in a premature stop codon downstream of the zinc-finger domain. *lola-F*^{ZNF} lacks the entire zinc-finger motif. (Bottom) Immunoblotting using the anti-Lola zf5 and anti-Lola antibody on control and *lola-F* KO lysates of stage 15 embryos is shown. Arrowheads depict a band specific for Lola-F.

(B) Anti-Lola zf5 immunostaining (green) on stage 13 embryos. Lola-F protein is undetectable in *lola-F*^{stop} embryos.

(C) *In situ* hybridization shows *lola-F* mRNA (magenta) enrichment in the nervous system, which is absent in *lola-F*^{ZNF} embryos. *lola-F* mRNA co-localizes with both the neuronal marker Elav (blue) and NSC marker Dpn (green, lateral view, stage 10/11).

(D) Immunostaining of the VNC using an anti-Fasciclin II antibody (green). *lola-F* mutants display strong midline crossing of axons (arrowheads), while *lola*^{E76} embryos show more severe axon growth defects (arrows). Neuronal *lola-F* expression in wild-type disrupts axonal tracts, but it is sufficient to rescue the phenotype in a *lola-F* mutant background (stage 15/16 embryos, ventral view). Ectopic *lola-H* expression is unable to rescue the axonal defects in *lola-F*^{Stop} mutants.

See also Figures S2 and S3.

dedifferentiate into NSCs in the developing nervous system (Southall et al., 2014) and that Lola-N is able to rescue this phenotype. We found that depletion of *lola-N* in the larval or adult brain by mosaic analysis with a repressible cell marker (MARCM) did not alter the differentiation state of postmitotic neurons (Figure S2E; data not shown), hinting to possible functional redundancy between isoforms. This potential functional redundancy between isoforms might also prevent us from uncovering additional roles for Lola. Consistent with this, reducing the level of both Lola-L and Lola-F was recently shown to alter NSC number, while reduction of either one alone had no effect (Wissel et al., 2016).

Lola-F Is the Main Isoform Required for Axon Guidance in the Developing Embryo

We generated two different *lola-F* alleles that were both lethal during late embryogenesis (Figures 1D, 2A, and S1). One allele specifically lacks the zinc-finger motif (*lola-F*^{znf}), whereas the second one carries a 2-bp deletion downstream of the zinc-finger domain (*lola-F*^{stop}), leading to a frameshift and premature stop codon. We confirmed the depletion of Lola-F protein in both homozygous mutant embryos, while the overall levels of other isoforms were virtually unchanged or only slightly reduced (Figure 2A). Immunostaining using a Lola-F-specific antibody further confirmed the absence of Lola-F protein in *lola-F*^{Stop} mutant

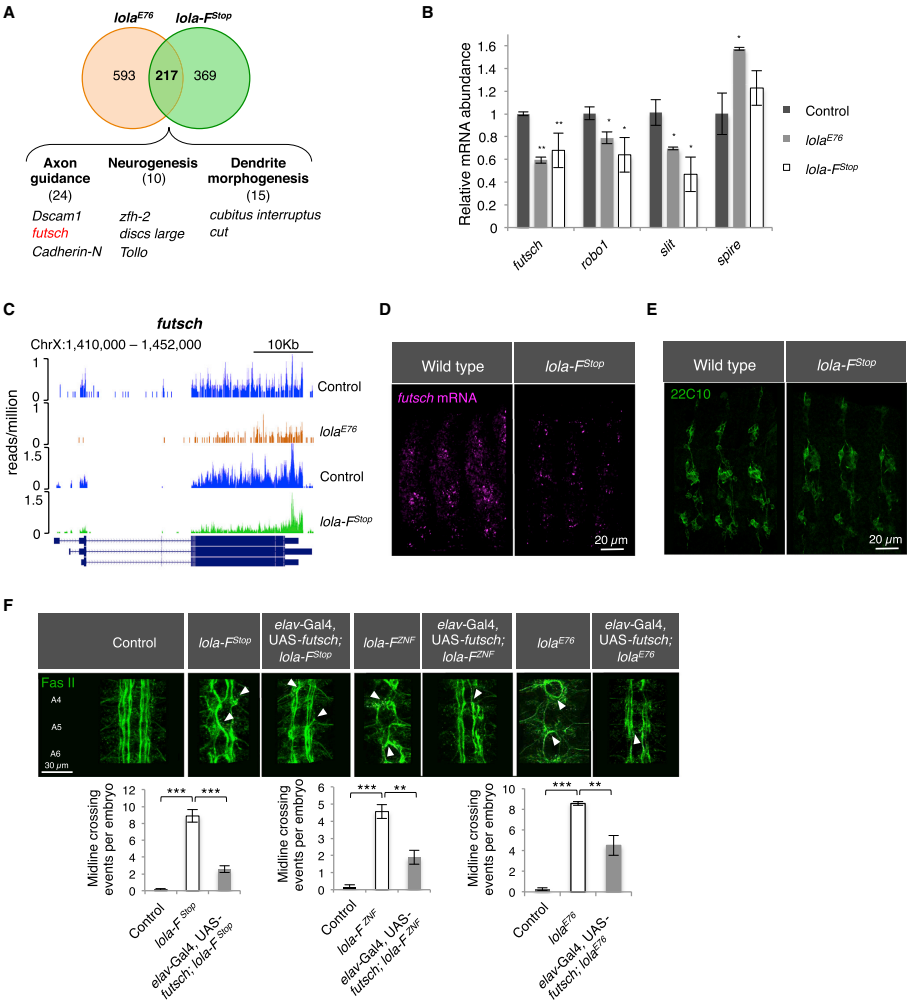

Figure 3. Lola-F Regulates Neuronal Projection by Activation of Axon Guidance Genes

(A) Transcriptome analysis of *lola-F*^{Stop} and *lola*^{E76} embryos reveals 217 commonly downregulated genes. Highlighted are examples of shared target genes involved in neuronal development.

(B) qRT-PCR for selected genes on *lola*^{E76} and *lola-F*^{Stop} mutant RNA extracted from stage 15 embryos. ANOVA t test was performed (**p < 0.01 and *p < 0.05). Data are represented as median ± SD from three technical replicates.

(C) Track example of poly-A-selected RNA-seq at the *futsch* locus.

(D) *In situ* hybridization reveals reduced *futsch* mRNA (magenta) in *lola-F*^{Stop} embryos (stage 15, lateral view).

(E) Anti-22C10 immunostaining (green) detects reduced Futsch levels in *lola-F*^{Stop} mutants (stage 15 embryo, lateral view).

(legend continued on next page)

embryos (Figure 2B). Moreover, expression of a *lola* genomic construct rescued the lethal effect of both mutants, confirming the specificity of our alleles (data not shown). Expression analysis by *in situ* hybridization revealed a strong enrichment of *lola-F* mRNA in the developing CNS, which was lost in *lola-F*^{ZNF} embryos (Figure 2C). More precisely, *lola-F* localized in both NSCs and differentiated neurons, suggesting possible functions during neurogenesis. At late embryogenesis and in larvae, *lola-F* RNA expression became mainly restricted to NSCs (Figures 2C and S3A).

To address the role of Lola-F, we stained control and *lola-F* KO embryos with anti-Fasciclin II to label axon tracts of stage 15 embryos (Figure 2D). The loss of all Lola isoforms was previously shown to impair axonal growth and pathfinding at the ventral midline, a phenotype we could recapitulate using the *lola*^{E76}-null mutant allele. Remarkably, depletion of Lola-F also resulted in severe disruptions of the ventral nerve cord (VNC). Compared to the null mutant, axons extended slightly further but several crossing defects were observed. The number of neurons, NSCs or glial cells, was, however, unaffected (Figures S3B and S3C). Both alleles and transheterozygous combinations gave indistinguishable phenotypes (Figure 2D; data not shown), and expression of a *lola*-BAC was sufficient to rescue the axonal guidance defects (data not shown), confirming the specific role of this isoform in this process. We further generated a transgenic line expressing Lola-F under the control of UAS promoter. Strikingly, neuronal Lola-F expression in wild-type embryos disrupted the VNC, mimicking the *lola-F* mutant phenotype (Figure 2D). However, neuronal Lola-F cDNA expression in *lola-F* KO embryos completely restored the axonal guidance defects, which was not the case upon neuronal expression of Lola-H or Lola-O cDNA (Figure 2D; data not shown). Altogether, these data indicate that Lola-F plays a major role in establishing axonal guidance at the ventral midline, and they suggest that its physiological levels must be tightly controlled to ensure its correct function.

We next wondered whether other isoforms that are essential during embryonic development were also involved in controlling axonal pathfinding. As previously shown by *in situ* hybridization (Goeke et al., 2003), we confirmed by RNA sequencing (RNA-seq) of neuronal sorted cells from stage 15/16 embryos that most isoforms were expressed in neurons. Lola-A, -F, -H, -K, and -N were most strongly expressed, while Lola-J, -M, -O, and -B were barely detectable (Figure S4A). Lola-K and -L were already shown to control muscle innervation by ISNb motoneurons, a phenotype we could recapitulate; we also could demonstrate that Lola-F plays a similar function (Figure S2C). However, neither the depletion of Lola-K and -L nor the absence of Lola-N and -T altered axon guidance at the ventral midline (Figure S2F). Only *lola-K* mutants occasionally displayed crossing defects between the A5 and A6 hemisegments. Hence, our data indicate that Lola-F is the major isoform required in axonal pathfinding at the ventral midline for which *lola* is named.

Lola-F Activates Expression of Several Genes Involved in Axon Guidance

Previous studies reported the involvement of Lola in axon guidance, in part by upregulating the levels of the repulsive ligand Slit and its receptor Robo at the ventral midline (Crowner et al., 2002), while its effect on axon growth could partly be explained by downregulation of the actin nucleation factor Spire (Gates et al., 2011). To get further insights into the mechanisms by which Lola controls axon growth and guidance, we took advantage of our specific *lola-F*^{stop} allele to perform transcriptome analysis at stage 15, when the majority of axon guidance events are taking place. We also included samples from *lola*^{E76}-null mutant embryos to compare the affected genes with the absence of *lola-F*. We found that 465 and 586 genes were significantly upregulated and downregulated in *lola-F* KO embryos, respectively (adjusted p value < 0.01). Intriguingly, gene ontology (GO) term analysis revealed enrichment for genes involved in cell adhesion and axon extension specifically for downregulated genes, underlining the role of Lola-F in regulating axonogenesis (Figures 3A and S5A). 217 (37%) downregulated genes were mutually found in the *lola*-null mutant, including the previously described targets *slit* and *robo1* (Figures 3A, 3B, S5B, and S5C). However, in contrast to the null allele, *lola-F* mutants showed no significant change in *spire* expression (Figures 3B and S5D), indicating that other isoforms must control its level. The absence of *spire* regulation by Lola-F might account for the milder effect observed on axon growth compared to the complete loss of *lola* (Figure 2D). Furthermore, potential antagonistic isoform-specific Lola functions might nullify each other's effect, thus explaining that a subset of genes affected in the *lola-F* mutant is not present in the null allele.

Among the top 15 downregulated genes in both *lola*^{E76} and *lola-F*^{Stop} mutants is *futsch*, a well-characterized and conserved axon guidance gene (Figure 3A). The axonal defects observed for *lola-F* KO embryos mimicked the previously characterized *futsch*^{K68} mutant phenotype, as embryos showed disrupted VNC motoraxons and stalling of the peripheral ISNb motornerve (Hummel et al., 2000; Figure S2C). The reduction in *futsch* levels was confirmed by qRT-PCR and *in situ* hybridization (Figures 3B–3D). Immunostaining using a Futsch-specific antibody on *lola-F*^{Stop} embryos showed an overall reduced fluorescent intensity, indicating that the protein level was also decreased (Figure 3E). To examine whether the effect on *futsch* expression in the absence of Lola-F activity contributes to the observed phenotypes, we wondered whether restoring its levels could rescue some of the *lola* defects. To this purpose, an EP element insertion line containing UAS-regulatory elements located in the promoter region of *futsch* was crossed with the neuronal *elav*-GAL4

(F) (Top) Immunostaining of VNC using anti-Fasciclin II antibody (green) to analyze midline-crossing events. Ectopic neuronal Futsch expression partially rescues axonal midline crossing of *lola-F*^{stop}, *lola-F*^{ZNF}, and *lola*^{E76} embryos. Arrowheads indicate axon guidance defects. (Bottom) Quantification of midline-crossing events is shown (n = 9 for *lola-F*^{stop}and *lola*^{E76}; n = 8 for *lola-F*^{ZNF}). Significance was tested using ANOVA one-way t test (***p < 0.001 and **p < 0.01). Data are represented as average ± SEM.
See also Figure S5.

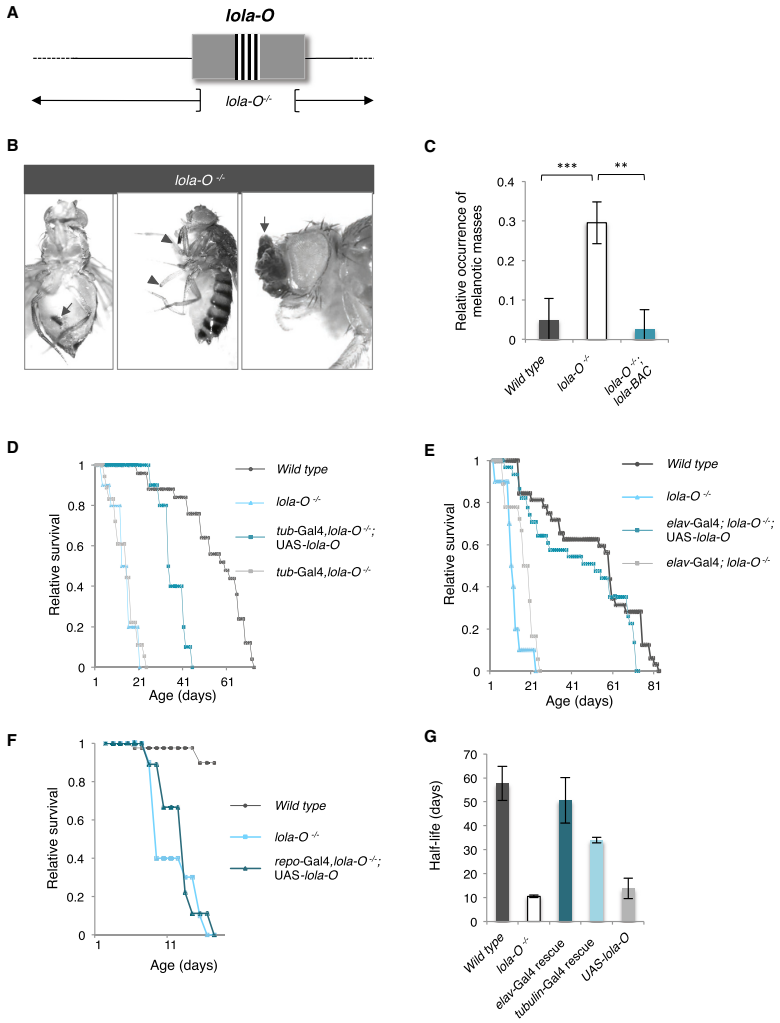

Figure 4. *lola-O* KO Flies Display a Severe Neuronal Degeneration Phenotype

(A) Scheme of the *lola-O* genomic region and expected deletion.

(B) *lola-O* KO adult flies display melanotic masses (arrows), eventually leading to the loss of affected limbs (arrowhead).

(C) Phenotypic penetrance of melanotic masses is reduced to control levels by recombination with a *lola* genomic construct. 10 flies were examined in four replicates at 11 days of age. ANOVA one-way t test was performed (***$p < 0.001$). Data are represented as average ± SEM.

(D–F) Survival curves of adult *Drosophila*. The average of three biological replicates is shown, and *lola-O* mutants recombined with the driver line serve as a control. (D) Ubiquitous ectopic expression (*Tub*-GAL4) of *lola-O* cDNA elongates the lifespan of *lola-O* mutants by 2-fold. (E) Neuronal *lola-O* expression (*elav-*

(legend continued on next page)

driver line. We found that embryonic progeny derived from this cross displayed ectopic Futsch levels, yet axonal guidance was normal (Figures S5E and S5G). Similar elevated Futsch levels were observed in embryos deficient for Lola-F. Remarkably, this ectopic Futsch expression was sufficient to partially restore both VNC and ISNb axonal defects for both *lola-F* alleles and the *lola*-null mutant (Figures 3F and S5F). It is noteworthy that neuronal overexpression of *lola-F* did not result in elevated *futsch* levels, indicating that ectopic *lola-F* expression alone was not sufficient to transcriptionally activate *futsch* (Figures S5H and S5I). Furthermore, previous findings have shown that Futsch expression is negatively regulated by a splice variant of Tramtrack (Ttk) (Giesen et al., 1997). To analyze whether the observed axon guidance phenotype in *lola-F* mutants was mediated by a change in Ttk levels, we analyzed *ttk* expression in *lola-F*^{Stop} embryos (Figure S5J). We found that both *ttk* isoforms displayed a slight downregulation upon Lola-F depletion, indicating that the observed axon guidance phenotype was not a consequence of increased Ttk levels. Collectively, our findings demonstrate that Lola-F regulates axonal pathfinding by activating numerous axon guidance genes, including the microtubule-associated encoded gene *futsch*.

lola-O Mutant Flies Display a Severe Degeneration Phenotype

We next investigated the function of Lola-O *in vivo*. We generated one mutant allele that was expected to disrupt the entire zinc-finger domain (Figure 4A). The lack of mRNA expression was confirmed by qRT-PCR and RNA-seq using RNA extracts from control and mutant strains (Figures S6A and S6B). Depletion of *lola-O* results in homozygous viable animals, yet adult flies displayed several abnormalities, including reduced lifespan and severe locomotion defects (Figures S6C and S6D). In addition, females exhibited cuticle malformation and suffered from partial sterility (Figures S6E and S6F). Both males and females also frequently formed melanotic masses (also called pseudotumors), which occurred predominantly on abdomen and limbs (Figures 4B and 4C). Melanotic masses were also occasionally observed in third instar larvae (Figure S6G). Importantly, all these phenotypes could be rescued by a genomic construct restoring *lola-O*, ruling out off-target effects. Likewise, ubiquitous or ectopic neuronal *lola-O* expression was sufficient to restore the lifespan and reduce phenotypic penetrance of *lola-O* KO flies (Figures 4D, 4E, 4G, and S6H). In contrast, glial expression had no effect (Figure 4F). Taken together, these findings indicate a neuronal role for Lola-O in regulating multiple physiological functions.

lola-O Is Specifically Expressed in OA Neurons

To obtain insights into Lola-O function, we sought to address its localization *in vivo*. For this purpose, we took advantage of a fly line carrying a *lola*-BAC encoding a Lola-O-GFP fusion protein (Spokony and White, 2012). We found that Lola-O was generally expressed at a very low level in the larval brain, just at the limit of its detection. However, the low Lola-O-GFP expression was refined to only a subset of cells, which included the midline and lateral midline of the ventral ganglion and a few groups of cells in the central brain (Figure 5A). To reveal the identity of these cells, we crossed flies carrying a UAS-GFP transgene reporter with flies expressing GAL4 under the control of various neuronal promoters, and the resulting GFP expression was subsequently compared to the expression pattern of Lola-O. Interestingly, GFP expression driven by the *Tdc2*-GAL4 driver was reminiscent of the expression of Lola-O-GFP (Figure 5B).

Tdc2 stands for *Tyrosine-decarboxylase* and encodes for an enzyme required for the synthesis of OA (Figure 6A). OA acts as a neurotransmitter, neuromodulator, and neurohormone in insects, and it is involved in diverse physiological functions. Notably, perturbation of its level results in phenotypes reminiscent of the loss of Lola-O, including locomotion defects, cuticle deformity, the appearance of pseudotumors, female sterility, and the shortening of lifespan (Figure 6B; Monastirioti et al., 1996; Stathakis et al., 1999; Saraswati et al., 2004; Li et al., 2016). Its synthesis requires the amino acid tyrosine, which is modified to tyramine by the Tyrosine-decarboxylase 2 (Tdc2). Subsequently, Tyramine β-hydroxylase (TBH) hydrolyzes tyramine to produce OA (Figure 6A; Barron et al., 2010; Li et al., 2016).

To confirm the expression of Lola-O in OA neurons, larval brains were stained for both Lola-O-GFP and an antibody that recognizes TBH, which was shown to be a faithful marker of OA cells (Selcho et al., 2012). We found that TBH and Lola-O-GFP co-localized in a cluster of dorsomedial cells in the larval brain and along the midline of the VNC. Single cells lateral of the midline were only positive for Lola-O-GFP (Figure 5C). Therefore, our data suggest that Lola-O function may be linked to the OA pathway. We also performed transcriptome analysis on OA cells sorted via fluorescence-activated cell sorting (FACS) of stage 17 embryos. We found that *lola-A*, *lola-K*, and *lola-L* were strongly expressed, while the read coverage was not sufficient to detect *lola-O* mRNA, confirming that this isoform is expressed at low levels in OA cells (Figure S4B).

Expression of *lola-O* cDNA in OA Neurons Is Sufficient to Rescue Most *lola-O* Mutant Defects

To address a potential role of Lola-O in the OA pathway, we performed a drug-feeding assay in which *lola-O* KO flies were supplied with OA-enriched food. Interestingly, ectopic feeding of OA to *lola-O* mutants was sufficient to elongate the half-life by 2-fold (12 days ± 2.6 versus 21 days ± 3.6, p value < 0.05), while feeding the same flies with tyrosine had no effect (Figures 6C and 6D). We verified that feeding *Tbh*^{nM18} mutant flies with OA rescues the half-life to a similar extent (Figure 6B). Furthermore,

GAL4) restores longevity of *lola-O* mutant flies to wild-type levels. (F) Glial cell-specific (*repo*-GAL4) *lola-O* expression is unable to rescue premature lethality of *lola-O* KO flies.
(G) Half-life quantification. Half-life is defined as the day with 50% survival. Four biological replicates were analyzed. Data are represented as average ± SEM. See also Figure S6.

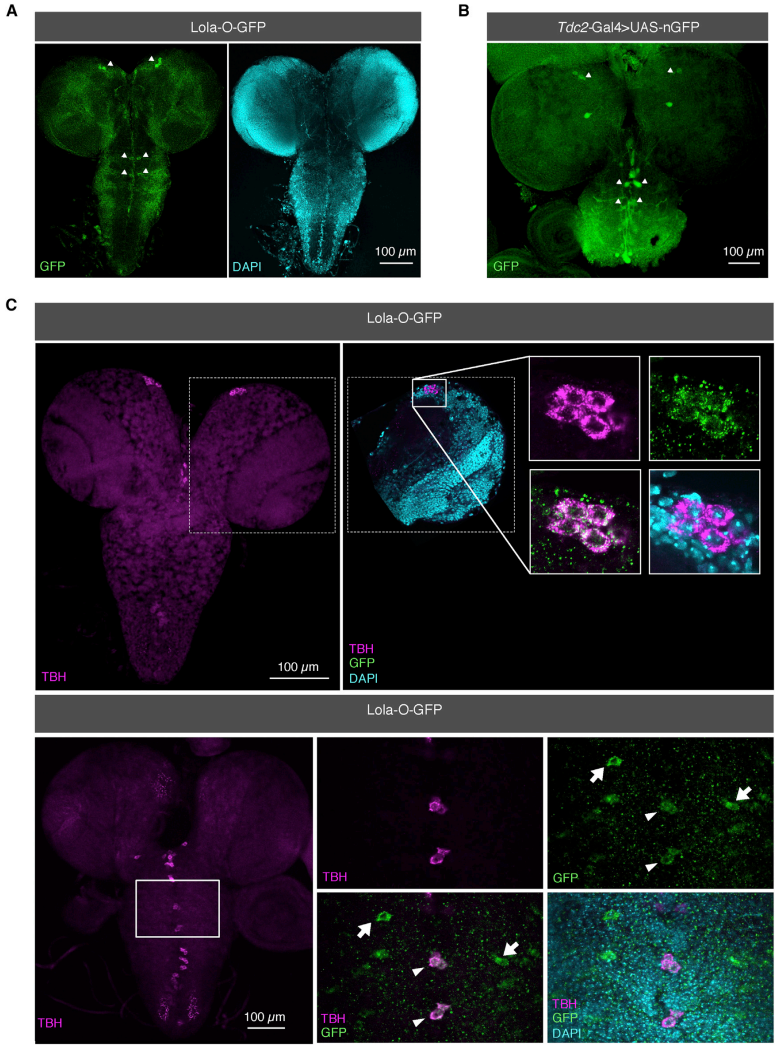

Figure 5. Lola-O Co-localizes with OA Neurons in the Larval Brain

(A) Immunostaining of Lola-O-GFP using an anti-GFP antibody (green; DAPI, cyan).

(B) *Tdc2*-GAL4 expression pattern in the larval brain revealed with an anti-GFP antibody (green). OA cells are present in the VNC along the midline and in a subset of cells in the central brain (arrowheads), similar to the Lola-O-GFP expression.

(C) Lola-O (anti-GFP, green) and TBH (magenta) co-localize in the larval central brain and in cells along the VNC (arrowheads). Individual Lola-O-positive cells at the lateral midline show no TBH immunoreactivity (arrows).

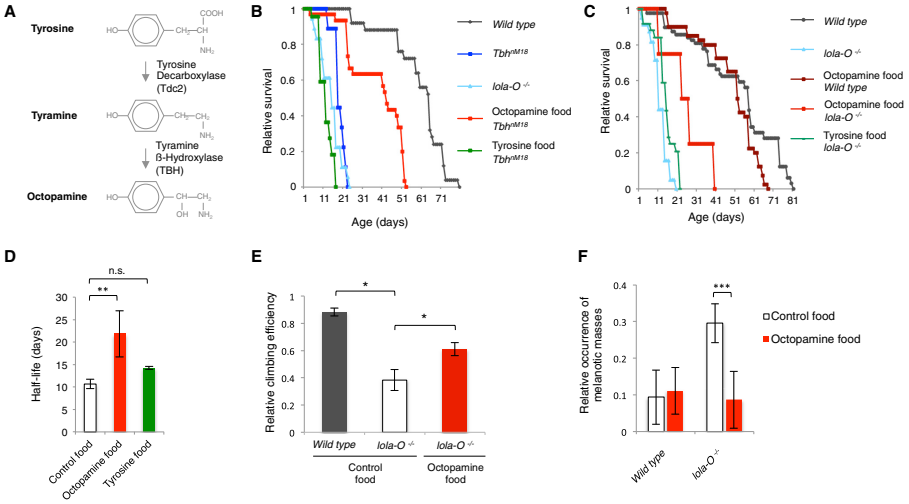

Figure 6. *lola-O* KO Flies Can Be Rescued by Feeding OA

(A) Scheme of the OA pathway.

(B) Longevity is drastically reduced in Tbh^{nM18} flies. Feeding OA extends the lifespan by more than 2-fold, while supplementing tyrosine has no effect. The average of two biological replicates is shown.

(C) Rearing *lola-O* KO flies on OA-enriched food elongates longevity by 2-fold, while tyrosine feeding has no effect on survival. The average of three biological replicates is shown.

(D) Quantification of the half-life deduced from (C). Feeding OA to *lola-O* mutants increases the half-life from 10.6 to 21.8 days. ANOVA t test was applied (**$p < 0.001$). Data are represented as the average of three biological replicates ± SD.

(E) Feeding OA to *lola-O* mutants enhances climbing efficiency. Three-day-old male flies were used for locomotion quantification in three biological replicates. ANOVA one-way t test was performed to test statistical significance (*$p < 0.05$). Data are represented as average ± SD.

(F) 10 freshly hatched males and females were analyzed for melanotic masses at 11 days. ANOVA one-way t test was applied (***$p < 0.0001$). Data are represented as the average of four biological replicates ± SEM.

See also Figure S6.

OA-enriched food improved locomotion of *lola-O* mutants, and it reduced the occurrence of pseudotumors close to wild-type levels (9.86% on OA-enriched food compared to 35.71% on control food) (Figures 6E and 6F). Thus, these results strongly suggest that the defects observed in *lola-O* KO flies result from reduced levels of OA.

We reasoned that if Lola-O function was solely required in OA cells, expressing Lola-O specifically in these cells should be sufficient to rescue all defects associated with its loss. To test this hypothesis, UAS-Lola-O flies were crossed with the *Tdc2*-GAL4 driver, which completely restored survival of *lola-O* mutants as well as their climbing ability and the appearance of pseudotumors (Figures 7A, S7A, and S7B). Furthermore, the fertility of mutant flies was also partially rescued, demonstrated by the improved egg-laying rate (Figure S7C). In contrast, expression of either UAS-Lola-F or UAS-Lola-H in OA cells was unable to restore the survival of *lola-O* KO flies (Figure S7D). Altogether, these experiments demonstrate that the primary activity of Lola-O is restricted to OA neurons.

Lola-O Regulates the OA Pathway via the Control of *Tβh* Expression

OA is synthetized via the activity of two enzymes, Tdc2 and TBH. To test whether Lola-O controls their expression *in vivo*, we analyzed transcript levels from RNA isolated from adult heads of control and *lola-O* KO flies by qRT-PCR. Intriguingly, while *Tdc2* expression was unaffected in *lola-O* mutants, the level of *Tbh* mRNA was significantly reduced (Figure 7B). A similar result was observed in a transheterozygous combination in which *lola-O* mutants were crossed with a *lola* deficiency line (data not shown). We also found that TBH protein levels were decreased, as shown by reduced TBH immunoreactivity in brains of *lola-O* KO larvae (Figure S7E). The specificity of the TBH staining was confirmed, as the signal was essentially absent in the brains of Tbh^{nM18} mutant larvae (Figure S7F). Collectively, these results indicate that Lola-O is required to maintain proper *Tbh* levels.

Given the reduced abundance of *Tbh* in *lola-O* mutants, we wondered whether ectopic expression of *Tbh* cDNA would restore longevity and phenotypic penetrance of these flies. We

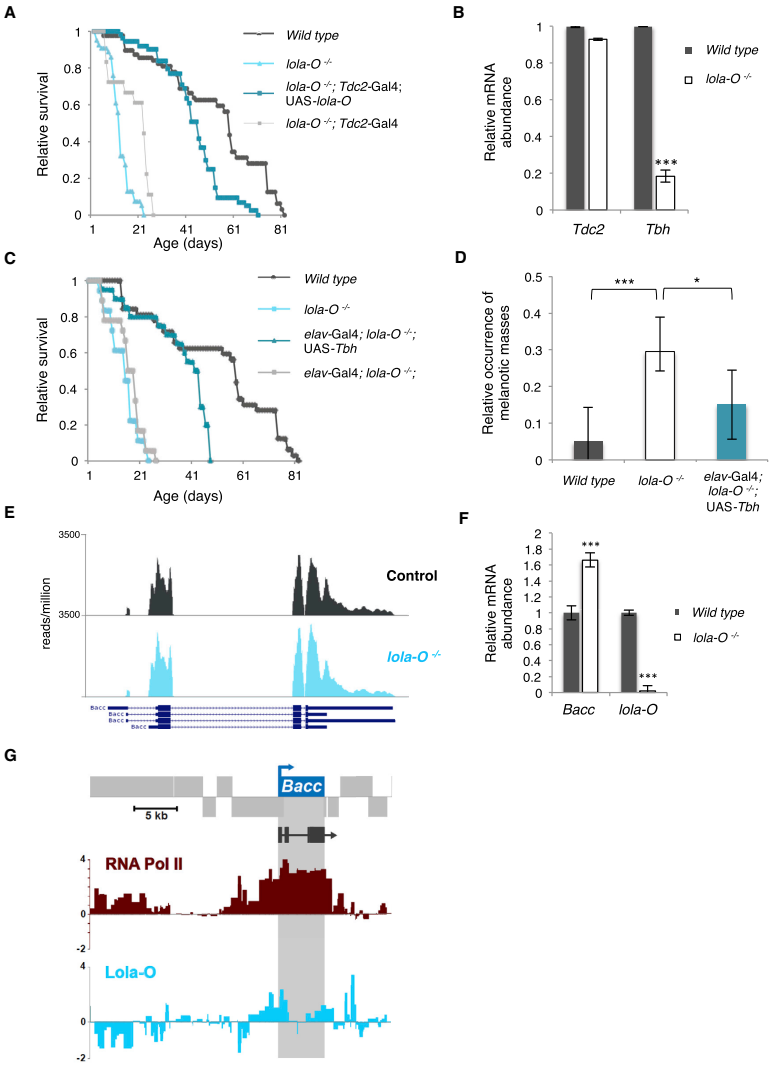

Figure 7. Lola-O Regulates the OA Pathway via the Activation of *Tbh* Expression

(A) Expression of *lola-O* in OA neurons restores wild-type longevity. The average of three biological replicates is shown.

(B) qRT-PCR using mutant RNA extract isolated from freshly eclosed adult male heads. ANOVA one-way t test was performed (***$p < 0.001$ and *$p < 0.05$). Data are represented as the median of three technical replicates ± SD.

(legend continued on next page)

generated flies with integrated *Tbh* under the control of a UAS-promoter, and we induced expression using different GAL4 lines. Strikingly, expression of *Tbh* using a neuronal driver line rescued fly survival and significantly decreased the occurrence of pseudotumors (Figures 7C and 7D). These findings therefore demonstrate that Lola-O regulates the OA pathway via the control of *Tbh* expression.

To uncover the transcriptional network regulated by Lola-O, we aimed to identify the Lola-O genome-wide binding sites, and we compared our findings with genes differentially expressed upon Lola-O depletion. For this purpose, we took advantage of the Targeted DamID (TaDa) approach to identify direct target genes in OA neurons (Southall et al., 2013). Expression of N-terminally tagged Dam-Lola-O was induced by the driver line *Tdc2*-GAL4, and embryos were processed at stage 17. The same experiment was repeated with Dam-RNA polymerase II (Pol II) to identify transcriptionally active genes in OA neurons. We found 1,449 genes bound by Pol II and 7,327 by Lola-O, while 905 were shared by Lola-O and Pol II (with a false discovery rate [FDR] of < 0.01). Furthermore, we found an overlap of 32.7% with differentially expressed genes (296) in *lola-O* mutants of the same developmental stage (Figure S7G). While *Tbh* was not among the Lola-O targets (Figure S7H), we identified the gene *Bacc*, which encodes a repressor of *Tbh* (Chen et al., 2013), as directly bound and repressed by Lola-O (Figures 7E–7G). Therefore, our results suggest a model whereby Lola-O regulates TBH levels indirectly, possibly via the repression of *Bacc* expression.

DISCUSSION

Here we describe a comprehensive functional characterization of the different Lola isoforms *in vivo*. Using the CRISPR/Cas9 approach, we generated mutants for every *lola* isoform, and we demonstrated that *lola-F* mutants mimic the characteristic *lola*-null mutant phenotype observed during embryogenesis. We further uncovered a function for Lola in the OA pathway mediated by Lola-O activity via the regulation of *Tbh*. In addition to revealing novel Lola functions, this study demonstrates that the recently developed CRISPR/Cas9 system can be used to systematically address isoform-specific functions *in vivo*.

Assigning Lola Function to Specific Isoforms

Lola is among the most complex loci in *Drosophila*, encoding for 20 different protein isoforms via the usage of 3′ alternative exons. Its complete loss of function gives rise to pleiotropic defects *in vivo*, which have been difficult to analyze at the molecular level due to the paucity of specific mutant isoforms. First described in 1993 by Giniger and colleagues, Lola was shown to control axon growth and guidance in both the CNS and peripheral nervous system (PNS) of the *Drosophila* embryo (Giniger et al., 1993). However, it remained unclear how it exerts these functions and whether these effects depend on a specific Lola isoform or on the activities of multiple ones. Our results clearly establish Lola-F as being the main isoform required in these early developmental processes.

A previous transcriptomic analysis from *lola*-null mutant extracts suggested that Lola controls axonal guidance by fine-tuning the expression of many genes involved in this process, and it is the sum of small changes on many genes that give rise to the severe *lola*-null mutant phenotype (Gates et al., 2011). Nevertheless, several key targets could be identified. For instance, in the CNS, Lola was suggested to repel longitudinal axons away from the midline by increasing the expression of the midline repellant Slit and its axonal receptor Robo (Crowner et al., 2002). In the PNS, Lola controls ISNb axonal growth partially via reducing the expression of the actin nucleation factor Spire (Gates et al., 2011). In spite of Lola-F being involved in both processes, we found that only *slit* and *robo* expression was altered, while *spire* was unchanged. Furthermore, our study revealed *futsch* as being a key target of Lola-F in axon growth. Futsch is a microtubule-associated protein whose expression levels need to be tightly controlled. For instance, heterozygous animals display mutant phenotypes, including slower growth rates and motor system abnormalities, indicating that its dosage is critical for its function (Edelmann et al., 1996). Moreover, its expression in the somatic and visceral musculature is repressed by Tramtrack (Giesen et al., 1997). It is interesting to note that Tramtrack, like Lola, encodes for a zinc-finger and BTB domain-containing protein, suggesting that this class of proteins plays a prominent role in either repressing or activating Futsch expression. Previous studies on several BTB-containing proteins demonstrated that the BTB domain mediates homomeric and heteromeric dimerization and transcriptional repression through the recruitment of diverse co-repressor proteins (Bardwell and Treisman, 1994; Dhordain et al., 1997). Our data, however, indicate that Lola-F is a general activator of neuronal genes. Further interactome studies will, therefore, be necessary to understand how different BTB proteins exert antagonistic molecular functions on gene expression.

The expression of Lola-F drops as *Drosophila* development progresses and becomes primarily restricted to NSCs. This finding suggests that neuronal gene expression outside the NSCs must be maintained by different means, such as via the activity of other transcription factors or via an epigenetic mechanism. Intriguingly, Lola-F was shown to interact early in development with the histone H3S10 kinase JII-1 (Zhang et al., 2003). Via this molecular activity, JIL-1 maintains euchromatic regions by antagonizing Su(var)3-9-mediated heterochromatin formation. Therefore, it is possible that, during early development, Lola-F establishes an active epigenetic state via its association with JIL-1, and, once established, its function may become dispensable. The remaining Lola-F expression in NSCs appears

(C and D) Neuronal *Tbh* expression (*elav*-GAL4) restores longevity (C) and the occurrence of melanotic masses (D) of *lola-O* KO flies. The average of two biological replicates is shown in (C).
(E and F) Track example of poly-A-selected RNA-seq at the *Bacc* locus. (E) *lola-O* KO embryos show upregulated *Bacc* levels, which were quantified by qRT-PCR in (F). RNA was isolated from stage 17 embryos (20–22 hr AEL). ANOVA one-way t test was performed and data are represented as average ± SD (*$p < 0.05$).
(G) Lola-O and Pol II binding to the *Bacc* locus in OA cells. Vertical bars show log2 ratio between the Dam-only and Dam-fusion signal.
See also Figure S7.

important to maintain their differentiation capacity, as the double knockdown (KD) of Lola-F and Lola-L leads to dramatic overproliferation of NSCs in the central brain (Wissel et al., 2016). It will be important to further identify the direct targets of Lola-F and Lola-L in this process to understand how these two isoforms cooperate to allow NSC differentiation.

Connection between Lola and the OA Pathway

Our findings demonstrate a regulatory role for Lola-O in the OA pathway by regulating *Tbh* expression, which encodes an enzyme required for the synthesis of OA, a monoamine that acts as a neurohormone, neuromodulator, and neurotransmitter (Nathanson, 1979). Monoamine neurotransmitter levels are usually tightly regulated, as their misregulation can lead to a wide range of disorders in humans (Ng et al., 2015). Accordingly, several lines of evidence indicate that the absolute levels of OA must also be tightly controlled. For instance, reducing its levels leads to diverse defects, including female sterility, locomotion, aggressiveness, and pseudotumor formation (Monastirioti et al., 1996; Saraswati et al., 2004; Zhou et al., 2008), while increasing its level also leads to similar abnormalities (Stathakis et al., 1999). Despite this dosage-function dependency, very little is known about the mechanisms controlling OA synthesis throughout the *Drosophila* life cycle. Studies on honeybees have shown that OA synthesis increases with age (Harris and Woodring, 1992), which might be also the case in *Drosophila*. Additionally, it has been shown that stress can induce OA synthesis in the hemolymph of both locusts and cockroaches (Davenport and Evans, 1984), implying that differential concentrations of OA are required in response to altered environmental circumstances. Recent reports demonstrated a FOXO-mediated increase in OA metabolism upon elevated temperatures in *Drosophila* (Gruntenko et al., 2016). It would, therefore, be interesting to test whether TBH expression is also stress induced and whether Lola-O contributes to this effect.

We show that Lola-O binds and negatively regulates *Bacc*, a previously characterized repressor of *Tbh*. Heterozygous *Bacc* mutants display only mild upregulation of *Tbh* levels, which is, however, sufficient to induce elevated OA synthesis, leading to acute ethanol sensitivity (Chen et al., 2013). These findings suggest that *Bacc* expression requires a precise regulation to control OA synthesis.

Future Directions

Our study illuminates a novel role for Lola in controlling neurotransmitter signaling. Interestingly, Lola-O expression appears to be completely restricted to TBH-positive cells in the larval CNS, albeit at very low levels. The mechanisms that restrict Lola-O expression to this subset of cells are currently unknown. It is widely known that promoter activity can influence and determine tissue-dependent gene expression, suggesting that expression of Lola-O in OA neurons might be a consequence of alternative promoter activity. *lola* is encoded by four promoters, with expression of all isoforms from all four promoters (Ohsako et al., 2003); yet, cell-type-specific promoter activity has not been addressed. Alternatively, a splicing regulator might be specifically expressed in OA-responsive cells, promoting the expression of Lola-O exclusively in these cells. Additional experiments are needed to further reveal the mechanism of the restricted expression of Lola-O in the brain and to address whether analogous mechanisms apply in vertebrates to control the level of norepinephrine upon normal and disease conditions.

EXPERIMENTAL PROCEDURES

Fly Stocks

Drosophila melanogaster w^{1118} was used as the wild-type control. For rescue experiments, the following driver lines were used: *Tdc2*-GAL4, *Tub*-GAL4, and $elav^{C155}$-GAL4. *Df(2R)ED2076* served for the generation of *trans*-heterozygous *lola* mutants. *PBac{lola.J-GFP.FLAG}VK00033* and *PBac{lola.GR-GFP.FLAG}* were used for rescue experiments (Spokony and White, 2012). For transcriptome analysis, $lola^{E76}$ and *lola-*F^{Stop} flies were balanced with *w*; P{sqh-mCherry.M}* to enable selection of homozygous embryos based on fluorescence (Martin et al., 2009). *P{w[+mC] = EP}futsch[EP1419]* served for the rescue experiment of *lola-*F^{Stop} embryos. MARCM clones were generated using the following lines: *lola-N*, *FRT42D/CyO*, *FRT42D/CyO* and *elav-GAL4*, *UAS-mCD8-GFP*, *hsFLP*; *FRT42D*, *tub-Gal80* (kind gift from C. Berger). Flies were obtained at the Bloomington *Drosophila* Stock Center. Tbh^{nm18} mutant flies were a kind gift from M. Monastirioti and *UAS-LT3-Dam-Pol II* and *UAS-LT3-Dam* flies were a kind gift from A. Brand.

CRISPR/Cas9 Mutant Flies

gRNA sequences were cloned into pBFv-U6.2B (Kondo and Ueda, 2013), sequenced, and injected in our lab into *y1 v1 P{nos-phiC31\int.NLS}X; attP40*. Transgenic flies were further crossed with y^2 cho^2 v^1; *attP40{nos-Cas9}/CyO*, and flies from the F1 generation were PCR-screened for the expected mutation using primer sequences flanking the gRNA sequences (Table S2). Obtained PCR amplicons were sequenced at GATC Biotech.

UAS Constructs

Coding sequences of *lola-A*, *-O*, *-F*, and *-H* and *Tbh* were amplified from cDNA and inserted into Gateway plasmids with N-terminal FLAG-Myc or FLAG-HA tag (pPFMW or pPFHW, respectively; obtained from *Drosophila* Genomics Resource Center at Indiana University). All constructs were sequenced prior to injection into w^{1118}. *Drosophila* germline injection for *lola-A* and *-F* and *Tbh* was performed in house. The construct for UAS-Lola-O and UAS-Lola-H was injected at BestGene.

Drug-Feeding Assay

Flies were collected within 10 hr of eclosion, gender-separated, and placed on medium containing 5 or 7.5 mg/mL OA or tyrosine for males and females, respectively. Flies were examined daily for survival rate and phenotypic penetrance. 20 flies were used for each condition.

Locomotion Assay

20 freshly hatched male and female flies were separated and staged until desired age. The locomotion was assessed using the climbing assay described previously (Bahadorani and Hilliker, 2008). Flies were taped to the bottom, and flies passing 8 cm in 10 or 5 s, respectively, were counted. Measurements were repeated five times in three biological replicates.

Lifespan Assay

20 control or experimental flies were gender-separated within 10 hr of eclosion and maintained at 25°C. Survival was analyzed every 2 days and flies were transferred to new vials twice a week.

Fertility Assay

10 female virgin flies were mated with 5 males for 3 days. Upon fertilization, females were transferred onto fresh agar plates every 12 hr, and the number of eggs laid was counted for 5 days.

Cell-Type-Specific Transcriptome Analysis

UAS-*mCherry* expression was induced in neurons by *elav*-GAL4 and in OA cells by *Tdc2*-GAL4. Eggs were collected for 3 hr and aged for 13 or 20 hr,

respectively. Cell isolation was performed as described previously (Salmand et al., 2011), and cells were sorted using the Becton Dickinson Aria III SORP flow cytometer. For RNA preparation, 10 cells per replicate were collected in lysis buffer and subjected to library preparation using the Smart-Seq2 Kit for Illumina.

Transcriptome Analysis

lola-F^{Stop} and *lola*^{E76} embryos were collected at 25°C for 2 hr and aged for 13 hr. Embryos were hand-sorted based on mCherry expression. *lola-O* KO embryos were collected at 25°C for 2 hr and developed for 20 hr. Mutant and control embryos were transferred into TRIzol reagent (Thermo Fisher Scientific), and they were subjected to RNA isolation using the manufacturer's protocol.

cDNA Library Preparation

RNA was isolated, DNase I- (New England Biolabs) treated, and subjected to library preparation using the NEBNext Ultra Directional RNA Library Prep Kit for Illumina. 1 μg total RNA was used as starting material for cDNA library preparation.

Computational Analysis

Libraries for transcriptome analyses were sequenced on the NextSeq500. Cells sorted via FACS were sequenced as single-read 76 bp; the other samples were sequenced as 42-bp paired end. Demultiplexing and fastq conversion were done with bcl2fastq (version [v.]2.19). Reads were mapped using STAR (v.2.5.2b) against ensembl release 87 (BDGP6). For the cells sorted via FACS, the reads were filtered for rRNA reads before mapping. Counts per gene were calculated using featureCounts (v.1.5.1) with ensembl release 87 as a reference. Differential expression analysis was done using DESeq2 (v.1.16.1) with an FDR filter of 1%. Transcript quantification for the cells sorted via FACS was performed using stringtie (v.1.3.3b) and visualized using ballgown (v.2.8.4). Splice junction quantification and visualization was done using SGSeq (v.1.10).

GO Term Method and Plot Outline

GO terms overrepresentation was calculated using GOStats (v.2.38.1) requiring a minimal amount of 5 genes per GO term and adjusted p value smaller than 1%. Afterwards, terms were summarized using semantic similarity (GOSemSim 1.30.3). Only GO terms with an odds ratio larger than 5 are displayed.

Targeted DamID

UAS-Dam-lola-O flies were generated by amplifying and cloning the Lola-O coding sequences into pUASTattB-LT3-NDam (kind gift from A. Brand). *UAS-LT3-Dam-lola-O* and *UAS-LT3-Dam-Pol II* flies and *UAS-LT3-Dam* flies (control) were crossed with *Tdc2*-GAL4 to induce octopaminergic expression of the Dam fusion proteins. DNA was isolated from embryos (20–22 hr after egg laying [AEL]), and subsequent treatments were performed as described (Marshall et al., 2016). Purified and processed genomic DNA of two biological duplicates was subjected to library preparation using the NebNext DNA Ultra II library kit (New England Biolabs) and sequenced on a NextSeq500. The first read was mapped to *Drosophila melanogaster* genome (BDGP6) using bowtie (v.2.2.9), binned to GATC fragments, and normalized against the Dam-only control (Marshall and Brand, 2015). Peaks were called and mapped to genes using a custom Perl program (available upon request).

qRT-PCR

Total RNA was transcribed into cDNA using MMLV reverse transcriptase (Promega). qRT-PCR analysis was performed using a ViiA7 real-time PCR system (Applied Biosystems). Measurements were done in triplicates. Relative RNA levels were normalized to *rpl15* levels. Primer sequences are listed in Table S2.

In Situ Hybridization

In situ hybridization was performed as previously described (Lence et al., 2016). For fluorescent *in situ* hybridization, anti-DIG-HRP (1:1,000, Roche) was applied, and probes were visualized using the tyramide signal amplification (Alexa Fluor 568, Thermo Fisher Scientific).

Whole-Mount Embryo Immunostaining

Embryos were fixed and washed with PBS with 0.3% Triton X-100. Primary antibodies used were the following: mouse anti-Fas II (1:20; 1D4, DSHB), rat anti-Elav (1:100; 7E8A10, DSHB), mouse anti-Repo (1:100; 8D12, DSHB), mouse anti-22C10 (1:50; DSHB), mouse anti-Lola zf5 (1:100; 1D5, DSHB), guinea pig anti-Dpn (1:50, kind gift from C. Berger), rat anti-TBH (1:75, kind gift from M. Monastirioti), and rabbit anti-GFP (1:500; TP401, Torrey Pines Biolabs). Appropriate combinations of secondary antibodies (Jackson ImmunoResearch Laboratories) were applied. Samples were analyzed with a Leica SP5 confocal microscope.

Larval L3 Brain Immunostaining

Larval CNS was dissected in cold PBS, fixed for 20 min in 4% paraformaldehyde in PBS, and subsequently treated as embryonic samples. A confocal stack was recorded using a Leica SP5 confocal microscope.

Western Blotting

Staged embryos were collected and homogenized in lysis buffer (140 mM NaCl, 10 mM Tris-HCl [pH 8], 1 mM EDTA [pH 8], and 0.5% Triton X-100). The protein extract was separated on 8% SDS-PAGE gel followed by western blot analysis with affinity-purified anti-Lola antibody (1:500, kindly provided by E. Giniger) or Lola-Zf5 antibody (1:100; DSHB). For visualization, ultra-sensitive enhanced chemiluminescent reagent (Thermo Fisher Scientific) was used.

Statistical Analysis

Statistical parameters and significance are reported in the figures and figure legends. For comparisons of the means of two groups, Student's t test was used. For comparisons among more than two groups, the one-way ANOVA was performed followed by multiple comparisons using t tests with Bonferroni normalization of p values.

DATA AND SOFTWARE AVAILABILITY

The accession number for the RNA-seq and DamID-seq data reported in this paper is GEO: GSE97836.

SUPPLEMENTAL INFORMATION

Supplemental Information includes seven figures and two tables and can be found with this article online at https://doi.org/10.1016/j.celrep.2017.11.015.

AUTHOR CONTRIBUTIONS

Conceptualization, J.-Y.R. and N.D.; Methodology, J.-Y.R., N.D., and V.M.; Investigation, N.D. and V.M.; Computation Analysis of RNA-Seq, N.K.; Computational Analysis of DamID-Seq, T.D.S.; Writing – Original Draft, N.D.; Writing – Review & Editing, J.-Y.R. and N.D.; Funding Acquisition, J.-Y.R.; Supervision, J.-Y.R.

ACKNOWLEDGMENTS

We would like to thank the Bloomington Drosophila Stock Center for fly reagents; the Developmental Studies Hybridoma Bank for antibodies; the Drosophila Genomics Resource Center for plasmids; M. Monastirioti for *Tbh* alleles and TBH antibody; E. Giniger for Lola antibody; C. Berger for Deadpan antibody; A. Brand for DamID constructs; members of the Roignant lab for fruitful discussion; the IMB Genomics, Cytometry, Bioinformatics and Microscopy Core facilities for tremendous support; and A. Dold, C. Berger, and J. Urban for critical reading of the manuscript. Research in the laboratory of J.-Y.R. is supported by the Deutsche Forschungsgemeinschaft (DFG) SPP1935 Grant RO 4681/4-1.

Received: May 8, 2017
Revised: September 12, 2017
Accepted: November 2, 2017
Published: December 5, 2017

REFERENCES

Bahadorani, S., and Hilliker, A.J. (2008). Cocoa confers life span extension in Drosophila melanogaster. Nutr. Res. *28*, 377–382.

Bardwell, V.J., and Treisman, R. (1994). The POZ domain: a conserved protein-protein interaction motif. Genes Dev. *8*, 1664–1677.

Barron, A.B., Søvik, E., and Cornish, J.L. (2010). The roles of dopamine and related compounds in reward-seeking behavior across animal phyla. Front. Behav. Neurosci. *4*, 163.

Bass, B.P., Cullen, K., and McCall, K. (2007). The axon guidance gene lola is required for programmed cell death in the Drosophila ovary. Dev. Biol. *304*, 771–785.

Chen, J., Wang, Y., Zhang, Y., and Shen, P. (2013). Mutations in Bacchus reveal a tyramine-dependent nuclear regulator for acute ethanol sensitivity in Drosophila. Neuropharmacology *67*, 25–31.

Crowner, D., Madden, K., Goeke, S., and Giniger, E. (2002). Lola regulates midline crossing of CNS axons in Drosophila. Development *129*, 1317–1325.

Davenport, A.P., and Evans, P.D. (1984). Stress-induced changes in the octopamine levels of insect haemolymph. Insect Biochem. *14*, 135–143.

Davies, E.L., Lim, J.G., Joo, W.J., Tam, C.H., and Fuller, M.T. (2013). The transcriptional regulator lola is required for stem cell maintenance and germ cell differentiation in the Drosophila testis. Dev. Biol. *373*, 310–321.

Dhordain, P., Albagli, O., Lin, R.J., Ansieau, S., Quief, S., Leutz, A., Kerckaert, J.P., Evans, R.M., and Leprince, D. (1997). Corepressor SMRT binds the BTB/POZ repressing domain of the LAZ3/BCL6 oncoprotein. Proc. Natl. Acad. Sci. USA *94*, 10762–10767.

Edelmann, W., Zervas, M., Costello, P., Roback, L., Fischer, I., Hammarback, J.A., Cowan, N., Davies, P., Wainer, B., and Kucherlapati, R. (1996). Neuronal abnormalities in microtubule-associated protein 1B mutant mice. Proc. Natl. Acad. Sci. USA *93*, 1270–1275.

Fukui, A., Inaki, M., Tonoe, G., Hamatani, H., Homma, M., Morimoto, T., Aburatani, H., and Nose, A. (2012). Lola regulates glutamate receptor expression at the Drosophila neuromuscular junction. Biol. Open *1*, 362–375.

Gates, M.A., Kannan, R., and Giniger, E. (2011). A genome-wide analysis reveals that the Drosophila transcription factor Lola promotes axon growth in part by suppressing expression of the actin nucleation factor Spire. Neural Dev. *6*, 37.

Giesen, K., Hummel, T., Stollewerk, A., Harrison, S., Travers, A., and Klämbt, C. (1997). Glial development in the Drosophila CNS requires concomitant activation of glial and repression of neuronal differentiation genes. Development *124*, 2307–2316.

Giniger, E., Jan, L.Y., and Jan, Y.N. (1993). Specifying the path of the intersegmental nerve of the Drosophila embryo: a role for Delta and Notch. Development *117*, 431–440.

Giniger, E., Tietje, K., Jan, L.Y., and Jan, Y.N. (1994). lola encodes a putative transcription factor required for axon growth and guidance in Drosophila. Development *120*, 1385–1398.

Goeke, S., Greene, E.A., Grant, P.K., Gates, M.A., Crowner, D., Aigaki, T., and Giniger, E. (2003). Alternative splicing of lola generates 19 transcription factors controlling axon guidance in Drosophila. Nat. Neurosci. *6*, 917–924.

Gruntenko, N.E., Adonyeva, N.V., Burdina, E.V., Karpova, E.K., Andreenkova, O.V., Gladkikh, D.V., Ilinsky, Y.Y., and Rauschenbach, I.Y. (2016). The impact of FOXO on dopamine and octopamine metabolism in Drosophila under normal and heat stress conditions. Biol. Open *5*, 1706–1711.

Harris, J.W., and Woodring, J. (1992). Effects of stress, age, season, and source colony on levels of octopamine, dopamine and serotonin in the honey bee (*Apis mellifera* L.) brain. J. Insect Physiol. *38*, 29–35.

Horiuchi, T., Giniger, E., and Aigaki, T. (2003). Alternative trans-splicing of constant and variable exons of a Drosophila axon guidance gene, lola. Genes Dev. *17*, 2496–2501.

Hummel, T., Krukkert, K., Roos, J., Davis, G., and Klämbt, C. (2000). Drosophila Futsch/22C10 is a MAP1B-like protein required for dendritic and axonal development. Neuron *26*, 357–370.

Kondo, S., and Ueda, R. (2013). Highly improved gene targeting by germline-specific Cas9 expression in Drosophila. Genetics *195*, 715–721.

Lence, T., Akhtar, J., Bayer, M., Schmid, K., Spindler, L., Ho, C.H., Kreim, N., Andrade-Navarro, M.A., Poeck, B., Helm, M., and Roignant, J.Y. (2016). m(6)A modulates neuronal functions and sex determination in Drosophila. Nature *540*, 242–247.

Li, Y., Hoffmann, J., Li, Y., Stephano, F., Bruchhaus, I., Fink, C., and Roeder, T. (2016). Octopamine controls starvation resistance, life span and metabolic traits in Drosophila. Sci. Rep. *6*, 35359.

Madden, K., Crowner, D., and Giniger, E. (1999). LOLA has the properties of a master regulator of axon-target interaction for SNb motor axons of Drosophila. Dev. Biol. *213*, 301–313.

Marshall, O.J., and Brand, A.H. (2015). damidseq_pipeline: an automated pipeline for processing DamID sequencing datasets. Bioinformatics *31*, 3371–3373.

Marshall, O.J., Southall, T.D., Cheetham, S.W., and Brand, A.H. (2016). Cell-type-specific profiling of protein-DNA interactions without cell isolation using targeted DamID with next-generation sequencing. Nat. Protoc. *11*, 1586–1598.

Martin, A.C., Kaschube, M., and Wieschaus, E.F. (2009). Pulsed contractions of an actin-myosin network drive apical constriction. Nature *457*, 495–499.

Monastirioti, M., Linn, C.E., Jr., and White, K. (1996). Characterization of Drosophila tyramine beta-hydroxylase gene and isolation of mutant flies lacking octopamine. J. Neurosci. *16*, 3900–3911.

Nathanson, J.A. (1979). Octopamine receptors, adenosine 3′,5′-monophosphate, and neural control of firefly flashing. Science *203*, 65–68.

Neumüller, R.A., Richter, C., Fischer, A., Novatchkova, M., Neumüller, K.G., and Knoblich, J.A. (2011). Genome-wide analysis of self-renewal in Drosophila neural stem cells by transgenic RNAi. Cell Stem Cell *8*, 580–593.

Ng, J., Papandreou, A., Heales, S.J., and Kurian, M.A. (2015). Monoamine neurotransmitter disorders–clinical advances and future perspectives. Nat. Rev. Neurol. *11*, 567–584.

Ohsako, T., Horiuchi, T., Matsuo, T., Komaya, S., and Aigaki, T. (2003). Drosophila lola encodes a family of BTB-transcription regulators with highly variable C-terminal domains containing zinc finger motifs. Gene *311*, 59–69.

Peng, Q., Wang, Y., Li, M., Yuan, D., Xu, M., Li, C., Gong, Z., Jiao, R., and Liu, L. (2016). cGMP-Dependent Protein Kinase Encoded by foraging Regulates Motor Axon Guidance in Drosophila by Suppressing Lola Function. J. Neurosci. *36*, 4635–4646.

Salmand, P.A., Iché-Torres, M., and Perrin, L. (2011). Tissue-specific cell sorting from Drosophila embryos: application to gene expression analysis. Fly (Austin) *5*, 261–265.

Saraswati, S., Fox, L.E., Soll, D.R., and Wu, C.F. (2004). Tyramine and octopamine have opposite effects on the locomotion of Drosophila larvae. J. Neurobiol. *58*, 425–441.

Selcho, M., Pauls, D., El Jundi, B., Stocker, R.F., and Thum, A.S. (2012). The role of octopamine and tyramine in Drosophila larval locomotion. J. Comp. Neurol. *520*, 3764–3785.

Southall, T.D., Gold, K.S., Egger, B., Davidson, C.M., Caygill, E.E., Marshall, O.J., and Brand, A.H. (2013). Cell-type-specific profiling of gene expression and chromatin binding without cell isolation: assaying RNA Pol II occupancy in neural stem cells. Dev. Cell *26*, 101–112.

Southall, T.D., Davidson, C.M., Miller, C., Carr, A., and Brand, A.H. (2014). Dedifferentiation of neurons precedes tumor formation in Lola mutants. Dev. Cell *28*, 685–696.

Spletter, M.L., Liu, J., Liu, J., Su, H., Giniger, E., Komiyama, T., Quake, S., and Luo, L. (2007). Lola regulates Drosophila olfactory projection neuron identity and targeting specificity. Neural Dev. *2*, 14.

Spokony, R., and White, K. (2012). Spokony insertions. http://flybase.org/reports/FBrf0220060.html.

Stathakis, D.G., Burton, D.Y., McIvor, W.E., Krishnakumar, S., Wright, T.R., and O'Donnell, J.M. (1999). The catecholamines up (Catsup) protein of

Drosophila melanogaster functions as a negative regulator of tyrosine hydroxylase activity. Genetics *153*, 361–382.

Tripathy, R., Kunwar, P.S., Sano, H., and Renault, A.D. (2014). Transcriptional regulation of Drosophila gonad formation. Dev. Biol. *392*, 193–208.

Wissel, S., Kieser, A., Yasugi, T., Duchek, P., Roitinger, E., Gokcezade, J., Steinmann, V., Gaul, U., Mechtler, K., Förstemann, K., et al. (2016). A Combination of CRISPR/Cas9 and Standardized RNAi as a Versatile Platform for the Characterization of Gene Function. G3 (Bethesda) *6*, 2467–2478.

Zhang, W., Wang, Y., Long, J., Girton, J., Johansen, J., and Johansen, K.M. (2003). A developmentally regulated splice variant from the complex lola locus encoding multiple different zinc finger domain proteins interacts with the chromosomal kinase JIL-1. J. Biol. Chem. *278*, 11696–11704.

Zheng, L., and Carthew, R.W. (2008). Lola regulates cell fate by antagonizing Notch induction in the Drosophila eye. Mech. Dev. *125*, 18–29.

Zhou, C., Rao, Y., and Rao, Y. (2008). A subset of octopaminergic neurons are important for Drosophila aggression. Nat. Neurosci. *11*, 1059–1067.

9. Literature

Adams, M. D. (2000) 'The Genome Sequence of Drosophila melanogaster', *Science*, 287(5461), pp. 2185–2195. doi: 10.1126/science.287.5461.2185.

Atwood, H. L., Govind, C. K. and Wu, C. -F (1993) 'Differential ultrastructure of synaptic terminals on ventral longitudinal abdominal muscles in Drosophila larvae', *Journal of Neurobiology*, 24(8), pp. 1008–1024. doi: 10.1002/neu.480240803.

Bahadorani, S. and Hilliker, A. J. (2008) 'Cocoa confers life span extension in Drosophila melanogaster', *Nutrition Research*, 28(6), pp. 377–382. doi: 10.1016/j.nutres.2008.03.018.

Balfanz, S. *et al.* (2005) 'A family of octopamine [corrected] receptors that specifically induce cyclic AMP production or Ca2+ release in Drosophila melanogaster.', *Journal of neurochemistry*, 93(2), pp. 440–51. doi: 10.1111/j.1471-4159.2005.03034.x.

Bao, H. *et al.* (2007) 'The atypical cadherin flamingo regulates synaptogenesis and helps prevent axonal and synaptic degeneration in Drosophila', *Molecular and Cellular Neuroscience*, 34(4), pp. 662–678. doi: 10.1016/j.mcn.2007.01.007.

Bardwell, V. J. and Treisman, R. (1994) 'The POZ domain: a conserved protein-protein interaction motif.', *Genes & development*, 8(14), pp. 1664–77. Available at:

Barron, A. B., Søvik, E. and Cornish, J. L. (2010) 'The roles of dopamine and related compounds in reward-seeking behavior across animal phyla.', *Frontiers in behavioral neuroscience*, 4(October), p. 163. doi: 10.3389/fnbeh.2010.00163.

Berger, C. *et al.* (2012) 'FACS Purification and Transcriptome Analysis of Drosophila Neural Stem Cells Reveals a Role for Klumpfuss in Self-Renewal', *Cell Reports*, 2(2), pp. 407–418. doi: 10.1016/j.celrep.2012.07.008.

Berget, S. M. (1995) 'Exon recognition in vertebrate splicing', *Journal of Biological Chemistry*, pp. 2411–2414. doi: 10.1074/jbc.270.6.2411.

Bhat, K. M., Gaziova, I. and Krishnan, S. (2007) 'Regulation of axon guidance by slit and netrin signaling in the drosophila ventral nerve cord', *Genetics*, 176(4), pp. 2235–2246. doi: 10.1534/genetics.107.075085.

Blumenthal, T. (2012) 'Trans-splicing and operons in C. elegans.', *WormBook : the online review of C. elegans biology*, pp. 1–11. doi: 10.1895/wormbook.1.5.2.
Boeke, J. *et al.* (2010) 'Phosphorylation of SU(VAR)3-9 by the chromosomal kinase JIL-1', *PLoS ONE*, 5(4). doi: 10.1371/journal.pone.0010042.

Bonchuk, A. *et al.* (2011) 'Drosophila BTB/POZ domains of "ttk group" can form multimers and selectively interact with each other.', *Journal of molecular biology*, 412(3), pp. 423–36. doi: 10.1016/j.jmb.2011.07.052.

Boothroyd, J. C. and Cross, G. A. (1982) 'Transcripts coding for variant surface glycoproteins of Trypanosoma brucei have a short, identical exon at their 5' end.', *Gene*, 20(2), pp. 281–9.

Bosco-Drayon, V. *et al.* (2012) 'Peptidoglycan sensing by the receptor PGRP-LE in the Drosophila gut induces immune responses to infectious bacteria and tolerance to microbiota', *Cell Host and Microbe*, 12(2), pp. 153–165. doi: 10.1016/j.chom.2012.06.002.

Boyle, M. and DiNardo, S. (1995) 'Specification, migration and assembly of the somatic cells of the Drosophila gonad.', *Development (Cambridge, England)*, 121(6), pp. 1815–25.

Brose, K. *et al.* (1999) 'Slit proteins bind Robo receptors and have an evolutionarily conserved role in repulsive axon guidance.', *Cell*, 96(6), pp. 795–806.

Cáceres, J. F. and Kornblihtt, A. R. (2002) 'Alternative splicing: multiple control mechanisms and involvement in human disease.', *Trends in genetics : TIG*, 18(4), pp. 186–93.

Carrasco-Rando, M. *et al.* (2016) 'Fear-of-intimacy-mediated zinc transport controls the function of zinc-finger transcription factors involved in myogenesis.', *Development (Cambridge, England)*, 143(11), pp. 1948–57. doi: 10.1242/dev.131953.

Cavaliere, V., Taddei, C. and Gargiulo, G. (1998) 'Apoptosis of nurse cells at the late stages of oogenesis of Drosophila melanogaster', *Development Genes and Evolution*, 208(2), pp. 106–112. doi: 10.1007/s004270050160.

Cavarec, L., Jensen, S., Casella, J. F., Cristescu, S. a, *et al.* (1997) 'Molecular cloning and characterization of a transcription factor for the copia retrotransposon with homology to the BTB-containing lola neurogenic factor.', *Molecular and cellular biology*, 17(1), pp. 482–94.

Cavarec, L., Jensen, S., Casella, J. F., Cristescu, S. A., *et al.* (1997) 'Molecular cloning and characterization of a transcription factor for the copia retrotransposon with homology to the BTB-containing lola neurogenic factor.', *Molecular and cellular biology*, 17(1), pp. 482–94.

Chen, J. *et al.* (2013) 'Mutations in Bacchus reveal a tyramine-dependent nuclear regulator for acute ethanol sensitivity in Drosophila', *Neuropharmacology*, 67, pp. 25–31. doi: 10.1016/j.neuropharm.2012.10.013.

Cong, L. *et al.* (2013) 'Multiplex genome engineering using CRISPR/Cas systems.', *Science (New York, N.Y.)*, 339(6121), pp. 819–23. doi: 10.1126/science.1231143.

Crocker, A. and Sehgal, A. (2008) 'Octopamine Regulates Sleep in Drosophila through Protein Kinase A-Dependent Mechanisms', *Journal of Neuroscience*, 28(38), pp. 9377–9385. doi: 10.1523/JNEUROSCI.3072-08a.2008.

Crowner, D. *et al.* (2002) 'Lola regulates midline crossing of CNS axons in Drosophila.', *Development (Cambridge, England)*, 129(6), pp. 1317–1325.

Crowner, D. *et al.* (2003) 'Notch steers Drosophila ISNb motor axons by regulating the Abl signaling pathway', *Current Biology*, 13(11), pp. 967–972. doi: 10.1016/S0960-9822(03)00325-7.

Davies, E. L. *et al.* (2013) 'The transcriptional regulator lola is required for stem cell maintenance and germ cell differentiation in the Drosophila testis', *Developmental Biology*, 373(2), pp. 310–321. doi: 10.1016/j.ydbio.2012.11.004.

Davies, E. L. *et al.* (2013) 'The transcriptional regulator lola is required for stem cell maintenance and germ cell differentiation in the Drosophila testis.', *Developmental biology*, 373(2), pp. 310–21. doi: 10.1016/j.ydbio.2012.11.004.

Edelmann, W. *et al.* (1996) 'Neuronal abnormalities in microtubule-associated protein 1B mutant mice', *Proceedings of the National Academy of Sciences of the United States of America*, 93(3), pp. 1270–1275. doi: 10.1073/pnas.93.3.1270.

El-Kholy, S. *et al.* (2015) 'Expression analysis of octopamine and tyramine receptors in Drosophila', *Cell and Tissue Research*. Springer Berlin Heidelberg, 361(3), pp. 669–684. doi: 10.1007/s00441-015-2137-4.

Elphick, M. R. and Egertova, M. (2001) 'The neurobiology and evolution of cannabinoid signalling', *Philosophical Transactions of the Royal Society B: Biological Sciences*, 356(1407), pp. 381–408. doi: 10.1098/rstb.2000.0787.

Elrod-Erickson, M. *et al.* (1996) 'Zif268 protein-DNA complex refined at 1.6 A: a model system for understanding zinc finger-DNA interactions.', *Structure (London, England : 1993)*, 4(10), pp. 1171–1180. doi: 10.1016/S0969-2126(96)00125-6.

Enuameh, M. S. *et al.* (2013) 'Global analysis of Drosophila Cys_2-His_2 zinc finger proteins reveals a multitude of novel recognition motifs and binding determinants.', *Genome research*, 23(6), pp. 928–40. doi: 10.1101/gr.151472.112.

Evans, P. D. and Robb, S. (1993) 'Octopamine receptor subtypes and their modes of action', *Neurochemical Research*. Kluwer Academic Publishers-Plenum Publishers, 18(8), pp. 869–874. doi: 10.1007/BF00998270.

Francis PT (2005) 'The interplay of neurotransmitters in Alzheimer's disease. LinkOut -more resources', *CNS Spectr*, 10(11), pp. 6–9.

Fukui, A. *et al.* (2012) 'Lola regulates glutamate receptor expression at the Drosophila neuromuscular junction', *Biol Open*, 1(4), pp. 362–375. doi: 10.1242/bio.2012448.

Fukushima, S., Yoshida, M. and Takatsuji, H. (2012) 'Role of Linkers between Zinc Fingers in Spacing Recognition by Plant TFIIIA-Type Zinc-Finger Proteins', *Journal of Amino Acids*, 2012, pp. 1–10. doi: 10.1155/2012/848037.

Gao, J.-L. *et al.* (2015) 'A conserved intronic U1 snRNP-binding sequence promotes trans-splicing in Drosophila.', *Genes & development*, 29(7), pp. 760–71. doi: 10.1101/gad.258863.115.

Gates, M. a, Kannan, R. and Giniger, E. (2011) 'A genome-wide analysis reveals that the Drosophila transcription factor Lola promotes axon growth in part by suppressing expression of the actin nucleation factor Spire.', *Neural development*. BioMed Central Ltd, 6(1), p. 37. A

Gibilisco, L. *et al.* (2016) 'Alternative Splicing within and between Drosophila Species, Sexes, Tissues, and Developmental Stages', *PLoS Genetics*, 12(12). doi: 10.1371/journal.pgen.1006464.

Giesen, K. *et al.* (1997) 'Glial development in the *Drosophila* CNS requires concomitant activation of glial and repression of neuronal differentiation genes.', *Development (Cambridge, England)*, 124, pp. 2307–2316.

Giniger, E. *et al.* (1994) 'lola encodes a putative transcription factor required for axon growth and guidance in Drosophila.', *Development (Cambridge, England)*, 120(6), pp. 1385–98. Available at: http://www.ncbi.nlm.nih.gov/pubmed/8050351.

Giot, L. *et al.* (2003) 'A protein interaction map of Drosophila melanogaster.', *Science (New York, N.Y.)*, 302(5651), pp. 1727–36. doi: 10.1126/science.1090289.

Goeke, S. *et al.* (2003) 'Alternative splicing of lola generates 19 transcription factors controlling axon guidance in Drosophila.', *Nature neuroscience*, 6(9), pp. 917–24.

Hammer, M. and Menzel, R. (no date) 'Multiple sites of associative odor learning as revealed by local brain microinjections of octopamine in honeybees.', *Learning & memory (Cold Spring Harbor, N.Y.)*, 5(1–2), pp. 146–56.

Harris, J. W. and Woodring, J. (1992) 'Effects of stress, age, season, and source colony on levels of octopamine, dopamine and serotonin in the honey bee (Apis mellifera L.) brain', *Journal of Insect Physiology*, 38(1), pp. 29–35. doi: 10.1016/0022-1910(92)90019-A.

Harris, R., Sabatelli, L. M. and Seeger, M. A. (1996) 'Guidance Cues at the Drosophila CNS Midline: Identification and Characterization of Two Drosophila Netrin/UNC-6 Homologs', *Neuron*, 17(2), pp. 217–228. doi: 10.1016/S0896-6273(00)80154-3.

von Hilchen, C. M. *et al.* (2010) 'Netrins guide migration of distinct glial cells in the Drosophila embryo', *Development*, 137(8), pp. 1251–1262. doi: 10.1242/dev.042853.

Horiuchi, T. and Aigaki, T. (2006) 'Alternative trans-splicing: a novel mode of pre-mRNA processing.', *Biology of the cell*, 98(2), pp. 135–40. doi: 10.1042/BC20050002.

Horiuchi, T., Giniger, E. and Aigaki, T. (2003) 'Alternative trans-splicing of constant and variable exons of a Drosophila axon guidance gene, lola', *Genes and Development*, 17(20), pp. 2496–2501.

Hummel, T. *et al.* (2000a) 'Drosophila Futsch/22C10 Is a MAP1B-like Protein Required for Dendritic and Axonal Development', *Neuron*, 26(2), pp. 357–370. doi: 10.1016/S0896-6273(00)81169-1.

Hummel, T. *et al.* (2000b) 'Drosophila Futsch/22C10 Is a MAP1B-like Protein Required for Dendritic and Axonal Development', *Neuron*, 26(2), pp. 357–370. doi: 10.1016/S0896-6273(00)81169-1.

Ishino Y., Shinagawa H., Makino K., Amemura M., N. A. (1988) 'Nucleotide-sequence of the iap gene, responsible for alkaline-phosphatase isozyme conversion in Escherichia coli, and identification of the gene-product', *Journal of Bacteriology*, 169 (12), pp. 5429–33.

Jefferis, G. S. X. E. *et al.* (2005) 'Development of wiring specificity of the Drosophila olfactory system', in *Chemical Senses*. doi: 10.1093/chemse/bjh130.

Jinek, M. *et al.* (2012) 'A programmable dual-RNA-guided DNA endonuclease in adaptive bacterial immunity.', *Science (New York, N.Y.)*, 337(6096), pp. 816–21. doi: 10.1126/science.1225829.

Johnson, J. M. (2003) 'Genome-Wide Survey of Human Alternative Pre-mRNA Splicing with Exon Junction Microarrays', *Science*, 302(5653), pp. 2141–2144. doi: 10.1126/science.1090100.

Keravala, A. and Calos, M. P. (2008) 'Site-specific chromosomal integration mediated by phiC31 integrase', *Methods Mol Biol*, 435, pp. 165–173. doi: 10.1007/978-1-59745-232-8_12.

Kidd, T. *et al.* (1998) 'Roundabout controls axon crossing of the CNS midline and defines a novel subfamily of evolutionarily conserved guidance receptors.', *Cell*, 92(2), pp. 205–15.

Kolodziej, P. A. *et al.* (1996) 'frazzled encodes a Drosophila member of the DCC immunoglobulin subfamily and is required for CNS and motor axon guidance.', *Cell*, 87(2), pp. 197–204.

Konarska, M. M. *et al.* (1985) 'Characterization of the branch site in lariat RNAs produced by splicing of mRNA precursors.', *Nature*, 313(6003), pp. 552–557. doi: 10.1038/313552a0.

Kondo, S. and Ueda, R. (2013) 'Highly improved gene targeting by germline-specific Cas9 expression in Drosophila.', *Genetics*, 195(3), pp. 715–21. doi: 10.1534/genetics.113.156737.

Koon, A. C. *et al.* (2010) 'Autoregulatory and paracrine control of synaptic and behavioral plasticity by octopaminergic signaling', *Nature Publishing Group*, 14(2). doi: 10.1038/nn.2716.

Koon, a. C. and Budnik, V. (2012) 'Inhibitory Control of Synaptic and Behavioral Plasticity by Octopaminergic Signaling', *Journal of Neuroscience*, 32(18), pp. 6312–6322. doi: 10.1523/JNEUROSCI.6517-11.2012.

Kowarz, E. *et al.* (2011) 'Premature transcript termination, trans-splicing and DNA repair: a vicious path to cancer.', *American journal of blood research*, 1(1), pp. 1–12.

.

Krause, M. and Hirsh, D. (1987) 'A trans-spliced leader sequence on actin mRNA in C. elegans.', *Cell*, 49(6), pp. 753–61.

Krishna, S. S., Majumdar, I. and Grishin, N. V (2003) 'Structural classification of zinc fingers: survey

and summary.', *Nucleic acids research*, 31(2), pp. 532–50.

Kurz, C. L. *et al.* (2017) 'Peptidoglycan sensing by octopaminergic neurons modulates Drosophila oviposition', *eLife*, 6. doi: 10.7554/eLife.21937.

Lander, E. S. *et al.* (2001) 'Initial sequencing and analysis of the human genome', *Nature*, 409(6822), pp. 860–921. doi: 10.1038/35057062.

Landgraf, M. and Thor, S. (2006) 'Development of Drosophila motoneurons: specification and morphology.', *Seminars in cell & developmental biology*, 17(1), pp. 3–11. doi: 10.1016/j.semcdb.2005.11.007.

Laski, F. A., Rio, D. C. and Rubin, G. M. (1986) 'Tissue specificity of Drosophila P element transposition is regulated at the level of mRNA splicing', *Cell*, 44(1), pp. 7–19. doi: 10.1016/0092-8674(86)90480-0.

Lee, H.-G., Rohila, S. and Han, K.-A. (2009) 'The Octopamine Receptor OAMB Mediates Ovulation via Ca^{2+}/Calmodulin-Dependent Protein Kinase II in the Drosophila Oviduct Epithelium', *PLoS ONE*, 4(3), p. e4716. doi: 10.1371/journal.pone.0004716.

Lee, M. S. *et al.* (1989) 'Three-dimensional solution structure of a single zinc finger DNA-binding domain.', *Science (New York, N.Y.)*, 245(4918), pp. 635–7. doi: 10.1126/science.2503871.

Li, Y. *et al.* (2015) 'The octopamine receptor octß2r is essential for ovulation and fertilization in the fruit fly drosophila melanogaster', *Archives of Insect Biochemistry and Physiology*, 88(3), pp. 168–178. doi: 10.1002/arch.21211.

Li, Y. *et al.* (2016) 'Octopamine controls starvation resistance, life span and metabolic traits in Drosophila', *Scientific Reports*, 6(October), p. 35359. doi: 10.1038/srep35359.

Lim, K. H. *et al.* (2011) 'Using positional distribution to identify splicing elements and predict pre-mRNA processing defects in human genes', *Proc Natl Acad Sci U S A*, 108(27), pp. 11093–11098. doi: 10.1073/pnas.1101135108.

Luo, J. *et al.* (2014) 'Drosophila insulin-producing cells are differentially modulated by serotonin and octopamine receptors and affect social behavior', *PLoS ONE*, 9(6). doi: 10.1371/journal.pone.0099732.

Madden, K., Crowner, D. and Giniger, E. (1999) 'LOLA has the properties of a master regulator of axon-target interaction for SNb motor axons of Drosophila.', *Developmental biology*, 213(2), pp. 301–313.

Mali, P. *et al.* (2013) 'RNA-guided human genome engineering via Cas9.', *Science (New York, N.Y.)*, 339(6121), pp. 823–6. doi: 10.1126/science.1232033.

Maqueira, B., Chatwin, H. and Evans, P. D. (2005) 'Identification and characterization of a novel family of Drosophila β-adrenergic-like octopamine G-protein coupled receptors', *Journal of Neurochemistry*, 94(2), pp. 547–560. doi: 10.1111/j.1471-4159.2005.03251.x.

Marshall, O. J. *et al.* (2016) 'Cell-type-specific profiling of protein-DNA interactions without cell isolation using targeted DamID with next-generation sequencing.', *Nature protocols*, 11(9), pp. 1586–98. doi: 10.1038/nprot.2016.084.

McManus, C. J. *et al.* (2010) 'Global analysis of trans-splicing in Drosophila', *Proceedings of the National Academy of Sciences*, 107(29), pp. 12975–12979.

Menzel, R. *et al.* (1996) 'Behavioral, neural and cellular components underlying olfactory learning in the honeybee.', *Journal of physiology, Paris*, 90(5–6), pp. 395–8.

Menzel, R. *et al.* (1999) 'Pharmacological dissociation between the reinforcing, sensitizing, and response-releasing functions of reward in honeybee classical conditioning.', *Behavioral neuroscience*, 113(4), pp. 744–54.

Minakhina, S. and Steward, R. (2006) 'Melanotic mutants in Drosophila: Pathways and phenotypes', *Genetics*, 174(1), pp. 253–263. doi: 10.1534/genetics.106.061978.

Monastirioti, M., Linn, C. E. and White, K. (1996) 'Characterization of Drosophila tyramine beta-hydroxylase gene and isolation of mutant flies lacking octopamine.', *The Journal of neuroscience : the official journal of the Society for Neuroscience*, 16(12), pp. 3900–3911.

Moussian, B. *et al.* (2005) 'Involvement of chitin in exoskeleton morphogenesis in Drosophila melanogaster', *Journal of Morphology*, 264(1), pp. 117–130. doi: 10.1002/jmor.10324.

Nathanson, J. A. (1979) 'Octopamine receptors, adenosine 3',5'-monophosphate, and neural control of firefly flashing.', *Science (New York, N.Y.)*, 203(4375), pp. 65–8.

Neumüller, R. A. *et al.* (2011) 'Genome-wide analysis of self-renewal in Drosophila neural stem cells by transgenic RNAi', *Cell Stem Cell*, 8(5), pp. 580–593.

NEZIS, I. *et al.* (2000) 'Stage-specific apoptotic patterns during oogenesis', *European Journal of Cell Biology*, 79(9), pp. 610–620. doi: 10.1078/0171-9335-00088.

Nilsen, T. W. (2003) 'The spliceosome: The most complex macromolecular machine in the cell?', *BioEssays*, pp. 1147–1149. doi: 10.1002/bies.10394.

Nilsen, T. W. and Graveley, B. R. (2010) 'Expansion of the eukaryotic proteome by alternative splicing', *Nature*, 463(7280), pp. 457–463. doi: 10.1038/nature08909.

Ohsako, T. *et al.* (2003) 'Drosophila lola encodes a family of BTB-transcription regulators with highly variable C-terminal domains containing zinc finger motifs', *Gene*, 311(1–2), pp. 59–69.

Ou, Q. *et al.* (2016) 'The Insect Prothoracic Gland as a Model for Steroid Hormone Biosynthesis and Regulation', *Cell Reports*, 16(1), pp. 247–262. doi: 10.1016/j.celrep.2016.05.053.

Paige Bass, B., Cullen, K. and McCall, K. (2007) 'The axon guidance gene lola is required for programmed cell death in the Drosophila ovary', *Developmental Biology*, 304(2), pp. 771–785.

Peng, Q. *et al.* (2016) 'cGMP-Dependent Protein Kinase Encoded by foraging Regulates Motor Axon Guidance in Drosophila by Suppressing Lola Function', *Journal of Neuroscience*, 36(16), pp. 4635–4646.

Pertea, M. and Salzberg, S. L. (2010) 'Between a chicken and a grape: estimating the number of human genes', *Genome Biology*, 11(5), p. 206. doi: 10.1186/gb-2010-11-5-206.

Pflüger, H.-J. and Duch, C. (2011) 'Dynamic neural control of insect muscle metabolism related to motor behavior.', *Physiology (Bethesda, Md.)*, 26(4), pp. 293–303. doi: 10.1152/physiol.00002.2011.

Pozzoli, U. and Sironi, M. (2005) 'Silencers regulate both constitutive and alternative splicing events in mammals', *Cellular and Molecular Life Sciences*, pp. 1579–1604. doi: 10.1007/s00018-005-5030-6.

Reid, D. C. *et al.* (2009) 'Next-generation SELEX identifies sequence and structural determinants of splicing factor binding in human pre-mRNA sequence', *Rna-a Publication of the Rna Society*, 15(12), pp. 2385–2397. doi: 10.1261/rna.1821809.

Renger, J. J. *et al.* (1999) 'Neuronal polymorphism among natural alleles of a cGMP-dependent kinase gene, foraging, in Drosophila.', *The Journal of Neuroscience*, 19(19), p. RC28.

Richardson, B. E. and Lehmann, R. (2010) 'Mechanisms guiding primordial germ cell migration: strategies from different organisms.', *Nature reviews. Molecular cell biology*, 11(1), pp. 37–49. doi: 10.1038/nrm2815.

Robberson, B. L., Cote, G. J. and Berget, S. M. (1990) 'Exon definition may facilitate splice site selection in RNAs with multiple exons.', *Molecular and cellular biology*, 10(1), pp. 84–94. doi: 10.1128/MCB.10.1.84.

Robertson, C. E., Ratai, E. M. and Kanwisher, N. (2016) 'Reduced GABAergic Action in the Autistic Brain', *Current Biology*, 26(1), pp. 80–85. doi: 10.1016/j.cub.2015.11.019.

Roeder, T. (1999) 'Octopamine in invertebrates', *Progress in Neurobiology*, pp. 533–561. doi: 10.1016/S0301-0082(99)00016-7.

Rubin, G. M. and Spradling, A. C. (1982) 'Genetic transformation of Drosophila with transposable element vectors.', *Science (New York, N.Y.)*, 218(4570), pp. 348–53.

Schaal, T. D. and Maniatis, T. (1999) 'Multiple distinct splicing enhancers in the protein-coding sequences of a constitutively spliced pre-mRNA', *Molecular and Cellular Biology*, 19(1), pp. 261–273. doi: 0270-7306/99.

Schwaerzel, M. *et al.* (2003) 'Dopamine and octopamine differentiate between aversive and appetitive olfactory memories in Drosophila.', *The Journal of neuroscience : the official journal of the Society for Neuroscience*, 23(33), pp. 10495–502.

Seinen, E. *et al.* (2011) 'RNAi-induced off-target effects in Drosophila melanogaster: Frequencies and solutions', *Briefings in Functional Genomics*, 10(4), pp. 206–214. doi: 10.1093/bfgp/elr017.

Selcho, M. *et al.* (2012) 'The role of octopamine and tyramine in Drosophila larval locomotion.', *The Journal of comparative neurology*, 520(16), pp. 3764–85. doi: 10.1002/cne.23152.

Sembulingam, K. and Sembulingam, P. (2012) *Essentials of Medical Physiology*, *California medicine*. doi: 10.1017/CBO9781139168403.

Silver, S. J. and Rebay, I. (2005) 'Signaling circuitries in development: insights from the retinal determination gene network.', *Development (Cambridge, England)*, 132(1), pp. 3–13. doi: 10.1242/dev.01539.

Southall, T. D. *et al.* (2014) 'Dedifferentiation of neurons precedes tumor formation in lola mutants', *Developmental Cell*. Cell Press, 28(6), pp. 685–696.

Spletter, M. L. *et al.* (2007) 'Lola regulates Drosophila olfactory projection neuron identity and targeting specificity.', *Neural development*. BioMed Central Ltd, 2, p. 14.

Stathakis, D. G. *et al.* (1999) 'The catecholamines up (Catsup) protein of Drosophila melanogaster functions as a negative regulator of tyrosine hydroxylase activity.', *Genetics*. Genetics Society of America, 153(1), pp. 361–82.

van Steensel, B. and Henikoff, S. (2000) 'Identification of in vivo DNA targets of chromatin proteins using tethered dam methyltransferase.', *Nature biotechnology*, 18(4), pp. 424–8. doi: 10.1038/74487.

Stogios, P. J. *et al.* (2005) 'Sequence and structural analysis of BTB domain proteins.', *Genome biology*, 6(10), p. R82. doi: 10.1186/gb-2005-6-10-r82.

Sugitani, Y. *et al.* (2002) 'Brn-1 and Brn-2 share crucial roles in the production and positioning of mouse neocortical neurons', *Genes and Development*, 16(14), pp. 1760–1765. doi:10.1101/gad.978002.

Sutton, R. E. and Boothroyd, J. C. (1986) 'Evidence for trans splicing in trypanosomes.', *Cell*, 47(4), pp. 527–35. Available at: http://www.ncbi.nlm.nih.gov/pubmed/3022935 (Accessed: 27 October 2016).

Tripathy, R. *et al.* (2014) 'Transcriptional regulation of Drosophila gonad formation', *Developmental Biology*. Academic Press Inc., 392(2), pp. 193–208.

Truman, J. W., Taylor, B. J. and Awad, T. A. (1993) 'Formation of the Adult Nervous System', *In the Development of Drosophila melanogaster, M. Bate and A. Martinez Arias, eds (Cold Spring Harbour, NY: Cold Spring Harbor Laboratory Press).*, Chapter 21, pp. 1245–1275.

Venken, K. J. T. *et al.* (2009) 'Versatile P[acman] BAC libraries for transgenesis studies in Drosophila melanogaster.', *Nature methods*, 6(6), pp. 431–4. doi: 10.1038/nmeth.1331.

Vitulo, N. *et al.* (2014) 'A deep survey of alternative splicing in grape reveals changes in the splicing machinery related to tissue, stress condition and genotype', *BMC Plant Biology*, 14(1), p. 99. doi: 10.1186/1471-2229-14-99.

Wang, Z. and Burge, C. B. (2008) 'Splicing regulation: from a parts list of regulatory elements to an integrated splicing code.', *RNA (New York, N.Y.)*. Cold Spring Harbor Laboratory Press, 14(5), pp. 802–13. doi: 10.1261/rna.876308.

Warf, M. B. and Berglund, J. A. (2010) 'Role of RNA structure in regulating pre-mRNA splicing', *Trends in Biochemical Sciences*, pp. 169–178. doi: 10.1016/j.tibs.2009.10.004.

Werner, F.-M. and Coveñas, R. (2011) 'Classical neurotransmitters and neuropeptides involved in generalized epilepsy: a focus on antiepileptic drugs.', *Current medicinal chemistry*, 18, pp. 4933–48. doi: BSP/CMC/E-Pub/2011/365 [pii].

Wierenga, J. M. and Hollingworth, R. M. (1990) 'Octopamine uptake and metabolism in the insect nervous system.', *Journal of neurochemistry*, 54(2), pp. 479–89.

Will, C. L. and Lührmann, R. (2011) 'Spliceosome structure and function', *Cold Spring Harbor Perspectives in Biology*, 3(7), pp. 1–2. doi: 10.1101/cshperspect.a003707.

Wissel, S. *et al.* (2016) 'A Combination of CRISPR/Cas9 and Standardized RNAi as a Versatile Platform for the Characterization of Gene Function.', *G3 (Bethesda, Md.)*. doi: 10.1534/g3.116.028571.

Wu, C.-S. *et al.* (2014) 'Integrative transcriptome sequencing identifies trans-splicing events with important roles in human embryonic stem cell pluripotency.', *Genome research*, 24(1), pp. 25–36. doi: 10.1101/gr.159483.113.

Yang, Y.-F. *et al.* (2017) 'Trans-splicing enhances translational efficiency in C. elegans', *Genome Research*, pp. 1–11. doi: 10.1101/gr.202150.115.6.

Yang, Z. *et al.* (2015b) 'Octopamine mediates starvation-induced hyperactivity in adult Drosophila.', *Proceedings of the National Academy of Sciences of the United States of America*. National Academy of Sciences, 112(16), pp. 5219–24. doi: 10.1073/pnas.1417838112.

Yang, Z. *et al.* (2015a) 'Octopamine mediates starvation-induced hyperactivity in adult Drosophila.', *Proceedings of the National Academy of Sciences of the United States of America*, 112(16), pp. 5219–24. doi: 10.1073/pnas.1417838112.

Yarali, A. and Gerber, B. (2010) 'A Neurogenetic Dissociation between Punishment-, Reward-, and Relief-Learning in Drosophila.', *Frontiers in behavioral neuroscience*, 4(December), p. 189. doi: 10.3389/fnbeh.2010.00189.

Younossi-Hartenstein, A. and Hartenstein, V. (1993) 'The Role of the Tracheae and Musculature during Pathfinding of Drosophila Embryonic Sensory Axons', *Developmental Biology*, 158(2), pp. 430–447. doi: 10.1006/dbio.1993.1201.

Zhang, W. *et al.* (2003) 'A developmentally regulated splice variant from the complex lola locus encoding multiple different zinc finger domain proteins interacts with the chromosomal kinase JIL-1', *Journal of Biological Chemistry*, 278(13), pp. 11696–11704.

Zheng, L. and Carthew, R. W. (2008) 'Lola regulates cell fate by antagonizing Notch induction in the Drosophila eye', *Mechanisms of Development*, 125(1–2), pp. 18–29.

Zhou, C. *et al.* (2012) 'Molecular Genetic Analysis of Sexual Rejection: Roles of Octopamine and Its Receptor OAMB in Drosophila Courtship Conditioning', *Journal of Neuroscience*, 32(41), pp. 14281–14287. doi: 10.1523/JNEUROSCI.0517-12.2012.

Zhou, C., Rao, Y. and Rao, Y. (2008) 'A subset of octopaminergic neurons are important for Drosophila aggression.', *Nature neuroscience*, 11(9), pp. 1059–67. doi: 10.1038/nn.2164.
Zhou, Z. *et al.* (2002) 'Comprehensive proteomic analysis of the human spliceosome', *Nature*, 419(6903), pp. 182–185. doi: 10.1038/nature01031.

Annex

List of reagents used in this study

Name	Source
Acidic-Phenol:Chloroform (pH 4.5)	Thermo Fisher Scientific
30% Acrylamide/Bis Solution	BioRad
Ambion nuclease-free water	Thermo Fisher Scientific
Ambion GlycoBlue™	Thermo Fisher Scientific
Ambion 3M Sodium acetate (NaAc)	Thermo Fisher Scientific
Ampure XP beads	Beckman Coulter
Ammonium Persulfate (APS)	BioRad
Bleach/ Sodium hypochlorite	Roth
Chloroform/ Trichlormethan	Roth
D-(+)Glucose	Sigma-Aldrich
D-(+)-Trehalose dihydrate	Sigma-Aldrich
Disodium hydrogen phosphate (Na_2HPO_2)	Sigma-Aldrich
Dry milk powder, non-fat	Cell Signaling
EDTA 0.5M, pH8	IMB CF, Media lab
Ethanol ≥99,5 %, ultra-pure	Thermo Fisher Scientific
Formamide	Sigma-Aldrich
Formaldehyde	Sigma-Aldrich
Glycerol	
HEPES ≥99,5 %	Sigma-Aldrich
Heparin sodium salt	Sigma-Aldrich
n-Heptane	Roth
Isopropanol/2-propanol, ultra-pure ≥99,8 %	Honeywell Research Chemicals
Magnesium chloride 2M	IMB CF, Media lab
Monosodium phosphate (NaH_2PO_4)	Sigma-Aldrich
Methanol ≥99 %	Roth
NBT/ BCIP	Roche
Octopamine hydrochloride ≥98 %	Sigma-Aldrich
Paraformaldehyde 95%	Sigma-Aldrich

Pluronic™ F-68 Non-ionic Surfactant	Thermo Fisher Scientific
Potassium chloride 1M (KCl)	IMB CF, Media lab
Potassium acetate (KAc)	Sigma-Aldrich
PVDF membrane, Immobilon®-P	Merck
Ribonucleic acid from torula yeast	Sigma-Aldrich
Schneider's *Drosophila* Medium	Thermo Fisher Scientific
Sodium bicarbonate ($NaHCO_3$)	Sigma-Aldrich
Sodium chloride 3M (NaCl)	IMB CF, Media lab
SSC (20x)	IMB CF, Media lab
Supersignal West Pico Chemiluminescent Substrate	Thermo Fisher Scientific
SYBR green PCR master mix	Applied Biosystems
TEMED/ N,N,N',N'-Tetramethylethylendiamin	Roth
Tris-HCl 1M, pH 7.5 or pH8	IMB CF, Media lab
Triton X-100	Sigma-Aldrich
TRIzol reagent	Thermo Fisher Scientific
Trypsin-EDTA (0.25%)	Thermo Fisher Scientific
Tween-20	Sigma-Aldrich
Vectashield	VECTOR laboratories
Western blot resolving buffer, pH 8.8	IMB CF, Media lab
Western blot running buffer (10x)	IMB CF, Media lab
Western blot stacking buffer, pH 6.8	IMB CF, Media lab
Western blot transfer buffer (10x)	IMB CF, Media lab

List of enzymes used in this study

Name	Source
OneTaq® DNA Polymerase	New England Biolabs
Phusion®-High Fidelity DNA Polymerase	New England Biolabs
T4-DNA Ligase	New England Biolabs
NotI-High Fidelity	New England Biolabs
EcoRI-High Fidelity	New England Biolabs

AscI	New England Biolabs
BglII	New England Biolabs
BbsI	New England Biolabs
XbaI	New England Biolabs
DNaseI, RNase-free	New England Biolabs
M-MLV reverse transcriptase	Promega
Murine RNase Inhibitor	New England Biolabs
MyTag™ HS polymerase	Bioline

List of commercially available kits used in this study

Name	Source
Agilent High Sensitivity DNA Kit	Genomics Agilent
Agilent RNA 6000 Pico Kit	Genomics Agilent
DIG RNA Labeling Kit (SP6/T7)	Sigma-Aldrich
Gateway® LR Clonase® II Enzyme mix	Thermo Fisher Scientific
GeneJET Gel Extraction Kit	Thermo Fisher Scientific
GeneJET Plasmid Miniprep Kit	Thermo Fisher Scientific
GeneJET PCR Purification Kit	Thermo Fisher Scientific
NEBNext® Ultra™ Directional RNA Library Prep Kit for Illumina®	New England Biolabs
NebNext® DNA Ultra II library kit for Illumina®	New England Biolabs
pENTR™/D-TOPO® Cloning Kit	Thermo Fisher Scientific
QIAprep® Miniprep Kit	QIAGEN
QIAprep® Midiprep Kit	QIAGEN
QIAamp® DNA Micro Kit	QIAGEN
Qubit™ dsDNA HS Sensitivity Assay	Thermo Fisher Scientific
TSA™ Plus Cyanine 3 System	Perkin Elmer

Abbreviation list

AA	Amino acid
AEL	After embryo laying
AS	Alternative splicing
AL	Antenna lobe
BAC	Bacterial artifical chromosome
Bacc	Bacchus
bp	Base pair
BTB	Broad-complex, Tramtrack, Bric a brac
BPS	Branch point sequence
cAMP	Cyclic adenosine monophosphate
CNS	Central nervous system
Co-IP	Co-immunoprecipitation
CRISPR	Clustered regularly interspaced palindromic repeats
Cys	Cystein
Cy3	Carbocyanine 3
Dam	DNA adenine methyltransferase
DamID	DNA adenine methyltransferase identification
DNA	Deoxyribonucleic acid
dnTP	2'-desoxy-nucleoside-5'-triphosphate
Dpn	Deadpan
Dscam1	Down syndrome cell adhesion molecule 1
EDTA	Ethylenediaminetetraacetic acid
Elav	Embryonic lethal abnormal vision
et al.	et alteres (Latin: and others)
EtOH	Ethanol
F	Forward
FACS	Fluorescent activated cell sorting
Fas2	Fasciclin 2
FDR	False discovery rate
Fra	Frazzled
FRT	Flipase recombination target
GFP	Green fluorescent protein
GLC	Germline stem cell
GO-term	Gene ontology term
GluR	Glutamate receptor
gRNA	guide RNA
hnRNP	Heterogeneous nuclear ribonucleoprotein
HCl	Hydrogenchloride
His	Histein
Hr	Hours
ISNb	Intersegmental nerve b
iVUM	ventral unpaired median
kB	Kilo Base
KCl	Potassium Chloride
KD	Knock-down
kDa	Kilo Dalton

KO	Knock-out
l	Litre
L3	Third instar larval stage
Lola	Longitudinals Lacking
M	Molar
MARCM	Mosaic analysis with a repressible cell marker
MeOH	Methanol
Mod(mdg4)	Modifier of mdg4
NaCl	Sodium Chloride
Nb	Neuroblast
NMJ	Neuromuscular junciton
Nos	Nanos
Oamb	Octopamine receptor in mushroom bodies
Octß1R	Octopamine ß1 receptor
Octß2R	Octopamine ß2 receptor
Octß3R	Octopamine ß3 receptor
PAK	p-21 activated kinase
PAM	Protospacer adjacent motif
PCR	Polymerase-chain reaction
PFA	Para-Formaldehyde
PKG	cGMP-dependent protein kinase
PN	Projection neuron
qRT-PCR	Quantitative reverse transcription polymerase chain reaction
R	Reverse
Repo	reversed polarity
RFP	Red fluorescent protein
RNA Pol II	RNA polymerase II
RNA	Ribonucleic acid
RNAi	RNA interference
Rpl15	Ribosomal protein L15
RT	Room temperature
mRNA	Messenger RNA
pre-mRNA	Pre-messenger RNA
SD	Standard deviation
SDS	Sodium dodecyl sulfate polyacrylamide
SEM	Standard error of the mean
SGP	Somatic gonadal precursor
SNP	Single nucleotide polymorphisms
snRNA	Small nuclear RNA
snRNP	Small nuclear ribonucleoprotein particle
SS	Splice site
TaDa	Targeted DamID
TBH	Tyramine-ß-hydroxylase
Tdc2	Tyrosine-decarboxylase 2
Ttk	Tramtrack
Tub	Tubulin
UAS	Upstream activating sequence
UTR	Untranslated region
VNC	Ventral nerve cord

WB	Western blot
WT	Wild type
ZF	Zinc finger

Acknowledgement

- Aus Datenschutzgründen entfernt –

Curriculum Vitae

- Aus Datenschutzgründen entfernt -